

Utilizing Structures of CYP2D6 and BACE1 Complexes To Reduce Risk of Drug–Drug Interactions with a Novel Series of Centrally Efficacious BACE1 Inhibitors

Michael A. Brodney,^{*,†} Elizabeth M. Beck,[†] Christopher R. Butler,[†] Gabriela Barreiro,[†] Eric F. Johnson,[#] David Riddell,[‡] Kevin Parris,^{||} Charles E. Nolan,[‡] Ying Fan,[#] Kevin Atchison,[‡] Cathleen Gonzales,[‡] Ashley E. Robshaw,[‡] Shawn D. Doran,[⊥] Mark W. Bundesmann,^{||} Leanne Buzon,[§] Jason Dutra,[§] Kevin Henegar,[§] Erik LaChapelle,[†] Xinjun Hou,[†] Bruce N. Rogers,[†] Jayvardhan Pandit,^{||} Ricardo Lira,[§] Luis Martinez-Alsina,[§] Peter Mikochik,[§] John C. Murray,[§] Kevin Ogilvie,[§] Loren Price,[§] Subas M. Sakya,[§] Aijia Yu,[∇] Yong Zhang,[∇] and Brian T. O'Neill[§]

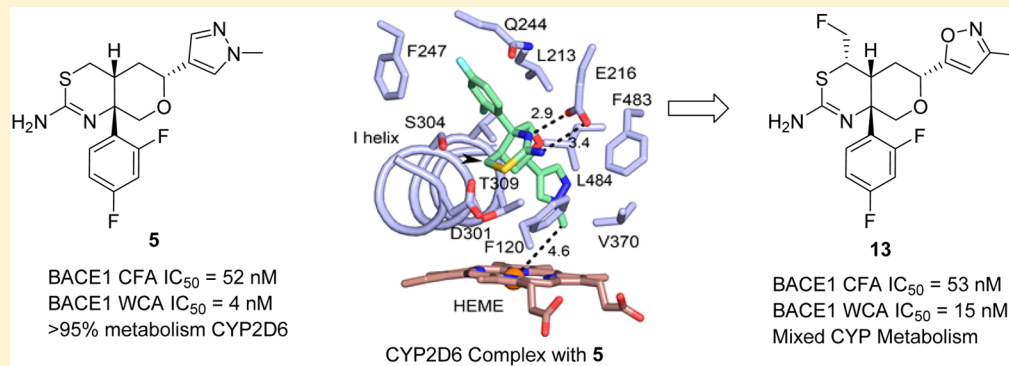
[†]Neuroscience Worldwide Medicinal Chemistry, [‡]Neuroscience Research Unit, Pfizer Worldwide Research and Development, 610 Main Street, Cambridge, Massachusetts 02139, United States

[§]Neuroscience Worldwide Medicinal Chemistry, ^{||}Center of Chemistry Innovation and Excellence, [⊥]Pharmacokinetics, Dynamics, and Metabolism, Pharmaceutical Sciences, Pfizer Worldwide Research and Development, 445 Eastern Point Road, Groton, Connecticut 06340, United States

[#]The Scripps Research Institute, 10550 North Torrey Pines Road, La Jolla, California 92024, United States

[∇]WuXi AppTec, 288 Fute Zhong Road, Waigaoqiao Free Trade Zone, Shanghai 200131, China

Supporting Information



ABSTRACT: In recent years, the first generation of β -secretase (BACE1) inhibitors advanced into clinical development for the treatment of Alzheimer's disease (AD). However, the alignment of drug-like properties and selectivity remains a major challenge. Herein, we describe the discovery of a novel class of potent, low clearance, CNS penetrant BACE1 inhibitors represented by thioamidine **5**. Further profiling suggested that a high fraction of the metabolism (>95%) was due to CYP2D6, increasing the potential risk for victim-based drug–drug interactions (DDI) and variable exposure in the clinic due to the polymorphic nature of this enzyme. To guide future design, we solved crystal structures of CYP2D6 complexes with substrate **5** and its corresponding metabolic product pyrazole **6**, which provided insight into the binding mode and movements between substrate/inhibitor complexes. Guided by the BACE1 and CYP2D6 crystal structures, we designed and synthesized analogues with reduced risk for DDI, central efficacy, and improved hERG therapeutic margins.

INTRODUCTION

The accumulation and aggregation of amyloid- β ($A\beta$) peptides is believed to be one of the underlying causes of Alzheimer's disease (AD), which is the most common reason for cognitive decline in the elderly.¹ AD pathology is characterized by the presence of extracellular plaques in the hippocampal and cortical regions of the brain, accompanied by intraneuronal neurofibrillary tangles and extensive neuronal loss.² $A\beta$, the major protein constituent of amyloid plaques, is derived from

sequential cleavage of the type I integral membrane protein, amyloid precursor protein (APP), by two proteases: BACE1 and γ -secretase.³ Proteolytic cleavage of APP by BACE1, a member of the aspartyl protease family of enzymes, takes place within the endosome at low pH, generating a soluble N-terminal ectodomain of APP (sAPP β) and C-terminal fragment

Received: February 2, 2015

Published: March 17, 2015

(C99).⁴ Subsequent cleavage of the membrane-bound C99 fragment by γ -secretase liberates the various $A\beta$ peptide species, of which $A\beta_{40}$ and $A\beta_{42}$ are the predominant forms.⁵ Mutations in APP near the BACE1 cleavage site have been reported that either increase $A\beta$ generation and are associated with early onset AD or decrease $A\beta$ generation and protect against AD.⁶ Together, these data suggest that limiting the generation of $A\beta$ through inhibition of BACE1 is an attractive approach for the treatment of this disease.

In recent years, the first generation of small molecule BACE1 inhibitors advanced into clinical studies. In contrast to the earlier chemical series, these compounds possess improved BACE1 potency and adequate CNS penetration and effectively lower $A\beta$ in the CSF of humans.⁷ While some clinical candidates continue to advance, unfortunately, there continues to be considerable attrition in this target space due to a range of safety findings, including hepatotoxicity and ocular toxicity. For example, BACE1 inhibitors from Eli Lilly (LY2811376) and Amgen (AMG-8718) led to accumulation of autofluorescent material and degeneration of the retinal pigment epithelium (RPE) layer of the eye in rat safety studies.⁸ In addition, Lilly terminated a phase II study with LY2886721 as a result of abnormal liver biochemical tests.⁹ With the requirement for longer duration studies in an aging population, a critical characteristic for a successful candidate will be fewer safety liabilities. As such, the next generations of BACE1 inhibitor clinical candidates will ideally exhibit improved CNS penetration, a reduced risk of safety findings, and a low daily dose.

RESULTS AND DISCUSSION

Projected Human Dose. We recently disclosed a novel series of thioamidine-containing BACE1 inhibitors, as represented by compound **1** (Figure 1), possessing excellent overall

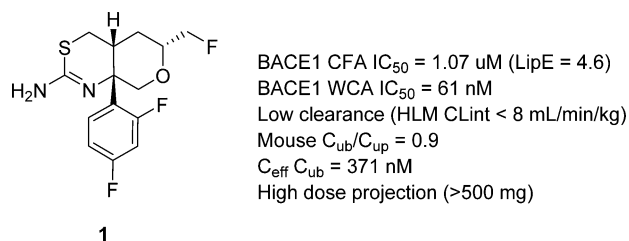


Figure 1. Potency, key ADME values, and projected dose for compound **1**.

properties including high CNS penetration (C_{ub}/C_{up} = 1) and in vivo efficacy in both an acute $A\beta$ -lowering model and in chronic dosing studies investigating plaque burden in a transgenic mouse model, as well as selectivity over the related aspartyl protease cathepsin D (CatD).¹⁰ Although compound **1** demonstrates robust efficacy in $A\beta$ -lowering models, the weak BACE1 in vitro potency, as measured by a cell-free fluorescence polarization assay (CFA IC_{50} = 1.07 μ M) or whole cell assay (WCA IC_{50} = 61 nM) in H4 human neuroglioma cells measuring sAPP β , translated to a requirement for a relatively high free brain concentration ($C_{eff} C_{ub}$ = 371 nM) in order to achieve 25% reduction of brain $A\beta_{x-42}$ (Figure 1). This C_{eff} resulted in a high projected human dose (>500 mg/day), which was outside the desired range for a viable clinical entry, given that minimizing the dose is one important factor in reducing compound attrition.¹¹

Objectives. The goal of the next-generation BACE1 inhibitor program was to develop a CNS-penetrant, small-molecule inhibitor with low projected human dose (<100 mg). To achieve the reduction in dose, we targeted improvements in potency (>10-fold) relative to compound **1**; clearly, this needed to be accomplished without negatively impacting the low clearance or excellent brain penetration of **1**. To track progress, lipophilic efficiency (LipE = BACE1 CFA pIC_{50} - log D) was used as a numerical index to ensure that potency improvements were not accomplished at the expense of ADME and safety profiles.¹²

Design Strategy. Analysis of the BACE1 costructure complex with inhibitor **1** (Figure 2) revealed direct hydrogen bonds between the amidine and the catalytic aspartic acids, while the difluorophenyl group occupied the S1 pocket.¹⁰ The fluoromethyl group on the THP ring forced Tyr71 to move to an “out” conformation, exposing a lipophilic pocket (S2') under the protein flap. This novel pocket is suboptimally filled by the fluoromethyl group (Figure 2A). This observation is consistent with previous SAR, wherein increasing the steric bulk at this position (fluoromethyl to cyclopropyl) improved BACE1 potency 3-fold.¹⁰ As shown in Figure 2B, the S2' pocket is mostly occupied with water molecules (O1–O6) that form a hydrogen-bond network with key residues of the S2' pocket (Arg128, Ile126, Tyr198, Ser35) and the protein flap (Tyr71, Trp76, Val69). We postulated that positioning a heteroaryl substituent in this pocket might function to improve potency, displacing one or more water molecules in the hydrogen-bond network while maintaining low overall lipophilicity and alignment of ADME properties.

Heteroaryl-Substituted BACE1 Inhibitors. Compound **2**, which bears an oxazole on the THP ring, was prepared according to Schemes 2–6 and showed ~2-fold improvement over **1** with respect to BACE1 potency (see Figure 1 and Table 1) and an improvement in LipE (5.2 vs 4.6). This supported the hypothesis that the induced pocket formed by movement of the protein flap could accommodate a polar heteroaryl ring (Table 1). In addition to the potency improvement, oxazole **2** maintained low clearance in human liver microsomes (h -CL_{int, app} < 8.7 mL/min/kg) and high passive permeability (RRCK P_{app} = 25.9) with no projected P-gp mediated efflux (MDR1 efflux ratio = 1).¹³ Unfortunately, oxazole **2** was determined to be a strong inhibitor of CYP2D6 (IC_{50} = 0.33 μ M). Molecular modeling of oxazole **2** in the S2' pocket highlighted the potential to further improve potency by introducing a methyl group at the 4-position of the oxazole to interact with Ser35, Tyr198, and Ile126. Results of modeling related methylated 5-membered ring heteroaryls such as isoxazole and pyrazole at the 3-position of the THP ring suggested comparable potency improvements. To this end, methyl-substituted oxazole **3**, isoxazole **4**, and pyrazole **5** were prepared as shown in Schemes 2–8 and profiled. We were gratified to find that all three methyl-substituted analogues (**3**, **4**, and **5**) exhibited significantly improved potency and lipophilic efficiency (LipE) relative to the fluoromethyl congener **1**. An X-ray structure of pyrazole **5** in BACE1 confirmed the binding mode and movement of Tyr71 in the protein flap (Figure 3). In this structure, the methyl group on the pyrazole ring displaced a water molecule just at the opening of the pocket formed by Ser35/Tyr198/Ile126 (O5 in Figure 2B). The remaining buried water molecules (O1–O4) in S2' were maintained in the cocrystal structure of pyrazole **5**. The pyrazole methyl filled a lipophilic cleft, which may account for

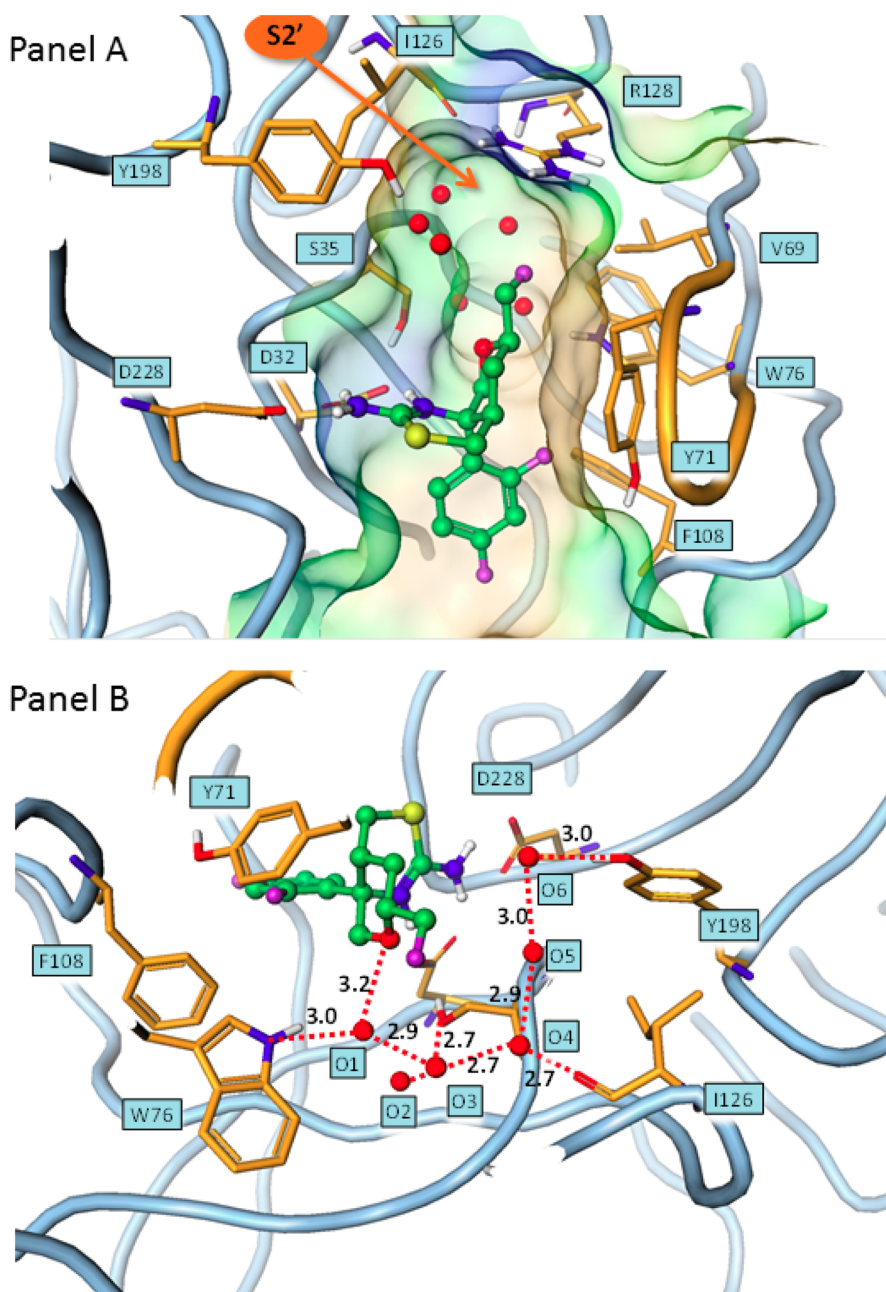


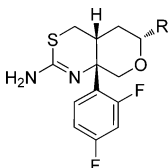
Figure 2. Cocrystal structure of compound 1 in BACE1. (A) The fluoromethyl group occupies the pocket near flap loop in orange. (B) An alternative view into the S2' pocket shows the crystal water (O1) interacting with oxygen of the THP and accepting a hydrogen bond from Trp76. Additional crystal waters (O2–O6) form a rich hydrogen-bond network in the S2' pocket.

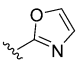
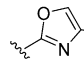
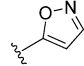
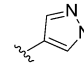
the approximately 10-fold improvement in potency over compound 2 that was observed for the methylated analogues 3, 4, and 5.

Despite the improved BACE1 potency of analogues 3, 4, and 5, we speculated that the additional methyl group on the oxazole/isoxazole ring may have provided a metabolic site for oxidation, based on the higher clearance observed for 3 and 4 in human liver microsomes (Table 1). The more polar pyrazole 5 maintained relatively low clearance in human liver microsomes and exhibited the best alignment of potency, reduced efflux, weak inhibition of hERG, high passive permeability (RRCK), and reduced inhibition of CYP2D6 ($IC_{50} = 13.9 \mu\text{M}$). Pyrazole 5 was selected for further in vivo profiling. To assess the brain penetration of pyrazole 5, a time-course study in mouse was

conducted, which revealed good distribution to the CNS compartment ($C_{ub}/C_{up} = 0.6$). The ability of pyrazole 5 to effect reduction in brain $A\beta_{x-42}$ was examined in wild-type mouse, using acute sc dosing at 3, 10, and 50 mpk (Figure 4); $A\beta_{x-42}$ levels were measured in brain, plasma, and CSF from 1 to 18 h (Supporting Information Figure 1). The corresponding drug exposure in brain was measured, in order to delineate the PK/PD relationship for BACE1 inhibition. A significant reduction was observed in brain for the 10 and 50 mpk doses, with a maximal reduction of 60% at 6 h for the 50 mpk dose. The exposure–response relationship was established based on an indirect response model, as previously described.¹⁴ The free concentration in brain to maintain an average 25% lowering of brain $A\beta_{x-42}$ (C_{eff}) at steady state is estimated to be

Table 1. In Vitro Pharmacology and ADME Properties for 2–5



Compound	2	3	4	5
R Group				
log D	1.0	1.4	1.6	1.2
CFA IC₅₀^a	614 nM (LipE = 5.2)	84 nM (LipE = 5.6)	78 nM (LipE = 5.3)	52 nM (LipE = 6.1)
WCA IC₅₀^b	27 nM	4 nM	3 nM	4 nM
CatD IC₅₀^c	74.9 μM	13.9 μM	9.4 μM	13.1 μM
<i>h</i>-CL_{int,s} (mL/min/kg)^d	< 8.7	69.6	55.2	9.1
MDR1 Er^e	1.0	2.0	1.2	1.8
RRCK (x10⁻⁶ cm/s)^f	25.9	19.9	17.4	17.3
CYP1A2 IC₅₀	29 μM	>30 μM	>30 μM	>30 μM
CYP2C8 IC₅₀	>30 μM	>30 μM	>30 μM	>30 μM
CYP2D6 IC₅₀^g	0.33 μM	5.5 μM	0.15 μM	13.9 μM
CYP3A4 IC₅₀	>30 μM	>30 μM	>30 μM	>30 μM
CYP2C19 IC₅₀	>30 μM	>30 μM	>30 μM	>30 μM
hERG IC₅₀^h	10.6 μM	2.3 μM	1.6 μM	4.9 μM
Mouse NeuroPkⁱ C_{ub}/C_{up}	ND	ND	ND	0.66
rCYP^j Contribution	95% 2D6	95% 2D6	95% 2D6	95% 2D6

^aIC₅₀ values obtained from BACE1 cell-free assay (CFA). ^bIC₅₀ values obtained from BACE1 whole-cell assay (WCA). ^cIC₅₀ values obtained from CatD cell-free assay (CFA). ^dPredicted human intrinsic clearance, apparent (*h*-CL_{int,app}) from human liver microsomal stability assay. ^eMDR1 efflux ratio (MDR Er) from MDR1-transfected MDCK cell line represents the ratio of permeability, *P*_{app} BA/AB using 1 μM test compound. ^fRRCK: Madin–Darby canine kidney cells with low transporter activity were isolated and used to estimate intrinsic absorptive permeability. ^gCYP2D6 inhibition was obtained by measuring inhibition of 5 μM dextromethorphan in pooled HLM (HL-MIX-102). ^hMeasured IC₅₀ in hERG-expressing CHO cells. ⁱDetermined from C_{ub}/C_{up} exposures (AUC-based) in WT mice. ^jRecombinant human CYPs (100 pmol/mL) with 1 μM probe substrate were used in 60 min incubations. ND = not determined.

50 nM. Relative to compound 1 (C_{eff} C_{ub} = 371 nM), pyrazole 5 represented a ~7 fold improvement with respect to in vivo potency.

Understanding Potential Drug–Drug Interactions of Pyrazole 5. Because of the encouraging efficacy and overall profile of the heteroaryl-substituted inhibitors, we profiled pyrazole 5 in human microsomes (CL_{int} = 9.1 mL/min/kg) and hepatocytes (CL_{int,app} < 6 μL/min/million) which confirmed low clearance. In vitro profiling with human recombinant CYPs (rCYP) showed that CYP2D6 significantly contributed (>95%) to the metabolism of pyrazole 5 as well as the other analogues in Table 1. Exclusive CYP2D6 metabolism was of particular concern due to the potential for victim based DDIs and variable clinical exposure due to polymorphic nature of this enzyme.¹⁵ While the in vitro rCYP data was utilized primarily as a higher throughput screen, the predicted contribution of CYP2D6 to the overall metabolism required additional investigation.

Metabolite identification following incubation of pyrazole 5 in human liver microsomes confirmed the primary metabolism was oxidative by CYP-P450s and not surprisingly showed formation of a major metabolite corresponding to the *N*-demethylated pyrazole 6 (Figure 5). Profiling of the *N*-H pyrazole 6 showed weaker BACE1 potency relative to *N*-Me pyrazole 5, an observation consistent with previous SAR in the oxazole analogues. However, pyrazole 6 was a very potent inhibitor of CYP2D6 (IC₅₀ = 0.36 μM), precluding pyrazole 5 from further development due to the high risk of a clinical DDI.

Structures of CYP2D6 Complexes with Compounds 5 and 6. To gain a more fundamental understanding of the DDI liability of the pyrazoles, with which to rationally design improved inhibitors, crystal structures of pyrazoles 5 and 6 bound to CYP2D6 were generated. Consistent with the observed site of metabolism for pyrazole 5, the pyrazole methyl group is oriented toward the heme iron at a distance of

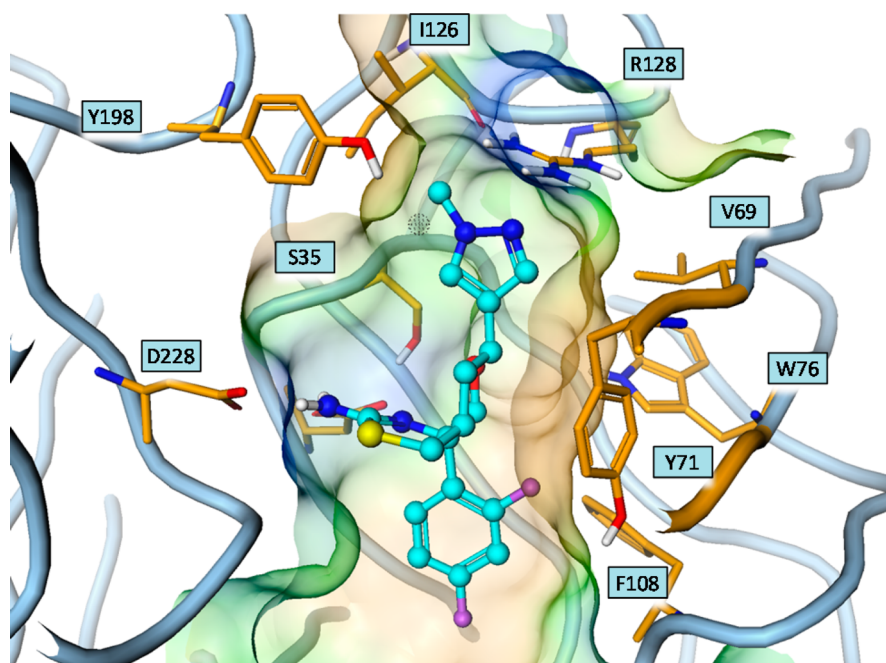


Figure 3. X-ray structure of pyrazole **5** bound to BACE1. The pyrazole occupies the S2' pocket near the flap loop (orange). The methyl group on the pyrazole fills a small lipophilic pocket formed by Ser35, Tyr198, and Ile126. A water molecule was displaced by the methyl group (represented by dotted sphere).

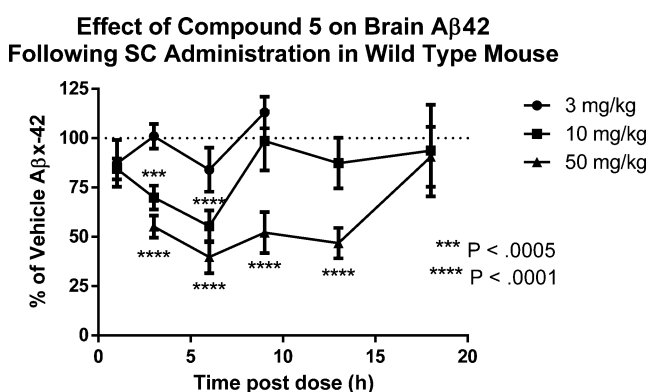


Figure 4. Effect of pyrazole **5** on brain A β x-42 following sc administration in wild-type mice.

4.6 Å (Figure 6A). This position of the methyl group is conducive to hydrogen abstraction from the methyl group by the iron-bound oxene. Presumably, the reactive intermediate derived from hydrogen abstraction binds to the hydroxyl radical

of the heme to form the corresponding hydroxymethyl compound. The latter undergoes cleavage of the carbon–nitrogen bond to form pyrazole **6** and formaldehyde. The high inhibitory potency of **6** is easily understood upon examination of its cocrystal structure (Figure 6B): the lone pair on the pyrazole nitrogen is seen to coordinate to the heme iron, with a coordinate covalent bond length of 2.0 Å. The pyrazole **5** is a very weak inhibitor because its methyl group prevents a close approach of the pyrazole nitrogen lone pair to the heme iron. A key feature of CYP2D6 is its capacity to complement positively charged ligands by ionic interactions between Glu216 and/or Asp301 and the ligand. In the complex with pyrazole **5**, the two carboxylate oxygens of Glu216 are positioned close to the two nitrogens of the thioamidine ring (Figure 6A). As the amine nitrogen is protonated at neutral and lower pH, the ability of CYP2D6 to interact with the charge of compounds **5** and **6** presumably contributes to the predominant role of CYP2D6 in the clearance of **5** and to the inhibitory potency of **6**. The binding of pyrazole **6** to the heme iron in the active site requires a significant shift in the position of **6** relative to **5** to enable the binding of the pyrazole lone pair of **6** with the heme

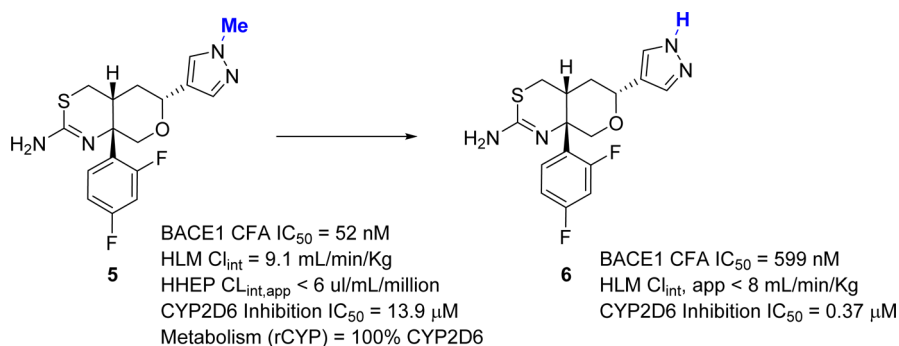


Figure 5. Metabolic fate of pyrazole **5** in human liver microsomes.

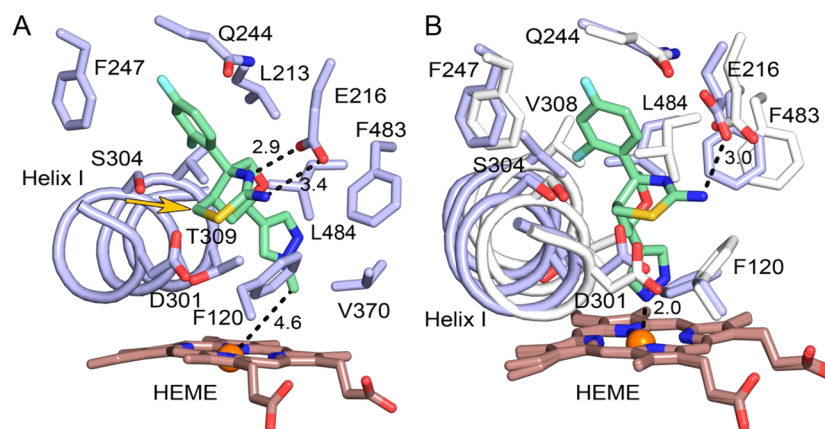


Figure 6. (A) Compound 5 bound in the active site of CYP2D6. Notable distance measurements are shown by dashed lines with the distance indicated in Å. A portion of helix I is rendered as a cartoon. Protein, heme, and substrate carbons are colored light-blue, brown, and pale-green, respectively. Oxygen, nitrogen, sulfur, fluorine, potassium, and iron atoms are colored red, blue, yellow, light-blue, gray, and orange, respectively. The carbon between the sulfur and the THP ring of 5 is indicated by the arrow. (B) Compound 6 bound in the active site of CYP2D6, where it forms a coordinate covalent bond to the heme iron. The difference in position of 6 relative to 5 is associated with significant changes for helix I, the helix F-G region, and surrounding residues. For reference, the protein structure of the complex with 5 is shown with gray carbons (B).

iron (Figure 6B). As a result, only one of the two carboxylate oxygens of Glu216 in the complex with 6 is sufficiently close to the amide nitrogen of the thioamide ring for hydrogen bonding. This reflects a limited range of motion of the Glu216 side chain coupled with displacement of the $C\alpha$ -carbon of the backbone (Figure 6B). The change in the $C\alpha$ position is part of a shift in the helix F–G region that is driven by ligand binding and the strong interaction of Glu216 with the thioamide ring. Additionally, helix I is bowed outward, compared to its position in Figure 6A, to accommodate the binding of the pyrazole moiety to the heme iron. This displacement is similar to that observed for the binding of prinomastat to CYP2D6, which is ligated to heme iron by a pyridine moiety.¹⁶ Helix I is bowed out in this region for the complexes with both 5 and 6 when compared to the structure PDB 3TBG of the CYP2D6 thioridazine complex, which is representative of the starting structure of CYP2D6 in the crystals used for exchange of thioridazine by pyrazoles 5 and 6. This outward movement of helix I for both complexes is required because of the width of the central bicyclic THP thioamide ring system.

Design for Reduced Substrate/Inhibition of CYP2D6.

The capacity of P450 enzymes to oxygenate structurally diverse ligands often limits efforts to reduce metabolism through structural modification of the inhibitor, as alternative binding modes or different CYP P450s may mediate metabolism of the new chemical entity. Nevertheless, the X-ray structures of pyrazole 5 bound to CYP2D6 and to BACE1 provided the basis to rationally design for reduced CYP2D6 inhibition while maintaining BACE1 potency. The CYP2D6 structure of pyrazole 5 showed that the thioamide ring is closely associated with a portion of the helix I backbone that is relatively rigid, suggesting that modification of the carbon adjacent to the sulfur (marked with an arrow in Figure 6A) might alter the orientation of 5 in the active site and reduce the rate of metabolism. Analysis of an internal database of BACE1 inhibitors highlighted a single example (compound 8) containing a methyl substituent (R_2) adjacent to the sulfur of the amidine group (Figure 7). Comparing the BACE1 potency of analogue 8 with that of the unsubstituted analogue 7 suggested that the methyl group at R_2 was well tolerated in BACE1, consistent with the crystal structure binding modes

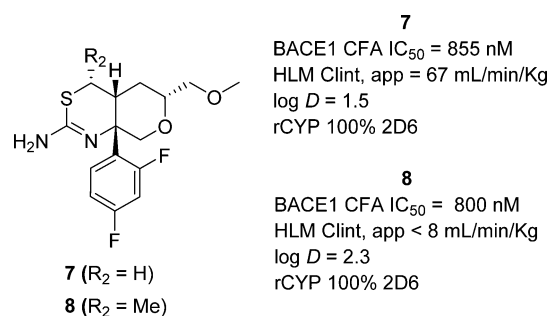


Figure 7. Impact of a methyl group adjacent to sulfur (R_2) on metabolism.

shown in Figures 2 and 3.¹⁰ Interestingly, a significant reduction in overall clearance was measured for compound 8 relative to 7 despite the increase in lipophilicity (0.8 unit increase in $\log D$ resulting from introduction of the methyl group). This was consistent with the notion that binding interactions for this series to CYP-P450s, rather than lipophilicity, were a key factor governing metabolic turnover.

To understand if this steric effect adjacent to the sulfur was a general solution to reducing clearance and CYP2D6 inhibition within this chemical series, we investigated the impact of adding the methyl group onto the set of heteroaryl-substituted THP analogues described above in Table 1. Compounds 9, 10, and 11 ($R_2 = Me$) were prepared following the route described in Schemes 5–8, and the properties were compared directly to the matched molecular pairs in which $R_2 = H$ from Table 1. Analogous to compounds 7 and 8, the substituted oxazole 9 ($R_2 = Me$) maintained comparable BACE1 cell-free and cellular potency relative to compound 3 but with significantly reduced clearance (HLM $Cl_{int, app} < 8$ mL/min/kg vs 69.6 mL/min/kg for compound 3) and no significant inhibition of the major CYP-P450s ($IC_{50s} > 30$ μM). Profiling of oxazole 9 in recombinant human P450s (rCYP) showed a balanced clearance profile through CYP3A4, CYP2D6, and CYP2C19, thereby reducing the potential for DDI and clinical variability liabilities relative to the compounds in Table 1. Profiling of isoxazole 10 and pyrazole 11 relative to their matched molecular pairs (compounds 4 and 5; $R = H$) confirmed the

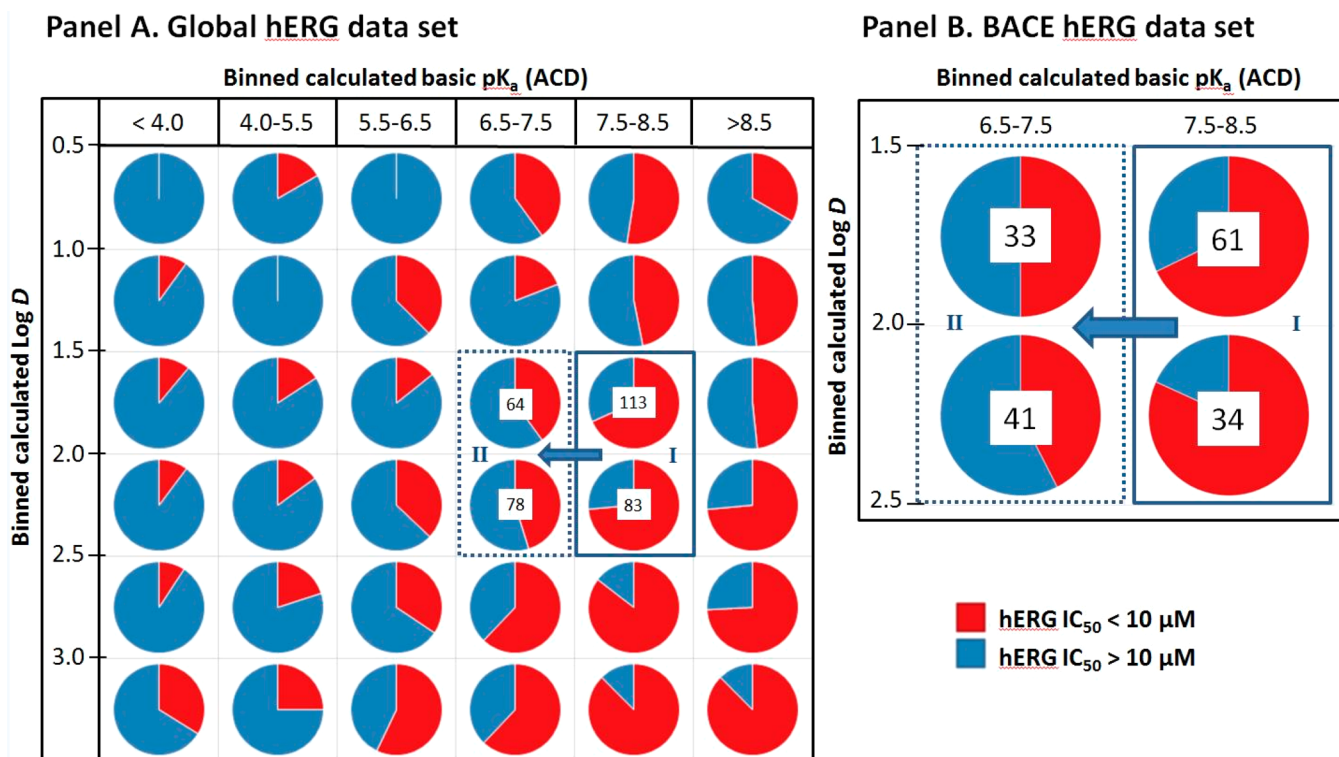


Figure 8. Effect of $\log D$ and pK_a on hERG IC_{50} . (A) Diverse Pfizer set of 2044 compounds. (B) Set of 169 BACE compounds from property space I and II. Red, hERG $IC_{50} < 10 \mu M$; blue, hERG $IC_{50} > 10 \mu M$. Total count per bin is highlighted in the center of the pie.

SAR trends, suggesting that the methyl substituent at R_2 reduced clearance and attenuated the contribution of CYP2D6 to the metabolism without negatively impacting potency, selectivity, or passive permeability. Overall, there was a small increase in the MDR efflux ratios for the compounds with the R_2 methyl group but CNS penetration was generally maintained, with isoxazole **10** exhibiting excellent brain penetration ($C_{ub}/C_{up} = 0.7$) and robust in vivo efficacy ($C_{eff} C_{ub} = 30 \text{ nM}$).¹⁴ In addition, plasma, CSF and brain $A\beta$ and drug levels were analyzed (see Supporting Information Figures 2–4).

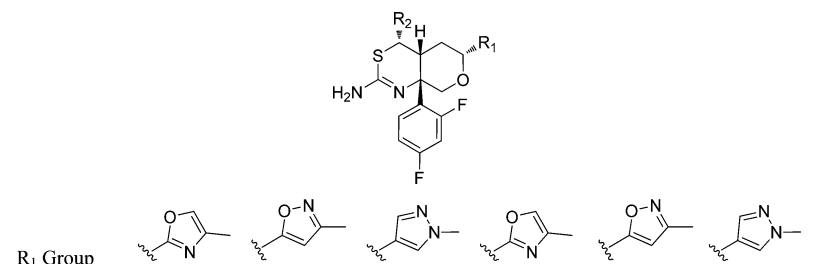
Designing for Improved hERG Safety Margins. Understanding potential cardiovascular risks such as QT prolongation as a result of inhibition of hERG (*human ether a go-go*) is an important factor in selecting compounds for clinical development.¹⁷ The methyl analogues **9–11** show weak inhibition of hERG ($IC_{50} = 2\text{--}5 \mu M$), which can be rationalized by their inherent structural features: a basic center with pendant aromatic and lipophilic moieties.¹⁸ Recent reports further suggest that minimizing hERG inhibition is a critical element in the design of BACE1 inhibitors with appropriate safety margins.¹⁹ We sought to understand the potential risks of weak inhibition of hERG relative to the targeted plasma concentrations in human ($C_{eff} C_{up}$). Examination of this relationship for isoxazole **10** shows that the margin between the projected concentration to maintain a 25% $A\beta$ lowering at steady state in plasma ($C_{eff} C_{up}$) and the hERG IC_{50} is 49-fold. From this analysis, we concluded that improvements in the margin between $C_{eff} C_{up}$ and hERG inhibition would be required for advancement of compounds from this chemical series into clinical development.

Previous literature reports^{18–20} and our analysis on a broad set of compounds (vide infra) highlighted basic pK_a and

lipophilicity as important factors in reducing activity at the hERG channel. Our analysis of a diverse set of over 2000 Pfizer compounds, profiled in the same hERG patch clamp assay, confirmed that reducing $\log D$ and lowering basic pK_a were important factors in reducing binding to the hERG channel (Figure 8A). Because a basic pK_a is required for inhibition of BACE1, we examined the factors influencing hERG activity in the relevant pK_a range of 6.5–8.5. This analysis suggested that in this property space (8A, area I) reducing the pK_a by a log unit (8A, area II) could be more effective in reducing hERG activity than lowering lipophilicity, particularly considering the goal of maintaining high CNS penetration. To ensure that the property trends were consistent between the diverse Pfizer set and compounds specifically prepared for the BACE1 project, we analyzed the BACE1 hERG set (8B) and observed similar probability trends.

With the design objective of reducing hERG, we estimated that a fluoromethyl group adjacent to the sulfur would reduce the pK_a by ~ 0.7 log units, relative to the methyl analogues **9**, **10**, and **11**, which have a measured pK_a of 7.7–7.8.²¹ Because the SAR suggested this position tolerated small substituents, we synthesized the fluoromethyl analogues **12**, **13**, and **14** (Table 2, Schemes 5–8). As expected, the $\log D$ for each matched molecular pair (F-Me vs Me) increased slightly, while the pK_a for the fluoromethyl derivatives was reduced (0.6–0.8 units). Analogous to the methyl analogues, the fluoromethyl congeners retained BACE1 potency without negatively impacting selectivity or ADME properties such as P-gp efflux (MDR Er) or passive permeability (RRCK). Analogues **12**, **13**, and **14** exhibited low clearance in HLM, with no projected DDI as measured both by the lack of CYP inhibition ($IC_{50} > 30 \mu M$) and mixed CYP contribution to oxidative metabolism (rCYP contribution). High CNS penetration and potent in vivo

Table 2. In Vitro Pharmacology and ADME Properties for 9-14



Cmpd	9 (R ₂ = CH ₃)	10 (R ₂ = CH ₃)	11 (R ₂ = CH ₃)	12 (R ₂ = CH ₂ F)	13 (R ₂ = CH ₂ F)	14 (R ₂ = CH ₂ F)
log D/pK _a	1.8/7.8	2.1/7.7	1.7/7.8	2.2/7.0	2.4/7.0	2.2/7.2
CFA IC ₅₀ ^a (LipE)	103 nM (5.1)	74 nM (5.0)	34 nM (5.8)	116 nM (4.7)	53 nM (4.9)	63 nM (5.0)
WCA IC ₅₀ ^b	6 nM	6 nM	3 nM	10 nM	15 nM	7 nM
CatD IC ₅₀ ^c	15.7 μM	14.2 μM	19.3 μM	19.1 μM	8.0 μM	6.6 μM
<i>h</i> -CL _{int} (mL/min/kg) ^d	< 8	< 8	< 8	27.8	< 8	< 8
MDR1 Er ^e	2.9	1.7	4.2	2.8	1.6	4.7
RRCK (x10 ⁻⁶ cm/s) ^f	24	17.8	15.8	19.1	14.8	12.2
1A2 IC ₅₀	>30 μM	>30 μM	>30 μM	>30 μM	>30 μM	>30 μM
2C8 IC ₅₀	>30 μM	>30 μM	>30 μM	>30 μM	>30 μM	>30 μM
2D6 IC ₅₀ ^g	>30 μM	14.2 μM	19.8 μM	>30 μM	>30 μM	26.4 μM
3A4 IC ₅₀	>30 μM	>30 μM	>30 μM	>30 μM	>30 μM	>30 μM
2C19 IC ₅₀	> 30 μM	> 30 μM	> 30 μM	> 30 μM	> 30 μM	> 30 μM
rCYP % contribution ^h	38% 3A4; 34% 2C19; 28% 2D6	100% 2C19	< LLQ	80% 3A4; 17% 2C19; 3% 2D6	68% 2C19; 32% 3A4;	65% 2C19; 35% 3A4
hERG IC ₅₀	4.8 μM	2.1 μM	4.8 μM	19.6 μM	10.1 μM	13.8 μM
Mouse Neuropk ⁱ	ND	0.70	ND	0.82	0.93	ND
C _{ub} /C _{up}						
Mouse C _{ub} ^j C _{ub} ^j	ND	30.1 nM	ND	27.4 nM	24.6 nM	ND

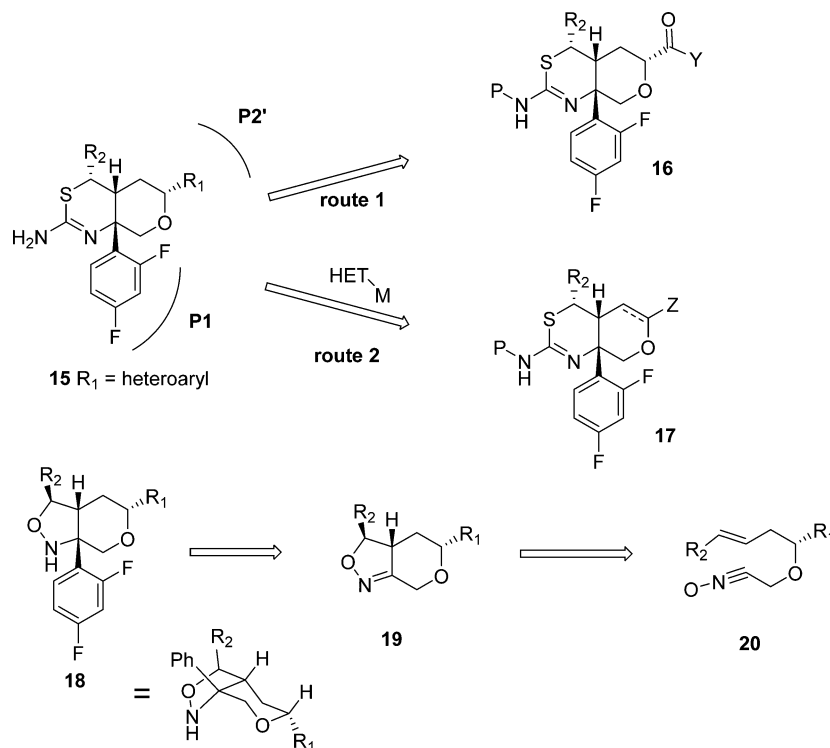
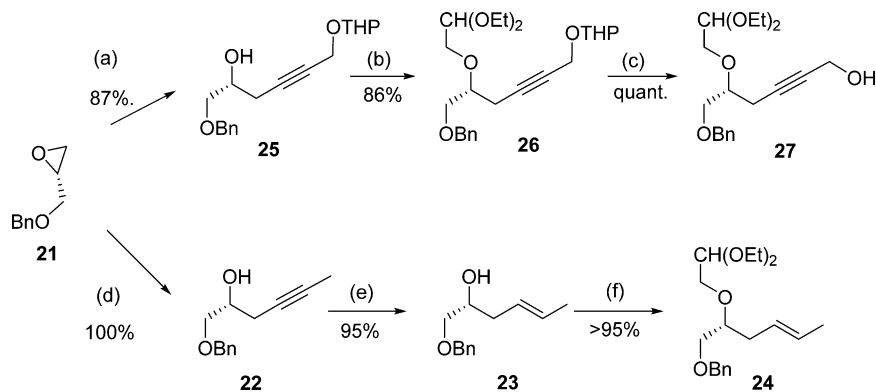
^aIC₅₀ values obtained from BACE1 cell-free assay (CFA). ^bIC₅₀ values obtained from BACE1 whole-cell assay (WCA). ^cIC₅₀ values obtained from CatD cell-free assay (CFA). ^dPredicted human intrinsic clearance, apparent (*h*-CL_{int,app}) from human liver microsomal stability assay. ^eMDR1 efflux ratio (MDR Er) from MDR1-transfected MDCK cell line represents the ratio of permeability, *P*_{app} BA/AB using 1 μM test compound. ^fRRCK: Madin–Darby canine kidney cells with low transporter activity were isolated and used to estimate intrinsic absorptive permeability. ^gCYP2D6 inhibition was obtained by measuring inhibition of 5 μM dextromethorphan in pooled HLM (HL-MIX-102). ^hRecombinant human CYPs (100 pmol/mL) with 1 μM probe substrate were used in 60 min incubations. ⁱDetermined from C_{ub}/C_{up} exposures (AUC-based) in WT mice. ^jSee Supporting Information Figures 2–4.

efficacy were measured for analogues **12** (C_{ub}/C_{up} = 0.82; C_{eff} C_{ub} = 27.4 nM) and **13** (C_{ub}/C_{up} = 0.93; C_{eff} C_{ub} = 24.6 nM). Examination of the hERG margin for isoxazole **13** shows a greater than 7-fold improvement compared to isoxazole **10**, with an in vitro hERG therapeutic index (C_{eff} C_{up} relative to hERG IC₅₀) of 381-fold. The reduced drug exposure required for central efficacy suggested that the margins over CatD were adequate for advancement. Finally, the goal of reducing the projected human dose was achieved with compound **12** and compound **13**.

Chemistry. It was clear that a comprehensive SAR investigation incorporating structural elements that modify the basicity of the thioamidine, the impact on cytochrome P450

binding, and an exploration of the P2' region of BACE1 would require a broad extension of existing synthetic technology.²² We proposed a two-part strategy in which functionality would be installed as part of the ring skeleton construction while incorporating versatility to enable the late-stage introduction of diverse heteroaryls in P2' from a common intermediate. Finally, we desired versatile functional groups that could be modified separately and easily at key intervals in the synthesis. We envisioned several approaches for the creation of substituents directed toward the P2' region of the BACE1 protein, as shown in Scheme 1. In each case, it was essential to have high yielding and stereoselective syntheses of the THP-fused thioamidine cores **16** or **17** as a foundation for SAR exploration.

Scheme 1

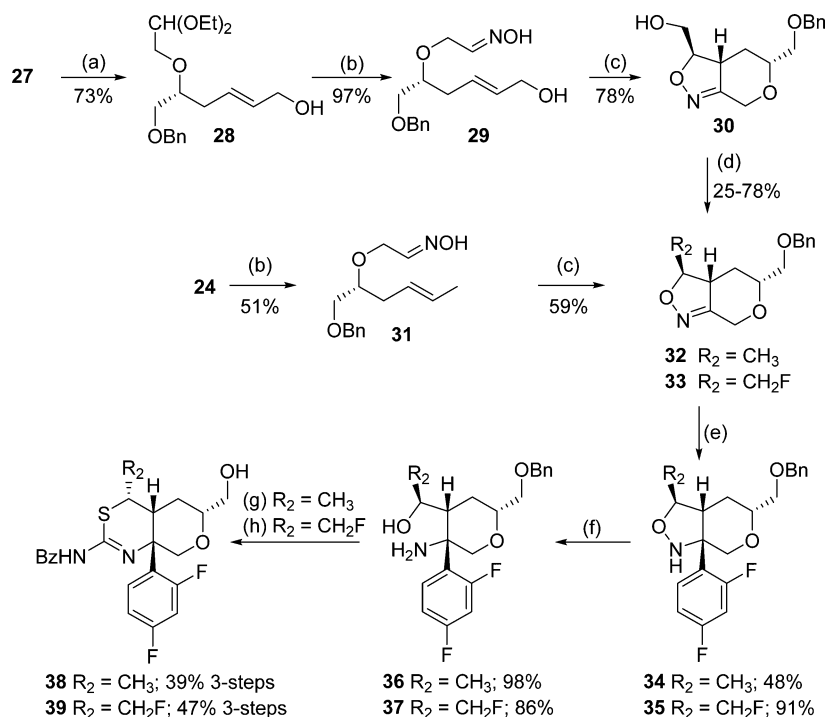
Scheme 2^a

^aReagents and conditions: (a) *O*-tetrahydropyranyl propargyl alcohol, *n*-BuLi then $BF_3 \cdot Et_2O$, then epoxide, THF, $-78^\circ C$; (b) NaH, then iodoacetaldehyde diethylacetal (via bromoacetaldehyde diethylacetal and NaI in acetone), THF, $50^\circ C$; (c) 10 mol % $PhSO_3H$ in EtOH; (d) propargyllithium, Et_2AlCl , toluene, $0^\circ C$; (e) $LiAlH_4$, DME, rt to $100^\circ C$; (f) NaH, then bromoacetaldehyde diethylacetal, THF, reflux.

We found that an optimum route for synthesis of the $S2'$ heteroaryl substituents on compound **15** involved construction of the heterocycles “in place” beginning from an alcohol, aldehyde, or acid functionality at the 6-position (R_1) of the fused THP ring system (Scheme 1, route 1). This approach opened the way to a variety of substituted heterocycles after a few straightforward transformations. Suitably substituted amides offered access to oxazole functionality by a ring closure dehydration.²³ Isoxazoles were prepared from amides by addition of ketone oxime anions followed by dehydration.²⁴ The aldehyde functionality could be converted indirectly to various pyrazole substitution patterns through homologation of the aldehyde to an acetaldehyde, formylation of the resulting aldehyde enol, and subsequent condensation of the resulting dialdehyde diacetal with hydrazine.²⁵ Thus, in an average of three steps, readily accessible functionality could be converted

into the desired heterocyclic ring systems. These approaches were developed after more convergent approaches failed to provide a direct approach to this class of compound. These included direct Csp^3-Csp^2 coupling of a suitably activated halide or sulfone with a heterocyclic organometallic or Csp^2-Csp^2 coupling followed by reduction of a dihydropyran double bond (Scheme 1, route 2). These two approaches were less successful because the activated THP derivatives proved to be unstable, and reduction of the dihydropyran intermediates was competitive with heterocycle reduction.

We previously described the synthesis of compound **1** ($R_2 = H$),¹⁰ which was prepared through an intramolecular [3 + 2] cycloaddition to form an enantioenriched, substituted, fused THP ring system [4.3.0] whose geometric constraints enabled later stereocontrolled addition at the ring fusion. By adding further constraining substituents (R_2 and R_1) as part of the

Scheme 3^a

^aReagents and conditions: (a) LiAlH₄, THF, 0 °C to rt; (b) aq HCl, 60 °C, then NH₂OH·HCl, EtOH/water, 70 °C, then NaOAc; (c) bleach, DCM, 18–22 °C; (d) DAST, CH₂Cl₂, –70 °C to rt or XtalFluor-E, TEA, TEA·3HF, acetonitrile, 105 °C, carried out via continuous flow technology; (e) 2,4-difluoro-1-iodobenzene/*n*-BuLi, then BF₃·Et₂O, then isoxazole in 9:1 toluene:THF, –78 °C; (f) zinc dust, AcOH, rt; (g) (i) BzNCS, CH₂Cl₂, rt, (ii) Ph₃P, DEAD, THF, 0 °C, (iii) cool to 0 °C, then add BCl₃, CH₂Cl₂; (h) (i) BzNCS, DCM, rt, isolate, (ii) Ghosez reagent, CH₂Cl₂, rt, 18 h, (iii) BCl₃, CH₂Cl₂, 0 °C or replace (ii) and (iii) w/TfOH in DCE, 60 °C, 3 h.

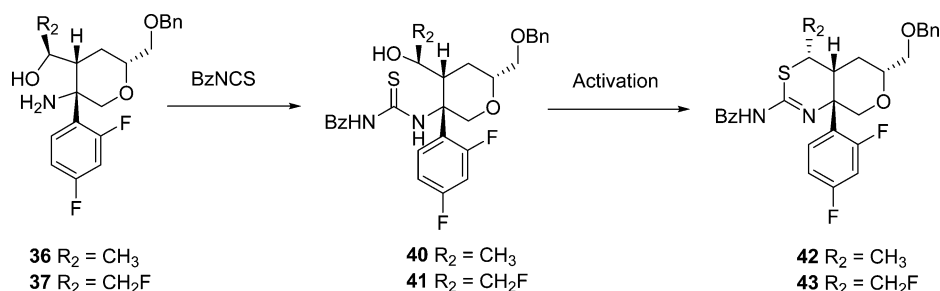
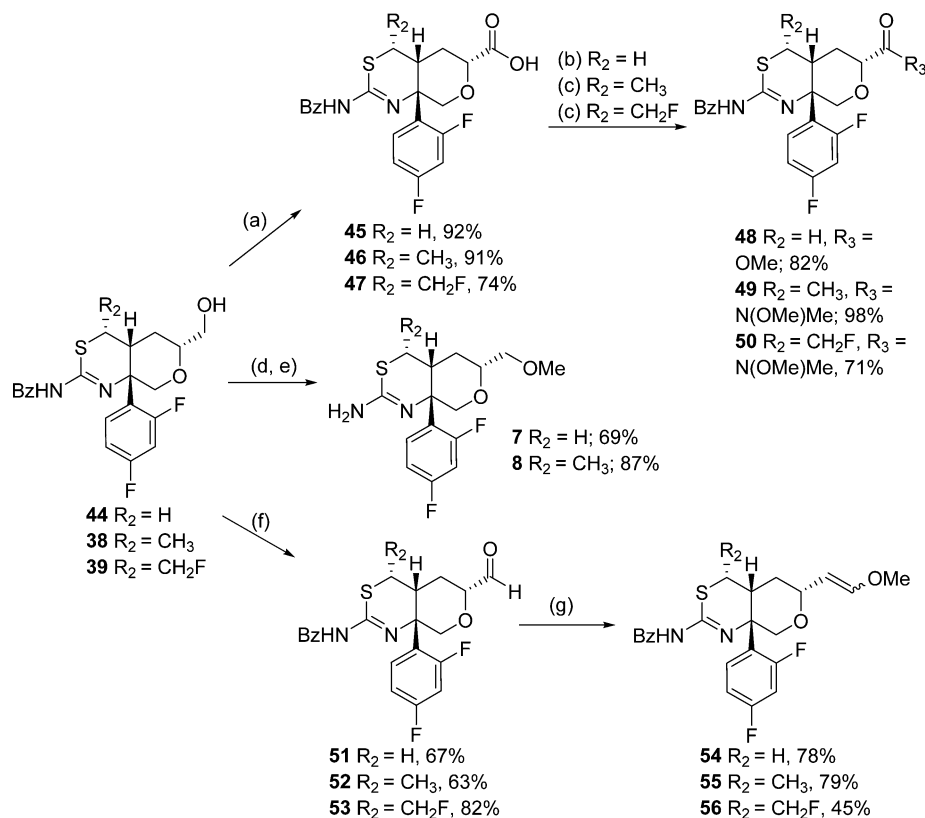
dipolarophile/nitrile oxide **20**, the stereocontrol of the cycloaddition can be extended to other ring substituents. To expand the functionality attached to the thioamidine ring (R₂ in **15**) to a methyl or fluoromethyl group, we extended the original terminal olefin to the *E*-alkene **20**. We expected excellent stereocontrol in the [3 + 2] cycloaddition to form **19** based on previous work.²⁶ Introduction of the S1 aryl group occurred on the convex face of **19**, again with excellent stereocontrol, to afford **18**; subsequent ring expansion provided the thioamidine functionality needed for **15**.²² The olefin geometry is thus transferred during the cycloaddition process, affording fully controlled relative stereochemistry between R₁, R₂, and the bicyclic core in **18**.

Synthesis of cycloaddition precursors such as **20** (where R₂ = Me) was initiated via Lewis acid-mediated propargyl anion addition to chiral epoxide **21** to form **22** (Scheme 2). Reduction of the alkyne **22** to the *E*-olefin **23** was accomplished using lithium aluminum hydride, likely activated by the neighboring alcohol.²⁷ The homoallylic alcohol **23** was elaborated to **24** through an alkylation with bromoacetaldehyde acetal. The acetal was hydrolyzed to the aldehyde and, without isolation, was progressed to oxime formation under standard conditions to afford **31** (Scheme 3). Direct nitrile oxide formation and [3 + 2] cycloaddition occurred in straightforward fashion to generate the fused tetrahydropyran ring system **32** as a single stereoisomer but with a small amount of accompanying nitrile oxide dimer or intermolecular isoxazoline formation (Scheme 3). Stereochemical assignment of compound **32** was confirmed using 2D-NMR (see Supporting Information). Using a similar strategy, the synthesis of cycloaddition precursor **27** (Scheme 2) proceeded via addition

of a THP-protected propargyl alcohol anion to epoxide **21**. Alkylation to afford the acetal **26** was followed by selective THP solvolysis and deprotection, to provide propargylic alcohol **27**.

Lithium aluminum hydride reduction of the acetylenic alcohol **27** was used to form the *trans*-allylic alcohol **28** exclusively. This was followed by oxime formation to provide **29**, conversion of the oxime to the nitrile oxide with bleach, and in situ cycloaddition to afford the bicyclic isoxazoline **30** as a single isomer (Scheme 3). The final step for this sequence, fluorination of the hydroxyl group, was challenging due to unfavorable steric and electronic effects in and around the alcohol. The DAST reagent was successful in activating the alcohol **30** to form a difluoro sulfanamine (not shown), but displacement of the activated intermediate by fluoride was less successful at ambient temperature.²⁸ We found that elevated temperatures were beneficial in improving yields, however, solutions of the DAST reagent are known to be unstable, rapidly decomposing when heated.²⁹ We were able to overcome these issues and obtain more significant amounts of **33** by carrying out multiple reactions on a small scale at elevated temperature or, more effectively, through the use of XtalFluor-E³⁰ and continuous flow technology. The reaction under continuous flow conditions was accomplished as follows: A stock solution of **30** and triethylamine in acetonitrile and a second solution of XtalFluor-E and triethylamine hydrofluoride (TEA·3HF) were introduced simultaneously through separate reagent ports in a continuous flow apparatus heated to 105 °C. The solutions were introduced at an equal rate with a reaction time of 14.3 min. In this way, alcohol activation and fluorination were completed rapidly, essentially soon after

Scheme 4

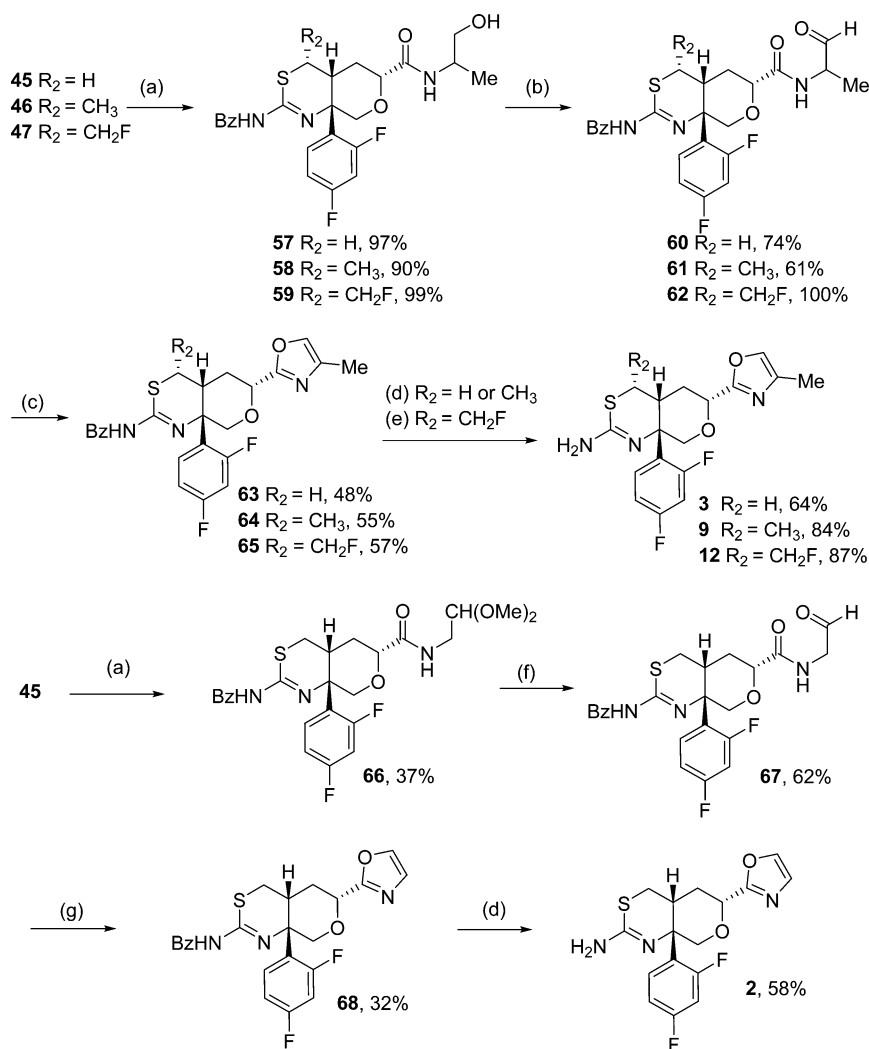
Scheme 5^a

^aReagents and conditions: (a) TPAP, NMO·H₂O, acetonitrile, rt; (b) (COCl)₂, cat. DMF, DCM, then MeOH, rt; (c) CDI, then *N,N*-dimethylhydroxylamine-HCl, DCE, rt; (d) MeI, NaH, THF, rt to 45 °C; (e) DBU, MeOH, 55 °C; (f) Py-SO₃, Et₃N, DMSO, DCM, rt; (g) (methoxymethyl)triphenylphosphonium chloride, *t*-BuOK, THF, 0 °C to rt.

mixing of the reagents, at a predetermined reaction temperature, allowing safe conversion on large scale. Stereochemical assignment of compound **33** was confirmed using 2D-NMR (see Supporting Information).

Creation of the final chiral center relied on a stereospecific anion addition to the convex face of the isoxazoline [4.3.0] imine functionality in **32** and **33** after activation with boron trifluoride etherate. The order of reactant introduction had a major influence on the yield. Halogen–metal exchange to form the difluorophenyl anion at –78 °C in the presence of BF₃·etherate, followed by slow addition of the isoxazoline, or alternatively anion formation followed by addition of the BF₃·complex of the isoxazoline, afforded the highest yields of **34** and **35**. In this way, we were able to avoid deprotonation of the isoxazoline and the eventual recovery of starting material. The reaction provided a single stereoisomer, bearing the *cis* ring fusion, as a precursor to the thioamidine ring system.

Thioamidine ring formation began with reduction of the N–O bond of the isoxazolines **34** and **35** with zinc in acetic acid (Scheme 3). The amino alcohols **36** and **37** were readily converted into a thiourea intermediate by reaction with benzoyl isothiocyanate (**40** and **41**; Scheme 4). Thioamidine cyclization could be effected via a variety of methods.¹⁰ In most cases, the undesired oxamidine was a minor byproduct; this was more of an issue with these secondary alcohols than for previous cases in which a primary alcohol was activated in the cyclization. In addition, the fluoromethyl analogue **37** displayed some instability toward epoxide formation, which required that intermediates of this type be cyclized soon after they were generated. In the case of the methyl-substituted thiourea **40**, cyclization was completed by activation of the alcohol in situ with triphenylphosphine and diethyl azodicarboxylate (TPP-DEAD), followed by S_N2 displacement with inversion to give **42**. At 0 °C, the cyclization produced the thioamidine **42**

Scheme 6^a

^aReagents and conditions: (a) TPTU, corresponding amino alcohol or acetal, DIPEA, DMF, rt; (b) Dess–Martin periodinane, DCM, rt; (c) Burgess reagent, THF, 125 °C, microwave, 2 min; (d) DBU, MeOH, 55–60 °C (e) neat propylamine; (f) 2 M HCl aq, THF, 40 °C; (g) Burgess reagent, THF, 66 °C.

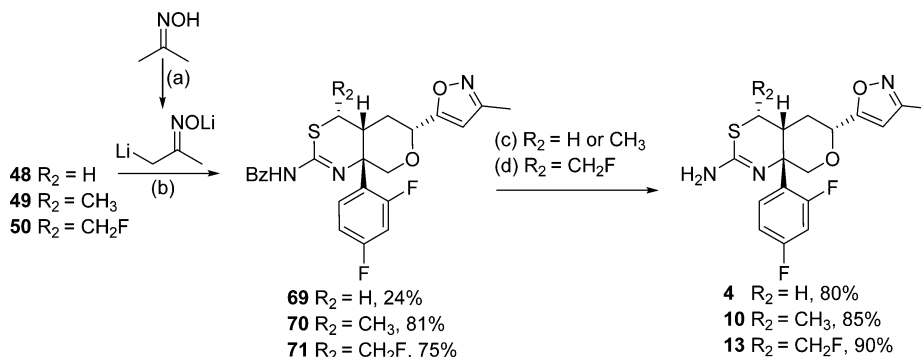
almost exclusively, while at higher temperature we observed significant formation of the oxamidine. Thus, in this system there was only a small difference between the desired activation of the secondary alcohol by the phosphorane and activation of the thiourea. The benzyl ether was selectively removed by treatment with BCl_3 to afford **38**.

In the case of the fluoromethyl-substituted thioamidine, we found that ring closure of the thioamidine alcohol **41** was more efficiently mediated by Ghosez's reagent³¹ than by TPP-DEAD. Product **39** was obtained in good yield from **43** after debenzoylation with BCl_3 (Scheme 3). We also found that fluoromethyl thioamidine **39** could be made directly from thiourea **41** via treatment with triflic acid. In this case, a mixture of triflic acid and anisole was found to effect initial deprotection of the benzyl ether, followed by protonation of the secondary alcohol and stereoselective thiourea cyclization with inversion of configuration. The stereochemistry of compound **38** and compound **39** was verified by single crystal X-ray analysis (see Supporting Information).

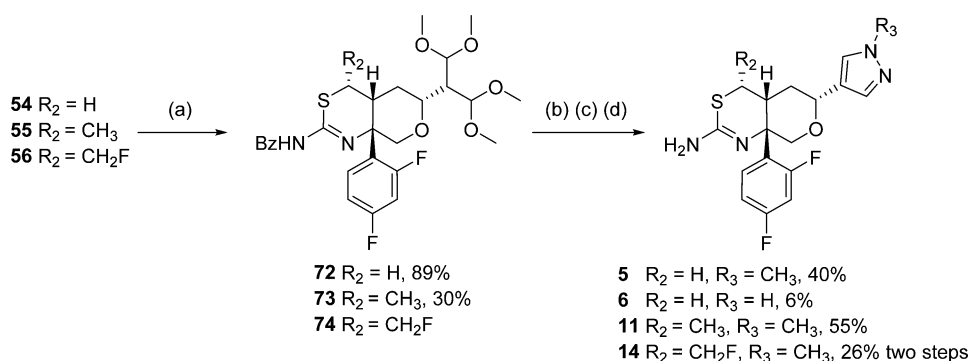
With the absolute and relative stereochemistry set for the thioamidine cores ($R_2 = \text{H}$, **44**; $R_2 = \text{CH}_3$, **38**; $R_2 = \text{CH}_2\text{F}$, **39**),

we turned our attention to installation of a range of heteroaryl groups on the THP ring (Scheme 5). Our plan was to modify the primary hydroxy group into various heteroaryl precursors to enable facile synthesis of the desired functional groups required for our SAR investigation. Conversion of the alcohols to acids **45**, **46**, and **47** with TPAP or to aldehydes **51**, **52**, and **53** using Parikh–Doering conditions (Scheme 5) was straightforward and applicable to all of these thioamidine series. The alcohols **38**, **39** and **44** could also be easily transformed into a variety of ethers, including the methyl ethers **7** and **8** shown, through reaction with the corresponding alkyl halide and base. Structural confirmation of compound **8** was verified through HSQC NMR (see Supporting Information). In preparation for the synthesis of an isoxazole series, the acids were converted to the Weinreb amides **49** and **50** or ester **48** in good yield. To prepare the pyrazole series, the aldehydes **51**, **52**, and **53** were homologated to enol ethers **54**, **55**, and **56** under Wittig conditions.

Synthesis of the oxazole series was initiated (Scheme 6) by amide coupling reactions of **45**, **46**, and **47** using the appropriate amino alcohol or amino acetal; these generated

Scheme 7^a

^aReagents and conditions: (a) 2.5 M *n*-BuLi in hexane, THF, -10 °C; (b) inverse addition of ester or Weinreb amide to anion, -10 to 0 °C in THF, then H₂SO₄; (c) DBU in MeOH, 55–60 °C; (d) methylamine, EtOH, rt.

Scheme 8^a

^aReagents and conditions: (a) trimethyl orthoformate, BF₃·Et₂O, DCM, 0 °C to rt; (b) MeNHNH₂·H₂SO₄, EtOH, 45 °C–60 °C; (c) N₂H₄·H₂SO₄, EtOH, 70 °C; (d) DBU, MeOH, 60 °C.

methyl-substituted compound **57**, **58**, and **59** and *des*-methyl analogue **66**. We initially approached the oxazole functionality via dehydration of the hydroxyethyl amides **57**, **58**, and **59** to the corresponding oxazolines. Unfortunately, the subsequent oxidation step to generate oxazoles such as **2**, **3**, **9**, and **12** was inefficient or completely ineffective under a variety of conditions. The synthesis of oxazoles with substitution adjacent to oxygen seemed to be more challenging due to the substrate possessing a secondary rather than a primary alcohol. We then found that utilizing the aldehyde rather than the alcohol provided an efficient route to each of the desired substitution patterns, as dehydration with the Burgess reagent³² proceeded smoothly under microwave heating (Scheme 6). Thus, for synthesis of the methyl oxazoles, 2-aminopropanol was coupled to the acids **45**, **46**, and **47**, followed by oxidation of the resulting alcohols **57**, **58**, and **59** with the Dess–Martin reagent. Aldehydes **60**, **61**, and **62** were treated with the Burgess reagent under microwave irradiation or extended reflux in THF to afford the oxazoles **63**, **64**, and **65** in good yield. For the unsubstituted oxazole **2**, acid **45** was coupled with acetaldehyde dimethyl acetal to afford **66**. Subsequent hydrolysis to the aldehyde amide **67**, followed by a similar dehydration, afforded the oxazole **68** in reasonable yield. Removal of the benzoyl group, under standard conditions with DBU in methanol or with neat propylamine, yielded the desired oxazoles **2**, **3**, **9**, and **12**.

To prepare the corresponding isoxazoles (Scheme 7), the Weinreb amides **49** and **50**, or in the case of the unsubstituted thioamide (R₂ = H) the methyl ester **48**, were treated with the

dianion of acetone oxime, followed by cyclization and dehydration with sulfuric acid to isoxazoles **69**, **70**, and **71**. Deprotection via treatment with alcohol and base afforded compounds **4**, **10**, and **13**.

Finally, to prepare the desired pyrazoles for this study, the key aldehyde intermediates **51**, **52**, and **53** were homologated to the enol ethers **54**, **55**, and **56** via a Wittig reaction on the aldehydes (Scheme 5). We found that these enol ethers were not readily hydrolyzed to stable aldehydes; an alternative strategy was designed involving the addition of a second aldehyde surrogate, which facilitated the subsequent reaction with hydrazine. Activation of trimethyl orthoformate with BF₃·etherate generated an excellent electrophile for formylation of the vinyl ethers, affording the bis-acetals **72**, **73**, and **74** (Scheme 8). Treatment of these bis-acetals under nonaqueous conditions with hydrazine or methylhydrazine afforded the desired pyrazoles and in most cases also effected removal of the benzamide protecting group. The stereochemistry of **5** was confirmed by single crystal X-ray crystallography on the benzoyl protected precursor (see Supporting Information).

CONCLUSION

In conclusion, a novel series of BACE1 inhibitors was developed which exhibited improved potency and projected human dose while maintaining CNS penetration similar to the previous lead molecule **1**. On the basis of the BACE1 crystal structure, a series of novel heterocycle-substituted analogues were designed to fill an induced pocket (S2') formed by movement of the protein flap. The synthetic strategy

undertaken to prepare these molecules utilized a late-stage diversification of THP-fused thioamidines into a variety of substituted heterocycles through efficient three-step transformations, which resulted in analogues with improved LipE. However, exclusive metabolism via CYP2D6 precluded advancement of these molecules due to the potential for clinical DDI. Cocrystal structures of the CYP2D6 substrate pyrazole **5** and the resultant CYP2D6 inhibitor *N*-H pyrazole **6** with CYP2D6 suggested that substituents (R_2) adjacent to the thioamidine sulfur could reduce binding of these inhibitors to CYP2D6. To prepare these complex structures, a significant synthetic investment was required to stereoselectively form the bicyclic thioamidines bearing appropriate functional handles oriented toward $S2'$ and positioned adjacent to the thioamidine sulfur (R_2). Our route emanated from chiral pool starting materials that could be elaborated and fashioned into a fully substituted and versatile ring skeleton. In this manner, SAR investigation and synthesis preceded in concert with multiple parameter optimizations. The combination of $S2'$ heterocycles with a thioamidine methyl group (R_2) resulted in lower clearance and conferred a more balanced CYP metabolism profile, significantly reducing the potential for DDIs. To improve the hERG margins of the initial analogues, in which $R_2 = \text{CH}_3$, an analysis of a diverse set of Pfizer compounds was conducted which indicated a strong effect of basic pK_a and $\log D$ on hERG potential. On the basis of the requirement for a basic amine for BACE1 inhibition, we successfully reduced the pK_a of the basic thioamidine by incorporating a fluoromethyl group adjacent to the sulfur. Subsequent profiling of compounds **12** and **13** showed excellent potency, alignment of ADME, improved hERG margins, and reduced dose relative to previous analogues. On the basis of the promising overall profile of compounds **12** and **13**, we advanced these compounds into long-term safety studies; results will be reported in due course.

EXPERIMENTAL SECTION

Biology. sAPP β Whole-Cell Assay (WCA). sAPP β , the primary cleavage product of BACE1, was determined in H4 human neuroglioma cells overexpressing the wild-type human APP₆₉₅. Cells were treated for 18 h with compound in a final concentration of 1% DMSO. sAPP β levels were measured by ELISA with a capture APP N-terminal antibody (Affinity BioReagents, OMA1-03132), wild-type sAPP β -specific reporter antibody p192 (Elan), and tertiary anti-rabbit-HRP (GE Healthcare). The colorimetric reaction was read by an EnVision (PerkinElmer) plate reader.

BACE1 Enzyme Cell-Free Assay (FP). Beta secretase-1 activity was assessed with soluble BACE1 and the synthetic APP substrate Biotin-GLTNIKTEEISEISYEVEFR-C[Oregon green]KK-OH in the presence of compounds in a fluorescence polarization (FP) *in vitro* assay. Enzyme, substrate, and test compounds were incubated in 15 μL of 100 mM sodium acetate pH 4.5 buffer containing 0.001% Tween-20 for 3 h at 37 $^\circ\text{C}$. Following the addition of saturating immunopure streptavidin, fluorescence polarization was measured with a PerkinElmer EnVision plate reader (Ex485 nm/Em530 nm).

In Vivo Experiments. All procedures were carried out in compliance with the National Institutes of Health Guide for the Care and Use of Laboratory Animals (1985), under approval of an Institutional Animal Care and Use Committee (IACUC).

Acute Treatment in Mice. Male 129/SVE wild-type mice (20–25 g) were in a nonfasted state prior to subcutaneous dosing with vehicle, or compound **5**, **10**, **12**, or **13**, using a dosing volume of 10 mL/kg in 5:5:90 DMSO:Cremophor:saline vehicle. Mice ($n = 5$ per group) were sacrificed at 1, 3, 5, 7, 14, 20, and 30 h postdose. Whole blood samples (0.5–1.0 mL) were collected by cardiac puncture into ethylenediaminetetraacetic acid (EDTA)-containing tubes, and plasma

was separated by centrifugation (1500g for 10 min at 4 $^\circ\text{C}$). The generated plasma was distributed into separate tubes on wet ice for exposure measurements (50 μL) and A β analysis (remainder). CSF samples (8–12 μL) were obtained by cisterna magna puncture using a sterile 25 gauge needle and collected with a P-20 Eppendorff pipet. CSF samples were distributed into separate tubes on dry ice for exposure measurements (3 μL) and A β analysis (remainder). Whole brain was removed and divided for exposure measurements (cerebellum) and A β analysis (left and right hemispheres), weighed, and frozen on dry ice. All samples were stored at -80 $^\circ\text{C}$ prior to assay.

Measurement of Rodent Amyloid- β . Frozen mouse hemibrains were homogenized (10% w/v) in 5 M guanidine HCl, using a Qiagen TissueLyser. Each sample was homogenized with a 5 mm stainless steel bead, four times, at a shaking rate of 24 times/s for 90 s, then incubated at 25 $^\circ\text{C}$ for 3 h, and ultracentrifuged at 125000g for 1 h at 4 $^\circ\text{C}$. The resulting supernatant was removed and stored in a 96-well polypropylene deep well plate at -80 $^\circ\text{C}$. The A β peptides were further purified through solid-phase extraction using Waters Oasis reversed-phase HLB 96-well column plates (60 mg). Column eluants in 98% MeOH and 2% NH_4OH from 500 to 800 μL of original brain supernatant were evaporated to complete dryness and stored at -80 $^\circ\text{C}$ until assay. For plasma analysis, 140–175 μL of mouse plasma was treated 1:1 with 5 M guanidine HCl and incubated overnight with rotation at 4 $^\circ\text{C}$. The entire volume was then purified through solid-phase extraction as indicated above.

Samples were analyzed using a dissociation-enhanced lanthanide fluorescent immunoassay (DELFLIA) platform enzyme-linked immunosorbent assay (ELISA). Configuration of the antibodies used in determining the level of A β x-40 and A β x-42 utilizes a common detect antibody (4G8) in combination with specific C-terminal antibodies for the 40 and 42 cleavage sites. For the A β x-40 assay, a 384-well black Nunc Maxisorp plate was coated with 15 μL /well (4 $\mu\text{g}/\text{mL}$) capture antibody (Rinat 1219) in 0.1 M sodium bicarbonate coating buffer, pH 8.2. For the A β x-42 assay, 15 μL /well (8 $\mu\text{g}/\text{mL}$) capture antibody (Rinat 10G3) was used. The plates were sealed and incubated at 4 $^\circ\text{C}$ overnight. Plates were washed with phosphate-buffered saline containing 0.05% Tween-20 (PBS-T) and blocked with 75 μL of blocking buffer (1% BSA in PBS-T) for 2 h at 25 $^\circ\text{C}$.

After the plates had been washed with PBS-T, rodent A β x-40 (California Peptide) or A β x-42 (California Peptide) standard was serially diluted in blocking buffer and 15 μL was applied to the plate in quadruplicate. Dried brain samples were reconstituted in 120 μL of blocking buffer, which corresponds to a 4.16–6.67-fold concentration. Then 15 μL of undiluted brain sample was added to the A β x-42 assay plate in triplicate, or 15 μL of a 1:2 diluted brain sample was added to the A β x-40 assay plate in triplicate. Dried plasma samples were reconstituted in 40 μL of blocking buffer, which corresponds to a 3.5–4.38-fold concentration, and 15 μL was added to the A β x-40 assay plate in duplicate. CSF samples were diluted 1:8 in blocking buffer, and 15 μL was added to the A β x-40 assay plate in duplicate. Plates were incubated with sample or standards for 2 h at 25 $^\circ\text{C}$. The plates were washed with PBS-T and 15 μL of detect antibody (4G8-Biotin, Covance), 200 ng/mL in blocking buffer, was added to each well, and incubation was carried out for 2 h at 25 $^\circ\text{C}$. The plates were then washed with PBS-T, and 15 μL of europium-labeled streptavidin (PerkinElmer), 50 ng/mL in blocking buffer, was added for a 1 h incubation in the dark at 25 $^\circ\text{C}$. The plates were washed with PBS-T, and 15 μL of PerkinElmer Enhancement solution was added to each well with 20 min incubation at RT. Plates were read on an EnVision plate reader using DELFLIA time-resolved fluorimetry (Exc340/Em615), and samples were extrapolated against a standard curve using four-parameter logistics.

Neuropharmacokinetic Studies in Male CD-1 Mice. The *in-life* and bioanalytical portions of these studies were conducted at BioDuro, Pharmaceutical Product Development Inc. (Beijing, China). Male CD-1 mice were obtained from PUMC, China. Mice received a 10 mg/kg subcutaneous (sc) dose of compounds **5**, **10**, **12**, or **13**. The doses were prepared in 5% DMSO/95% (0.5% methylcellulose) and delivered in a volume of 5 mL/kg. Animals were sacrificed in a CO_2

chamber. Blood, brain, and CSF samples were collected at 1, 4, and 7 h postdosing. Plasma was isolated after centrifugation. The plasma, brain, and CSF samples were stored at $-80\text{ }^{\circ}\text{C}$ prior to analysis.

General Multipoint Cocktail DDI IC_{50} Assay Conditions. Standard marker activity substrates were incubated with pooled human liver microsomes (HL-MIX-102) in the presence of NADPH (1.2 mM) in 100 mM KH_2PO_4 , pH 7.4, containing 3.3 mM MgCl_2 at $37\text{ }^{\circ}\text{C}$. The incubation volume was 0.1 mL, utilizing a 384-well plate format. The same microsomal protein concentration (0.1 mg/mL) and P450 concentration (0.035 μM) were used for each probe substrate at the following concentrations: tacrine (1A2) 2 μM , diclofenac (2C9) 5 μM , dextromethorphan (2D6) 5 μM , midazolam (3A4) 2 μM , taxol (2C8) 5 μM , and S-mephenytoin (2C19) 40 μM . Substrate concentrations are near K_m values that had been previously determined, and incubation times were selected based on determinations of reaction velocity linearity. Each test compound/prototypical inhibitor was tested at a concentration range of 0–30 mM in triplicate, in final vehicle solvent concentrations of 0.9% acetonitrile and 0.1% DMSO. Incubations were initiated with the addition of NADPH. At the end of the incubation period, termination solvent containing internal standard was added and the terminated incubation mixture was centrifuged to precipitate microsomal protein. Samples were directly injected on an HPLC/MS/MS system. A Biomek FX workstation was used for liquid handling and sample incubation.

General Recombinant Human CYP(rCYP) Conditions. Reaction mixtures containing phosphate buffer (100 mM, pH 7.4), magnesium chloride (3 mM), recombinant human CYPs (100 pmol/mL), and probe substrates (1 μM) were prepared. Reactions were initiated by the addition of NADPH (2 mM) and terminated by addition of 4 volumes of acetonitrile at predetermined time points (0, 3, 5, 10, 20, 30, and 60 min). After quenching and centrifugation at 1200g for 10 min, the supernatant was transferred to injection plates, mixed with 2 volumes of water, and analyzed by LC-MS. The LC/MS system consisted of two Jasco pumps, an ADDA dual arms autosampler (Apricot Designs), two 1.5 mm \times 5 mm polymethacrylate columns (11–03455-DB; Optimize Technologies), and a Sciex QTRAP 5500 mass spectrometer equipped with an electrospray ionization source (AB Sciex). A trap and elute gradient consisting of mobile phase A (5% methanol/5% acetonitrile/90% 2 mM ammonium acetate) and B (47.5% methanol/47.5% acetonitrile/5% 2 mM ammonium acetate) was used at a flow rate of 1.3 mL/min. The column was eluted at 0% B for 16 s to desalt and equilibrate the column, followed by a gradient of 0% to 100% B for 16 s to elute the analytes. The dual arm autosampler stacked 22 injections into a 6 min run. The injection volume was 20 μL /injection. For data analysis, peak area ratios were calculated using AB Sciex analyst software to calculate the half-life of parent depletion, in vitro Cl_{inv} and % rCYP contributions for 1A2, 2C8, 2C9, 2C19, 2D6, and 3A4.

Measurement of Fraction Unbound in Brain. The unbound fraction of each compound was determined in brain tissue homogenate using a 96-well equilibrium dialysis method as described by Kalvass et al.,³⁵ with the following exceptions. Brain homogenates were prepared from freshly harvested rat brains following dilution with a 4-fold volume of phosphate buffer and spiked with 1 μM compound. The homogenates were dialyzed against an equal volume (150 μL) of phosphate buffer at $37\text{ }^{\circ}\text{C}$ for 6 h. Following the incubation, equal volumes (50 μL) of brain homogenate and buffer samples were collected and mixed with 50 μL of buffer or control homogenate, respectively, for preparation of mixed matrix samples. All samples were then precipitated with internal standard in acetonitrile (200 μL), vortexed, and centrifuged. Supernatants were analyzed using an LC-MS/MS assay. A dilution factor of 5 was applied to the calculation of brain fraction unbound.

Generic Liquid Chromatography Tandem Mass Spectrometry (LC-MS/MS) Assay for Exposure Measurements in Plasma, Brain, and CSF. Plasma, brain, and CSF were collected as described above and frozen at $-80\text{ }^{\circ}\text{C}$ until analysis by LC-MS/MS. Standard curves were prepared in respective matrix via serial dilution at a concentration of 1.0–2000 ng/mL (plasma and CSF) or 0.5–2000 ng/g (brain). For plasma, a 50 μL aliquot of sample was precipitated with 500 μL of

MTBE containing an internal standard. Samples were vortexed for 1 min then centrifuged at 3000 rpm for 10 min. The supernatant was transferred to a 96-well plate. Frozen brain tissue was weighed, and an 2-propanol:water (60:40) volume equivalent to 4 times the mass was added before homogenization in a bead beater (BioSpec Products Inc., Bartlesville, OK). A 50 μL aliquot of sample was precipitated with 500 μL of MTBE containing an internal standard. Samples were vortexed for 1 min then centrifuged at 3000 rpm for 10 min. The supernatant was transferred to a 96-well plate. For CSF, a 50 μL aliquot of sample was precipitated with 500 μL of MTBE containing an internal standard. Samples were vortexed for 1 min then centrifuged at 3000 rpm for 10 min. The supernatant (300 μL) was transferred to a 96-well plate. LC-MS/MS analysis was carried out using a high-performance liquid chromatography system consisting of tertiary Shimadzu LC20AD pumps (Shimadzu Scientific Instruments, Columbia, MD) with a CTC PAL autosampler (Leap Technologies, Carrboro, NC) interfaced to an API 4000 LC-MS/MS quadrupole tandem mass spectrometer (AB Sciex Inc., Ontario, Canada). The mobile phase consisted of solvent A (water with 0.1% formic acid) and solvent B (acetonitrile with 0.1% formic acid). The gradient was as follows: solvent B was held at 5% for 0.4 min, linearly ramped from 5% to 95% in 0.5 min, held at 90% for 0.6 min, and then stepped to 5% over 0.01 min. The mass spectrometer was operated using positive electrospray ionization. All raw data was processed using Analyst Software version 1.4.2 (AB Sciex Inc., Ontario, Canada).

hERG Patch Clamp Assay. All testing was carried out in CHO cells transfected with the hERG gene, purchased from Millipore (PrecisION hERG-CHO Recombinant Cell Line CYL3038). The cell line was grown in DMEM/F-12, GlutaMAX with 10% fetal bovine serum, 1% penicillin–streptomycin, 1% geneticin, and 1% of 1 M HEPES buffer solution and maintained at approximately $37\text{ }^{\circ}\text{C}$ in a humidified atmosphere containing 5% carbon dioxide. The cells were passaged every 3–5 days based on confluency. On the day of the experiment, 50%–80% confluent cells were harvested from a 175 cm^2 culture flask using Detachin. After 10 min of exposure to Detachin at $37\text{ }^{\circ}\text{C}$, the cells were centrifuged for 1 min at 1000 rpm. The supernatant was removed, and the cell pellet was reconstituted in 5–8 mL of serum-free media with 2.5% of 1 M HEPES, placed on the Qstirrer, and allowed to recover. After a \sim 30 min recovery period, experiments were initiated.

hERG Potassium Channel Current Recordings. hERG current was elicited and recorded using the automated Qpatch HT system.³⁴ The suspended cells in the Qstirrer were transferred to 48 individual recording chambers on a Qplate 48 containing extracellular recording saline composed of (in mM) 132 NaCl, 4 KCl, 1.8 CaCl_2 , 1.2 MgCl_2 , 10 HEPES, and 11.1 glucose and adjusted to pH 7.35 ± 0.1 with NaOH. The intracellular recording saline was composed of (in mM) 70 KF, 60 KCl, 15 NaCl, 5 EGTA, and 5 HEPES and adjusted to pH 7.2 ± 0.1 with KOH. Membrane currents were recorded at room temperature.

hERG current was elicited from a holding potential of -80 mV with a voltage step to $+30\text{ mV}$ for 1 s, followed by a ramp back to -80 mV at 0.55 mV/ms. Test pulses were delivered at a frequency of 0.25 Hz. Up to four different concentrations were studied for each cell, each exposure lasting 5 min or until steady-state effects were observed. In a separate set of experiments, full concentration–response relationships were determined for the positive control, cisapride, and an IC_{50} was reported for this study.

hERG Data Analysis. Using Sophion Qpatch assay software, the amplitude of the peak outward hERG current upon repolarizing ramp was measured. Current amplitude was determined by taking the average of the last five current peaks under each treatment condition. Percent inhibition was determined by taking the ratio of the current measured at steady state in the presence of test article ($I_{\text{test article}}$) versus the control current (I_{control}) and expressed as % inhibition = $100 - (I_{\text{test article}}/I_{\text{control}}) \times 100$. When possible, a concentration–response curve was plotted and the data were fitted using Qpatch software to determine an IC_{50} . The $P < 0.05$ was considered statistically significant. Data were presented as mean \pm SEM.

X-ray Diffraction and Molecular Dynamics Studies. *Crystallization of BACE1.* Crystals of BACE1 were prepared as previously described.³⁵ Briefly, recombinant BACE1 lacking the pro-segment was concentrated to ~14 mg/mL in 20 mM Tris, pH 7.4, and 250 mM NaCl. Crystallization was carried out by the vapor diffusion method, using 2 μ L protein solution and 2 μ L reservoir solution (200 mM sodium citrate tribasic dihydrate, pH 6.6, 22% PEG 5K monomethyl ether, and 200 mM ammonium iodide). Crystals generally grew to $\sim 0.1 \times 0.1 \times 0.05$ mm³ over 2 weeks. The crystal form was determined as P6₂2₂, with a single molecule of BACE1 in the asymmetric unit and diffracted to high resolution ($d_{\text{min}} < 2.0$ Å) with typical X-ray exposure times.

Soaking of BACE Crystals. Soaking solutions were made by diluting the concentrated 30 mM DMSO compound mixtures 1:10 with reservoir solution. Crystals were transferred individually from their mother drops to a 10 μ L drop of soaking solution and allowed to equilibrate at 21 °C for ~3 h. Following this equilibration, crystals were flash-cooled for data collection by harvesting in rayon loops and plunging directly into liquid nitrogen.

Data Collection. X-ray diffraction data were collected at the 17-ID (IMCA) beamline at the APS with a Pilatus 6 M detector. For each crystal, a total of 180° of data were collected in 0.25° oscillations, generally yielding ~100% complete data coverage at 4–5 \times redundancy for accurate scaling and outlier rejection. Data processing was performed using HKL2000.³⁶

Structure Solution. Structures were determined by rigid body refinement using the program REFMAC.³⁷ The initial model was a 1.5 Å crystal structure of apo BACE1 that was solved as part of an ongoing structure-based drug design effort. As we expected, conformational variability in the “flap” region of BACE, residues 68–75 were excised from the model prior to refinement to minimize difficulty in interpretation of the mFo–dFc sigmaA-weighted difference maps. Binding of compounds to the BACE1 active site was assessed by visual inspection of the resulting difference maps using the program COOT.³⁸ Final refinement was done using AUTOBUSTER.³⁹ Refinement statistics are reported in Supporting Information.

Determination of Structures for CYP2D6 Complexed with Compounds 5 and 6. Complexes of 5 and 6 with CYP2D6 were prepared by soaking crystals of CYP2D6. CYP2D6 was crystallized in the presence of thioridazine, using conditions that produce a P2₁2₁2₁ crystal form with four molecules of the thioridazine complex in the asymmetric unit as previously described.⁴⁰ The crystals were soaked in an artificial mother liquor containing 1.5 μ L of protein buffer (20 mM KP_i (pH 7.4), 500 mM NaCl, 20% glycerol, and 0.2 mM Facile-EM), 0.25 μ L of 70 mM HEGA-10, 0.4 μ L of precipitin solution (16% PEG3350, 0.2 M Na acetate, pH 7, 0.1 M Na cacodylate pH 7, 2.25 mM Zn(OAc)₂), and either a 5 mM of 5 or a 1 mM of 6 final concentration (prepared from 10 \times DMSO stock solutions). The structure of the CYP2D6 complex with 5 was determined from a crystal that was soaked for 3 days with seven transfers to fresh mother liquor. The structure of the CYP2D6 complex with 6 was obtained from a crystal soaked for 6 days, with daily transfers to fresh artificial mother liquor. Following addition of 0.5 μ L of glycerol to the mother liquor, crystals were harvested and frozen in liquid nitrogen for remote data collection. Data sets were collected at 100 K on SSRL beamlines 11–1 and 7–1 with a limiting resolution of 2.5 and 2.4 Å, respectively, for the complexes with 5 and 6. The data were indexed and scaled using XDS,⁴¹ and the reflections were merged using Aimless.⁴² The space group and unit cell dimensions were similar to those for the crystals used for determination of the PDB 3TBG structure of the thioridazine complex that is representative of the starting crystals for the soaking experiments.⁴⁰ Rigid body refinement of each chain in the 3TBG structure provided initial phasing information. The structures were adjusted using Coot³⁸ and refined using Phenix.⁴² Data merging and model refinement statistics are shown in Supporting Information.

Chemistry. General Methods. Solvents and reagents were of reagent grade and were used as supplied by the manufacturer. All reactions were run under a N₂ atmosphere. Organic extracts were routinely dried over anhydrous Na₂SO₄. Concentration refers to rotary evaporation under reduced pressure. Chromatography refers to flash

chromatography using disposable RediSepRf 4 to 120 g silica columns or Biotage disposable columns on a CombiFlash Companion or Biotage Horizon automatic purification system. Microwave reactions were carried out in a SmithCreator microwave reactor from Personal Chemistry. Purification by mass-triggered HPLC was carried out using Waters XTerra PrepMS C18 columns, 5 μ m, 30 mm \times 100 mm. Compounds were presalted as TFA salts and diluted with 1 mL of dimethyl sulfoxide. Samples were purified by mass-triggered collection using a mobile phase of 0.1% trifluoroacetic acid in water and acetonitrile, with a gradient of 100% aqueous to 100% acetonitrile over 10 min at a flow rate of 20 mL/min. Elemental analyses were performed by QTI, Whitehouse, NJ. All target compounds were analyzed using ultra high performance liquid chromatography/ultraviolet/evaporative light scattering detection coupled to time-of-flight mass spectrometry (UHPLC/UV/ELSD/TOFMS). LC-MS analyses were performed on a Waters Acquity UPLC-MS system with a Waters Acquity HSS T3, 1.7 μ m C18 column (50 mm \times 2.1 mm). UPLC conditions: mobile phase A = 0.1% formic acid in water (v/v), mobile phase B = 0.1% formic acid in acetonitrile; flow rate = 1.25 mL/min; compounds were eluted with a gradient of 5% B/A to 95% B/A for 1.1 min. Unless otherwise noted, all tested compounds were found to be >95% pure by this method.

UHPLC/MS Analysis. The UHPLC was performed on a Waters Acquity UHPLC system (Waters, Milford, MA), which was equipped with a binary solvent delivery manager, column manager, and sample manager coupled to ELSD and UV detectors (Waters, Milford, MA). Detection was performed on a Waters LCT premier XE mass spectrometer (Waters, Milford, MA). The instrument was fitted with an Acquity Bridged Ethane Hybrid (BEH) C18 column (30 mm \times 2.1 mm, 1.7 μ m particle size, Waters, Milford, MA) operated at 60 °C.

(2R)-1-(Benzyloxy)hex-4-yn-2-ol (22). Prop-1-yne was bubbled through a solution of *n*-butyllithium (2.5 M in hexanes, 1.06 L, 2.65 mol) in toluene (5 L) at 0 °C for 1.5 h until a thin suspension was obtained. Diethylaluminum chloride (1 M in hexanes, 2.44 L, 2.44 mol) was added, and the reaction mixture was stirred at 0 °C for 2 h, whereupon (2R)-2-[(benzyloxy)methyl]oxirane 21 (200 g, 1.22 mol) was added. After 10 min, the reaction was quenched with water (100 mL) and then with aqueous hydrochloric acid (2 M, 2 L). The mixture was extracted with ethyl acetate (2 L), and the combined organic layers were dried over sodium sulfate, concentrated, and purified by chromatography on silica gel (gradient: 2–17% ethyl acetate in petroleum ether) to afford the product 22 as a pale-brown oil. Yield: 250 g, 1.22 mol, 100%. ¹H NMR (400 MHz, CDCl₃) δ 7.28–7.41 (m, 5H), 4.58 (s, 2H), 3.89–3.97 (s, 1H), 3.60 (dd, half of ABX pattern, *J* = 9.5, 3.9 Hz, 1H), 3.50 (dd, half of ABX pattern, *J* = 9.5, 6.7 Hz, 1H), 2.50 (br s, 1H), 2.38–2.43 (m, 2H), 1.79 (t, *J* = 2.6 Hz, 3H).

(2R,4E)-1-(Benzyloxy)hex-4-en-2-ol (23). Lithium aluminum hydride (93 g, 2.4 mol) was gradually added portionwise to a 10–20 °C solution of 22 (167 g, 0.818 mol) in 1,2-dimethoxyethane (2.2 L), and the reaction was heated at 100 °C for 16 h. The reaction mixture was allowed to cool to room temperature and was then quenched with ice followed by aqueous hydrochloric acid (2 M, 2 L) at 10–20 °C. The resulting mixture was extracted with ethyl acetate (2 L), and the combined organic layers were dried over sodium sulfate and concentrated, affording the product as a pale-brown oil. This material was used for the next step without further purification. Yield: 160 g, 0.78 mol, 95%. ¹H NMR (400 MHz, CDCl₃) δ 7.27–7.41 (m, 5H), 5.49–5.60 (m, 1H), 5.39–5.49 (m, 1H), 4.56 (s, 2H), 3.80–3.88 (m, 1H), 3.51 (dd, half of ABX pattern, *J* = 9.5, 3.4 Hz, 1H), 3.39 (dd, half of ABX pattern, *J* = 9.3, 1.9 Hz, 1H), 2.4 (br s, 1H), 2.16–2.24 (m, 2H), 1.66–1.70 (m, 3H).

([(2R,4E)-2-(2,2-Diethoxyethoxy)hex-4-en-1-yl]oxy)methylbenzene (24). To a 0 °C suspension of sodium hydride (60% in mineral oil, 93 g, 2.3 mol) in tetrahydrofuran (1.6 L) was slowly added 23 (160 g, 0.78 mol), and the reaction mixture was stirred at 0 °C for 1 h. 2-Bromo-1,1-diethoxyethane (460 g, 2.33 mol) was added to the cold mixture, which was then heated at reflux for 16 h. The reaction was carefully quenched by addition of water (1 L), and the mixture was extracted with ethyl acetate (2 L). The combined organic layers were dried over sodium sulfate and concentrated to provide the

product as a brown oil, which was used for the next step without purification. ^1H NMR (400 MHz, CDCl_3), characteristic peaks: δ 7.24–7.38 (m, 5H), 5.37–5.54 (m, 2H), 4.54 (s, 2H), 2.19–2.30 (m, 2H), 1.64 (br d, $J = 5.0$ Hz, 3H).

2-[[*(2R,4E)*-1-(benzyloxy)hex-4-en-2-yl]oxy]-*N*-hydroxyethanimine (**31**). To a solution of crude **24** (from the previous step, ≤ 0.78 mol) in tetrahydrofuran (1.5 L) was added aqueous hydrochloric acid (2 M, 850 mL, 1.7 mol) at 25 °C, and the reaction mixture was stirred at 60 °C for 1 h. After it had cooled to room temperature, it was saturated with solid sodium chloride and extracted with ethyl acetate (2 L). The combined organic layers were washed with saturated aqueous sodium chloride solution (3 \times 1 L), dried over sodium sulfate, and concentrated to afford [[*(2R,4E)*-1-(benzyloxy)hex-4-en-2-yl]oxy]acetaldehyde as a pale-brown oil, which was used for the next step without further purification. ^1H NMR (400 MHz, CDCl_3), characteristic peaks: δ 9.72 (br s, <1H), 7.27–7.40 (m, 5H), 5.4–5.57 (m, 2H), 1.66 (br d, $J = 5$ Hz, 3H).

To a solution of crude [[*(2R,4E)*-1-(benzyloxy)hex-4-en-2-yl]oxy]acetaldehyde (from the previous step, ≤ 0.78 mol) in a mixture of ethanol and water (2:1, 2.1 L) was added sodium acetate (472 g, 5.75 mol), followed by hydroxylamine hydrochloride (238 g, 3.42 mol). The reaction mixture was stirred at 60 °C for 16 h then concentrated to remove ethanol and extracted with dichloromethane (2 L). The combined organic layers were washed sequentially with saturated aqueous sodium carbonate solution (2 \times 1 L) and saturated aqueous sodium chloride solution (1 L), dried over sodium sulfate, and concentrated. Silica gel chromatography (gradient: 2–17% ethyl acetate in petroleum ether) provided the product as a pale-yellow oil. Yield: 105 g, 0.399 mol, 51% over three steps. LCMS m/z 264 [M + H] $^+$. ^1H NMR (400 MHz, CDCl_3) δ [7.51 (t, $J = 5.66$ Hz) and 6.96 (t, $J = 3.51$ Hz), total 1H (oxime)], 7.28–7.38 (m, 5H), 5.45–5.57 (m, 1H), 5.34–5.44 (m, 1H), 4.55 (d, $J = 3.9$ Hz, 2H), 4.48 (d, $J = 3.5$ Hz, 1H), 4.22 (t, $J = 5.7$ Hz, 1H), 3.45–3.60 (m, 3H), 2.22–2.29 (m, 2H), 1.66 (td, $J = 0.9, 6.2$ Hz, 3H).

(*3S,3aR,5R*)-5-[(benzyloxy)methyl]-3-methyl-3,3a,4,5-tetrahydro-7H-pyrano[3,4-*c*][1,2]oxazole (**32**). Aqueous sodium hypochlorite (6.15%, 1 L) was slowly added to a mixture of **31** (100 g, 0.38 mol) and triethylamine (2.9 g, 28.6 mmol) in dichloromethane (2 L). The reaction mixture was stirred at 25 °C for 1 h then washed with water (5 \times 2 L), dried over sodium sulfate, and concentrated. Silica gel chromatography (gradient: 2–17% ethyl acetate in petroleum ether) afforded the product as a white solid. Yield: 58 g, 0.22 mol, 58%. Additional purification could be carried out via recrystallization. To a solution of **32** (174 g) at reflux in *t*-butyl methyl ether (135 mL) was added heptane (430 mL) until a thin cloudy mixture was obtained. This was allowed to slowly cool to 25 °C and then kept motionless for 16 h. The resulting precipitate was collected via filtration and washed with heptane (100 mL) to provide a white solid (142 g); this was recrystallized again in the same manner to afford the product as a white solid. Yield: 102 g, 59%. LCMS m/z 262.2 [M + H] $^+$. ^1H NMR (400 MHz, CDCl_3) δ 7.26–7.39 (m, 5H), 4.70 (d, $J = 13.7$ Hz, 1H), 4.58 (AB quartet, $J_{AB} = 12.1$ Hz, $\Delta\nu_{AB} = 13.2$ Hz, 2H), 4.14–4.25 (m, 2H), 3.63–3.71 (m, 1H), 3.56 (dd, half of ABX pattern, $J = 10.2, 5.9$ Hz, 1H), 3.48 (dd, half of ABX pattern, $J = 10.1, 4.3$ Hz, 1H), 2.93 (ddd, $J = 11.3, 11.2, 6.7$ Hz, 1H), 2.12 (ddd, $J = 12.8, 6.6, 1.2$ Hz, 1H), 1.46 (d, $J = 6.2$ Hz, 3H), 1.45–1.57 (m, 1H).

(*3S,3aR,5R,7aS*)-5-[(benzyloxy)methyl]-7a-(2,4-difluorophenyl)-3-methylhexahydro-1H-pyrano[3,4-*c*][1,2]oxazole (**34**). Boron trifluoride diethyl etherate (60.1 mL, 474 mmol) was added to a solution of **32** (31.0 g, 119 mmol) in a 1:1 mixture of toluene and diisopropyl ether (1 L) at an internal temperature of –76 °C. The reaction was stirred at this temperature for 30 min then treated with 2,4-difluoro-1-iodobenzene (15.9 mL, 133 mmol). While the reaction temperature was maintained at –76 to –71 °C, *n*-butyllithium (2.5 M in hexanes, 50.4 mL, 126 mmol) was slowly added. The reaction mixture was stirred at –76 °C for 1.5 h then quenched with saturated aqueous ammonium chloride solution (1 L) and partitioned between water (1 L) and ethyl acetate (750 mL). After the mixture warmed to room temperature, the aqueous layer was extracted with ethyl acetate (3 \times 250 mL) and the combined organic layers were washed with saturated

aqueous sodium chloride solution (550 mL), dried over sodium sulfate, filtered, and concentrated in vacuo. Silica gel chromatography (gradient: 0–70% ethyl acetate in heptane) gave the product as a yellow oil. Yield: 21.5 g, 57.2 mmol, 48%. LCMS m/z 376.2 [M + H] $^+$. ^1H NMR (400 MHz, CDCl_3) δ 7.98 (ddd, $J = 9.1, 9.1, 6.8$ Hz, 1H), 7.28–7.40 (m, 5H), 6.87–6.93 (m, 1H), 6.80 (ddd, $J = 11.9, 8.6, 2.6$ Hz, 1H), 4.60 (AB quartet, $J_{AB} = 12.1$ Hz, $\Delta\nu_{AB} = 19.9$ Hz, 2H), 3.99–4.06 (m, 1H), 3.97 (dd, half of ABX pattern, $J = 12.9, 2.0$ Hz, 1H), 3.80–3.88 (m, 2H), 3.56 (dd, half of ABX pattern, $J = 10.2, 6.3$ Hz, 1H), 3.49 (dd, half of ABX pattern, $J = 10.2, 4.1$ Hz, 1H), 2.81–2.87 (m, 1H), 2.04 (ddd, $J = 14.2, 7.6, 2.8$ Hz, 1H), 1.48–1.59 (m, 1H), 0.79 (d, $J = 6.4$ Hz, 3H).

(*1S*)-1-[[*(2R,4R,5S)*-5-Amino-2-[(benzyloxy)methyl]-5-(2,4-difluorophenyl)tetrahydro-2H-pyran-4-yl]ethanol (**36**). Compound **34** (14.2 g, 37.8 mmol) was dissolved in acetic acid (126 mL) and treated with zinc powder (32.1 g, 491 mmol). The reaction mixture, which had warmed to 40 °C, was allowed to cool to room temperature and stir for 16 h. Insoluble material was removed via filtration through a pad of diatomaceous earth, and the pad was washed with ethyl acetate (3 \times 500 mL). The combined filtrates were neutralized with saturated aqueous sodium bicarbonate solution (2.5 L), and the aqueous layer was extracted with ethyl acetate (3 \times 500 mL). The combined organic layers were washed with saturated aqueous sodium chloride solution (1 L), dried over sodium sulfate, filtered, and concentrated in vacuo to provide the product as a thick yellow oil, which was used in the following reaction without additional purification. Yield: 13.96 g, 37.00 mmol, 98%. LCMS m/z 378.2 [M + H] $^+$. ^1H NMR (400 MHz, CDCl_3), characteristic peaks: δ 7.65–7.78 (br m, 1H), 7.27–7.40 (m, 5H), 6.93–7.02 (br m, 1H), 6.80 (ddd, $J = 12.6, 8.5, 2.6$ Hz, 1H), 4.06 (dd, $J = 11.7, 2.2$ Hz, 1H), 3.53 (dd, $J = 10.2, 3.7$ Hz, 1H), 2.50–2.61 (br m, 1H), 1.62 (ddd, $J = 14, 4, 2.5$ Hz, 1H), 0.89 (d, $J = 6.6$ Hz, 3H).

N-[[*(3S,4R,6R)*-6-[(benzyloxy)methyl]-3-(2,4-difluorophenyl)-4-[[*(1S)*-1-hydroxyethyl]tetrahydro-2H-pyran-3-yl]carbamothioyl]benzamide (**40**). Benzoyl isothiocyanate (4.97 mL, 36.8 mmol) was added to a solution of **36** (13.9 g, 36.8 mmol) in dichloromethane (0.37 L), and the reaction mixture was allowed to stir at room temperature for 18 h. After removal of solvent in vacuo, the residue was chromatographed on silica gel (gradient: 0–50% ethyl acetate in heptane) to afford the product as a yellow foam. Yield: 13.36 g, 24.71 mmol, 67%. LCMS m/z 539.2 [M – H] $^+$.

N-[[*(4R,4aR,6R,8aS)*-6-[(benzyloxy)methyl]-8a-(2,4-difluorophenyl)-4-methyl-4,4a,5,6,8,8a-hexahydroprano[3,4-*d*][1,3]thiazin-2-yl]benzamide (**42**). Diethyl azodicarboxylate (21.3 mL, 136 mmol) was added dropwise to a solution of triphenylphosphine (35.7 g, 136 mmol) in tetrahydrofuran (850 mL), and the mixture was stirred for 30 min before being cooled in an ice bath. A solution of *N*-[[*(3S,4R,6R)*-6-[(benzyloxy)methyl]-3-(2,4-difluorophenyl)-4-[[*(1S)*-1-hydroxyethyl]tetrahydro-2H-pyran-3-yl]carbamothioyl]benzamide (**40**) (24.5 g, 45.3 mmol) in tetrahydrofuran (115 mL) was added dropwise to the reaction mixture, which was then stirred for 1 h under ice cooling. After concentration in vacuo, the residue was loaded onto a silica gel column that had been equilibrated with dichloromethane and the column was eluted with 1:1 ethyl acetate/heptane. Fractions containing product were combined and concentrated under reduced pressure; the resulting material was triturated with 15% ethyl acetate in heptane, and the solid was removed via filtration. The filtrate was concentrated in vacuo and chromatographed on silica gel (gradient: 20–40% ethyl acetate in heptane), affording the product as a white solid. Yield: 17.23 g, 32.97 mmol, 73%. LCMS m/z 523.2 [M + H] $^+$. ^1H NMR (400 MHz, CDCl_3) δ 8.23 (br d, $J = 6.5$ Hz, 2H), 7.49–7.55 (m, 1H), 7.36–7.48 (m, 3H), 7.24–7.36 (m, 5H), 6.84–6.96 (m, 2H), 4.58 (AB quartet, $J_{AB} = 12.0$ Hz, $\Delta\nu_{AB} = 25.0$ Hz, 2H), 4.18 (dd, $J = 12.2, 1.7$ Hz, 1H), 3.87–3.94 (m, 1H), 3.84 (d, $J = 12.2$ Hz, 1H), 3.63 (dd, half of ABX pattern, $J = 10.2, 6.4$ Hz, 1H), 3.50 (dd, half of ABX pattern, $J = 10.2, 4.4$ Hz, 1H), 3.23–3.31 (m, 1H), 2.88–2.96 (m, 1H), 1.61–1.79 (m, 2H), 1.25 (d, $J = 6.9$ Hz, 3H).

N-[[*(4R,4aR,6R,8aS)*-8a-(2,4-Difluorophenyl)-6-(hydroxymethyl)-4-methyl-4,4a,5,6,8,8a-hexahydroprano[3,4-*d*][1,3]thiazin-2-yl]benzamide (**38**). Boron trichloride (1 M solution in heptane, 176 mL,

176 mmol) was added to a 0 °C solution of **42** (35.4 g, 67.7 mmol) in dichloromethane (300 mL). After 15 min, the reaction mixture was allowed to warm to room temperature and stirred for 4 h. Methanol (100 mL) was then added, first dropwise {Caution: violent reaction} and then at a steady rate, while the interior of the flask was flushed with nitrogen gas. The mixture was heated at reflux for 30 min, cooled to room temperature, and concentrated in vacuo. The residue was again dissolved in methanol, stirred, and concentrated in vacuo. The resulting material was taken up in dichloromethane and washed sequentially with 1 M aqueous sodium hydroxide solution, water, and saturated aqueous sodium chloride solution. The organic layer was dried over magnesium sulfate, filtered, and concentrated under reduced pressure. The crude product was triturated with dichloromethane rather than being purified by chromatography. The filtrate from the trituration was concentrated in vacuo, and a second crop of material was obtained via a second trituration with dichloromethane, affording the product in both cases as a white solid. Total yield: 23.12 g, 53.46 mmol, 79%. LCMS m/z 433.2 [M + H]⁺. ¹H NMR (400 MHz, CD₃OD) δ 8.12 (br d, J = 7 Hz, 2H), 7.51–7.57 (m, 1H), 7.40–7.49 (m, 3H), 7.02–7.11 (m, 2H), 4.15 (br d, J = 12 Hz, 1H), 3.91 (d, J = 11.9 Hz, 1H), 3.71–3.78 (m, 1H), 3.60 (d, J = 5.2 Hz, 2H), 3.19–3.28 (br m, 1H), 2.97–3.06 (br m, 1H), 1.74–1.82 (m, 1H), 1.49–1.62 (m, 1H), 1.26 (d, J = 7.0 Hz, 3H).

(4*R*,4*aR*,6*R*,8*aS*)-8*a*-(2,4-difluorophenyl)-6-(methoxymethyl)-4-methyl-4,4*a*,5,6,8*a*-hexahydropyrano[3,4-*d*][1,3]thiazin-2-amine (**8**). To a solution of *N*-((4*R*,4*aR*,6*R*,8*aS*)-8*a*-(2,4-difluorophenyl)-6-(hydroxymethyl)-4-methyl-4,4*a*,5,6,8*a*-hexahydropyrano[3,4-*d*][1,3]-thiazin-2-yl)benzamide **38** (65 mg, 0.15 mmol) stirring in tetrahydrofuran (2 mL) at rt under N₂ was added NaH (18 mg, 0.450 mmol 60% in mineral oil). The reaction mixture was stirred at ambient temperature for 30 min (fizzing ceased; reaction became light suspension) before adding methyl iodide (21.3 mg, 0.150 mmol in 400 μ L of THF) at rt. Following stirring at rt, the mixture was heated to 45 °C for 45 min, during which time the reaction mixture became a cloudy solution. The mixture was cooled to rt then quenched with saturated aqueous ammonium chloride (2 mL) and extracted with ethyl acetate (2 \times 5 mL). The combined organic layers were dried over Na₂SO₄, filtered, and then concentrated in vacuo to give the crude product (33 mg white foam). The residue was loaded onto a 4g CombiFlash silica gel column that had been equilibrated with heptanes, and the column was eluted with a gradient of 0–100% ethyl acetate in heptanes. Fractions containing product were combined and concentrated under reduced pressure, affording *N*-((4*R*,4*aR*,6*R*,8*aS*)-8*a*-(2,4-difluorophenyl)-6-(methoxymethyl)-4-methyl-4,4*a*,5,6,8*a*-hexahydropyrano[3,4-*d*][1,3]thiazin-2-yl)benzamide as a white solid. Yield: 46 mg, 0.103 mmol, 69%. LCMS consistent with desired ether LCMS m/z 447.1 [M + H]⁺. The material was used directly in the next step.

DBU (10 mL) was added to *N*-((4*R*,4*aR*,6*R*,8*aS*)-8*a*-(2,4-difluorophenyl)-6-(methoxymethyl)-4-methyl-4,4*a*,5,6,8*a*-hexahydropyrano[3,4-*d*][1,3]thiazin-2-yl)benzamide dissolved in methanol (1 mL), and the resulting solution was heated at 55 °C overnight. The resulting mixture was concentrated in vacuo, taken up in ethyl acetate (5 mL), and washed with saturated aqueous bicarbonate (2 mL). The aqueous layer was further extracted with ethyl acetate (2 \times 5 mL). The combined organic extracts were dried over sodium sulfate, filtered, and concentrated to afford the crude product which was chromatographed on a 4g RediSep Gold column (gradient: 0–15% methanol in dichloromethane). Fractions containing product were concentrated in vacuo to afford (4*R*,4*aR*,6*R*,8*aS*)-8*a*-(2,4-difluorophenyl)-6-(methoxymethyl)-4-methyl-4,4*a*,5,6,8*a*-hexahydropyrano[3,4-*d*][1,3]thiazin-2-amine **8** as a white solid. Yield: 30 mg, 0.089 mmol, 87%. Product confirmed by ¹H NMR, HSQC shows that the methyl singlet correlates to a carbon at 58.1 ppm, which is consistent with the desired *O*-alkylation product (vs *N*-methylation) from the previous step. This spectra can be found in the Supporting Information section. LCMS m/z 343.1 [M + H]⁺. ¹H NMR (400 MHz, CD₃OD) δ 7.32 (dt, J = 6.6, 9.2 Hz, 1H), 6.92–7.00 (m, 2H), 4.10 (dd, J = 2.2, 11.1 Hz, 1H), 3.75–3.82 (m, 1H), 3.73 (d, J = 11.3 Hz, 1H), 3.39–3.50 (m, 2H), 3.38 (s, 3H), 3.09 (dq, J = 3.3, 6.9 Hz,

1H), 2.75 (td, J = 3.8, 11.9 Hz, 1H), 1.56–1.62 (m, 1H), 1.36–1.47 (m, 1H), 1.17 (d, J = 7.0 Hz, 3H); [α]_D²² = +24.00 (c = 0.05g/100 mL; MeOH).

(2*R*)-1-(Benzyloxy)-6-((tetrahydro-2*H*-pyran-2-yl)oxy)hex-4-yn-2-ol (**25**). A solution of 2.5 M *n*-BuLi in hexane (52 mL, 130 mmol) was added to a –78 °C solution of 2-(prop-2-yn-1-yloxy)tetrahydro-2*H*-pyran (18.2 g, 130 mmol) in anhydrous THF (200 mL) dropwise. The reaction was stirred for 30 min before the addition of BF₃·OEt₂ (15.4 mL, 125 mmol) and (R)-2-((benzyloxy)methyl)oxirane **21** (16.4 g, 100 mmol) in THF (50 mL), and the reaction was then stirred for 15 min before quenching with saturated aqueous NaHCO₃ solution (150 mL) and saturated aqueous NH₄Cl solution (150 mL). The reaction was then warmed to room temperature. The reaction was extracted with ether (3 \times 300 mL), and the combined organic layers were washed with water (200 mL) and brine (200 mL), dried over sodium sulfate, concentrated, and purified by chromatography on silica gel (gradient: 0–50% ethyl acetate in heptane) to afford the product as a colorless oil. Yield: 24.5 g, 100 mmol, 87%. LCMS m/z 305.3 [M + H]⁺. ¹H NMR (400 MHz, CDCl₃) δ 7.31–7.46 (m, 5H), 4.82 (t, J = 3.5 Hz, 1H), 4.60 (s, 2H), 4.16–4.38 (m, 2H), 4.00 (dq, J = 3.9, 6.4 Hz, 1H), 3.87 (ddd, J = 2.9, 8.7, 11.4 Hz, 1H), 3.64 (dd, J = 3.9, 9.8 Hz, 1H), 3.48–3.59 (m, 2H), 2.53 (qd, J = 1.9, 6.2 Hz, 2H), 1.71–1.93 (m, 2H), 1.50–1.71 (m, 5H).

2-(((R)-6-(Benzyloxy)-5-(2,2-diethoxyethoxy)hex-2-yn-1-yl)oxy)-tetrahydro-2*H*-pyran (**26**). NaH (60% in mineral oil, 1.39 g, 34.8 mmol) was added to a solution of **25** (5.89 g, 48 mmol) in THF (19 mL) at 0 °C under nitrogen atmosphere in several portions. The reaction was stirred at rt for 30 min then cooled to 0 °C. 1,1-Diethoxy-2-iodoethane (7.32 g, 30 mmol) was then added dropwise, and the reaction was stirred at 55 °C for 18 h. The reaction was cooled to 0 °C and quenched with saturated aqueous NH₄Cl solution (50 mL) and with ether (3 \times 50 mL), and the combined organic layers were washed with brine (50 mL), dried over sodium sulfate, concentrated, and purified by chromatography on silica gel (gradient: 0–45% ethyl acetate in heptane) to afford the product as a colorless oil. Yield: 7.03 g, 19.4 mmol, 86%. ¹H NMR (400 MHz, CDCl₃) δ 7.30–7.44 (m, 5H), 4.53–4.69 (m, 3H), 4.16–4.36 (m, 2H), 3.44–3.93 (m, 12H), 2.56 (qd, J = 2.0, 6.2 Hz, 2H), 1.69–1.91 (m, 2H), 1.47–1.70 (m, 4H), 1.15–1.30 (m, 6H).

(R)-6-(Benzyloxy)-5-(2,2-diethoxyethoxy)hex-2-yn-1-ol (**27**). Benzenesulfonic acid (554 mg, 3.5 mmol) was added to a solution of **26** (13.4 g, 31.86 mmol) in ethanol (75 mL). The reaction was stirred under a nitrogen atmosphere for 5 h. The reaction was then poured into a solution of NaHCO₃ (1.61 g, 19.1 mmol) in water (75 mL). The organic layer was separated and extracted with ether (6 \times 50 mL), and the combined organic layers were washed with brine (50 mL), dried over sodium sulfate, filtered, and concentrated to yield crude product, which was carried on without further purification. Yield: 11.0 g, 32 mmol, quantitative. ¹H NMR (400 MHz, CDCl₃) δ 7.31–7.42 (m, 5H), 4.55–4.71 (m, 3H), 4.23 (t, J = 2.2 Hz, 2H), 3.48–3.78 (m, 9H), 2.55 (tdd, J = 2.3, 4.3, 6.2 Hz, 2H), 1.16–1.32 (m, 6H).

(R,E)-6-(Benzyloxy)-5-(2,2-diethoxyethoxy)hex-2-en-1-ol (**28**). A solution of 1 M lithium aluminum hydride in THF (55.3 mL, 55.33 mmol) was added dropwise to a 4 °C solution of **27** (11.0 g 32.7 mmol) in ethanol (75 mL) under a nitrogen atmosphere. The reaction was warmed to rt and stirred for 1.5 h. The reaction was cooled to 0 °C and quenched with a 5% solution of NaOH. Ether (75 mL) was added, and the reaction was stirred at rt for 15 min then filtered. The filter was washed with ether (150 mL), and the combined ether layers were dried over magnesium sulfate, filtered, concentrated, and purified by chromatography on silica gel (gradient: 0–100% ethyl acetate in heptane) to afford the product as a colorless oil. Yield: 8.17 g, 24.1 mmol, 73%. ¹H NMR (400 MHz, C₆D₆) δ 7.29 (d, J = 7.4 Hz, 2H), 7.13–7.22 (m, 2H), 7.05–7.13 (m, 1H), 5.62–5.74 (m, 1H), 5.50–5.60 (m, 1H), 4.69 (t, J = 5.1 Hz, 1H), 4.34 (s, 2H), 3.87 (t, J = 5.3 Hz, 2H), 3.75–3.82 (m, 1H), 3.65–3.71 (m, 1H), 3.50–3.65 (m, 3H), 3.32–3.48 (m, 4H), 2.23–2.32 (m, 2H), 1.08–1.18 (m, 6H).

2-(((1-(Benzyloxy)-6-hydroxyhex-4-en-2-yl)oxy)acetaldehyde Oxime (**29**). Hydroxylamine hydrochloride (2.4 g, 34.54 mmol) was added to a solution of **28** (8.1 g, 23.9 mmol) in ethanol (50 mL) and

water (10 mL). The reaction was equipped with a condenser, under nitrogen, and heated to 70 °C for 1.5 h. The reaction was cooled to rt, and then sodium acetate (4.0 g, 48.8 mmol) and water (9 mL) were added and the reaction stirred for 10 min. The reaction was concentrated and taken back up in water (75 mL) and DCM (150 mL). The aqueous layer was extracted with DCM (2 × 75 mL), and the combined organic layers were washed with saturated aqueous NaHCO₃ solution (75 mL), brine (75 mL), dried over sodium sulfate, filtered, and concentrated with no further purification. Yield: 6.54 g, 23.4 mmol, 97%. LCMS *m/z* 302 [M + Na]⁺. ¹H NMR (400 MHz, CDCl₃) δ 7.31–7.42 (m, 5H), 5.68–5.78 (m, 2H), 4.55–4.62 (m, 2H), 4.47–4.53 (m, *J* = 3.0 Hz, 1H), 4.24–4.32 (m, 1H), 4.17–4.25 (m, 1H), 4.09–4.17 (m, *J* = 4.3 Hz, 2H), 3.55–3.68 (m, *J* = 5.9, 10.9, 10.9 Hz, 1H), 3.49–3.55 (m, 2H), 2.27–2.41 (m, 2H).

(3*R*,3*aR*,5*R*)-5-((Benzyloxy)methyl)-3,3*a*,4,5-tetrahydro-7*H*-pyrano[3,4-*c*]isoxazol-3-yl)methanol (30). A lab grade NaOCl solution (Fisher Scientific, 5.65–6% NaOCl in water, 30 mL) was added dropwise to a solution of **29** (6.52 g, 23.3 mmol) in DCM (110 mL). The reaction was stirred for 10 min then diluted with water (90 mL) and extracted with DCM (2 ×, 150 mL). The combined DCM layers were washed with brine (2 ×, 100 mL), dried over sodium sulfate, filtered, concentrated, and purified by chromatography on silica gel (gradient: 0–100% ethyl acetate in heptane) to afford the product as a colorless oil. Yield: 5.08 g, 18.3 mmol, 78%. LCMS *m/z* 278 [M + H]⁺. ¹H NMR (400 MHz, CDCl₃) δ 7.30–7.44 (m, 5H), 4.73 (d, *J* = 13.7 Hz, 1H), 4.56–4.66 (m, 2H), 4.19–4.34 (m, 2H), 4.02 (dd, *J* = 2.9, 12.3 Hz, 1H), 3.69–3.80 (m, 2H), 3.55–3.63 (m, 1H), 3.49–3.55 (m, 1H), 3.39–3.49 (m, *J* = 6.6, 11.1, 11.1 Hz, 1H), 2.17 (ddd, *J* = 1.6, 6.6, 12.9 Hz, 1H), 1.57–1.72 (m, 1H).

(3*R*,3*aR*,5*R*)-5-((Benzyloxy)methyl)-3-(fluoromethyl)-3,3*a*,4,5-tetrahydro-7*H*-pyrano[3,4-*c*]1,2-oxazole (33). This reaction was carried out in 10 separate batches. To a –70 °C solution of **30** (5.0 g, 18 mmol) in dichloromethane (150 mL) was added (diethylamino)sulfur trifluoride (11.6 g, 72.0 mmol); the reaction mixture was stirred at –70 °C for 2 h then warmed to room temperature and stirred for 1 h. The reaction was quenched by addition of saturated aqueous sodium bicarbonate solution (500 mL), and the aqueous layer was extracted with dichloromethane (2 × 300 mL). The combined organic layers were dried over sodium sulfate, filtered, and concentrated. Silica gel chromatography (eluent: 5:1 petroleum ether/ethyl acetate) provided the product as a yellow oil. Combined yield: 12.6 g, 45.1 mmol, 25%. LCMS *m/z* 280.1 [M + H]⁺. ¹H NMR (400 MHz, CDCl₃) δ 7.28–7.41 (m, 5H), 4.51–4.76 (m, 5H), 4.30–4.42 (m, 1H), 4.22 (dd, *J* = 13.4, 1.1 Hz, 1H), 3.69–3.77 (m, 1H), 3.58 (dd, half of ABX pattern, *J* = 10.0, 5.8 Hz, 1H), 3.50 (dd, half of ABX pattern, *J* = 10.2, 4.4 Hz, 1H), 3.32–3.42 (m, 1H), 2.19 (br dd, *J* = 13, 7 Hz, 1H), 1.60–1.71 (m, 1H).

(3*R*,3*aR*,5*R*)-5-((Benzyloxy)methyl)-3-(fluoromethyl)-3,3*a*,4,5-tetrahydro-7*H*-pyrano[3,4-*c*]1,2-oxazole (33). This reaction was carried out on the Vaportec R4 continuous flow reactor. The system solvent was CH₃CN. Reagents were injected using the instrument's two reagent ports (ambient aspiration, 1/16 in. PFA tubing) for pump A (color coded orange) and pump B (color coded purple). The system pressure was maintained by a back pressure regulator (BPR, 100 psi rating), generating an average pressure of 6.7–7.8 bar. A length of 1/8 in. PFA reactor tubing was used with a total volume of 150 mL. The reactor tubing was submerged into a rotary evaporator oil bath and kept below the surface with weights. The temperature was maintained between 103.5 and 106 °C (external probe). The two pumps outputs were connected with a simple T joint. Each pump was run at 5.25 mL/min, for a combined pump rate of 10.5 mL/min. The anticipated residence time was approximately 14.3 min.

Stock Solution A. A 570 mL stock solution of ((3*R*,5*R*)-5-((benzyloxy)methyl)-3,3*a*,4,5-tetrahydro-7*H*-pyrano[3,4-*c*]isoxazol-3-yl)methanol **30** was prepared by solubilizing the alcohol (78.93g, 0.285 mol) with 80 mL of TEA (58 g, 0.573 mol), made up to a total volume of 570 mL (0.5 M in alcohol, and 1.0 M in TEA.)

Stock Solution B. Preparation of 700 mL (23% excess relative to stock A) of a stock solution of 0.875 M XtalFluor-E and 0.993 M TEA-3HF in CH₃CN (XtalFluor-E:140.1 g (611 mmol); TEA-3HF, 112 g

(695 mmol) per 700 mL). The addition of XtalFluor-E is endothermic, so the XtalFluor was added to 450 mL of CH₃CN first. The temperature of the solution was monitored, and when it stabilized at 21 °C, the solution was treated with TEA-3HF in 250 mL of CH₃CN. During the addition TEA-3HF in CH₃CN to the XtalFluor solution, there was no noted temperature rise. The reaction temperature was monitored due to the determination that the stock solution of XtalFluor-e and TEA-3HF is a high energy mixture with a low temperature of onset. Both solutions were simultaneously introduced through the reagent ports (port A and port B) on the instrument (substrate alcohol/TEA and XtalFluor/TEA-3HF) and into the flow stream at an equal rate, generating the stoichiometry of 1 equiv of the alcohol, 2 equiv of TEA, 1.75 equiv of XtalFluor, and 2 equiv of TEA-3HF. At a combined flow (both pumps) of 10.5 mL/min, anticipated reaction time was 14.3 min. The resulting concentration of the alcohol is 0.25 M. The very dark-colored output of the reaction was collected post BPR into two 2 L collection flasks containing 35 g of sodium bicarbonate (417 mmol, 1.5 equiv) and 100 mL of satd bicarb each. Each collection flask contained approximately half of the reaction mixture. As the effluent flowed into the collection flask, bubbling was observed. The collection flasks were continuously stirred during this process. After the collection of the first half of the reaction effluent, the mixture was observed to be pH 3–4. The pH was adjusted to slightly basic (pH ~ 8), with the portionwise addition of sodium bicarbonate (solid) and agitation of the mixture. The mixture was then diluted with 200 mL of water. The organic phase was separated, evaporated in vacuo, and chromatographed.

The second collection flask, prior to collection, had an additional 35 g of NaHCO₃ added (total of 70 g, 0.83 M). The flask was agitated as the effluent was collected. After collection, the reaction was further adjusted with another 20 g of NaHCO₃ and 200 mL water, and the pH was tested at about 8.

Work Up. The quenched flow reactor batches (in 79.5 g theoretical product) were combined and diluted to a total 3 L with water to dissolve most of the residual carbonate salts (pH ~ 8.5–9). The aqueous phase was extracted once with 1 L of ether followed by 3 × 800 mL ether. Analysis by TLC (2/1 hep/EA; UV), indicated there was no product in the dark aqueous layer. The combined dark upper ether extracts were dried over Na₂SO₄, filtered, and concentrated in vacuo to give 90g of a crude dark oil. The residue was diluted with 50 mL of DCM and loaded in roughly equal portions on separate 100 g Biotage SNAP columns and dried on low vacuum, then each was purified on separate 330 g RediSep Gold columns in parallel. The product fractions from each column were combined and concentrated then costripped by dissolving the dark-amber oil with 3 × 250 mL ether to afford (62.24 g, 0.22 mmol dark-amber oil) 78%. LCMS *m/z* 280.1 [M + H]⁺. ¹H NMR (400 MHz, CDCl₃) δ 7.28–7.41 (m, 5H), 4.51–4.76 (m, 5H), 4.30–4.42 (m, 1H), 4.22 (dd, *J* = 13.4, 1.1 Hz, 1H), 3.69–3.77 (m, 1H), 3.58 (dd, half of ABX pattern, *J* = 10.0, 5.8 Hz, 1H), 3.50 (dd, half of ABX pattern, *J* = 10.2, 4.4 Hz, 1H), 3.32–3.42 (m, 1H), 2.19 (br dd, *J* = 13, 7 Hz, 1H), 1.60–1.71 (m, 1H).

(3*R*,3*aR*,5*R*,7*aS*)-5-((Benzyloxy)methyl)-7*a*-(2,4-difluorophenyl)-3-(fluoromethyl)-hexahydro-1*H*-pyrano[3,4-*c*]1,2-oxazole (35). Boron trifluoride diethyl etherate (12.7 mL, 103 mmol) was added to a –78 °C solution of 2,4-difluoro-1-iodobenzene (12.6 mL, 105 mmol) in a 10:1 mixture of toluene and tetrahydrofuran (250 mL). *n*-Butyllithium (2.5 M in hexanes, 40.1 mL, 100 mmol) was added dropwise, and the reaction mixture was stirred at –78 °C for 15 min. A solution of (3*R*,5*R*)-5-((benzyloxy)methyl)-3-(fluoromethyl)-3,3*a*,4,5-tetrahydro-7*H*-pyrano[3,4-*c*]isoxazole **33** (14 g, 50 mmol) in minimal 10:1 toluene/tetrahydrofuran was added, and stirring was continued at –78 °C for 15 min. At this point, the reaction mixture was poured into aqueous ammonium chloride solution; the aqueous layer was extracted three times with ethyl acetate, and the combined organic layers were washed with water, washed with saturated aqueous sodium chloride solution, dried over sodium sulfate, filtered, and concentrated in vacuo. Chromatography on silica gel (gradient: 0–30% ethyl acetate in heptane) afforded the product as an oil. Yield: 18 g, 45.8 mmol, 91%. LCMS *m/z* 394.2 [M + H]⁺. ¹H NMR (400 MHz, CDCl₃) δ 7.94 (ddd, *J* = 9.1, 9.0, 6.7 Hz, 1H), 7.29–7.41 (m, 5H), 6.88–6.94 (m,

1H), 6.82 (ddd, $J = 11.9, 8.6, 2.5$ Hz, 1H), 6.42 (br s, 1H), 4.61 (AB quartet, $J_{AB} = 12.2$ Hz, $\Delta\nu_{AB} = 13.7$ Hz, 2H), 4.11–4.20 (m, 1H), 4.01 (dd, half of ABX pattern, $J = 12.9, 2.0$ Hz, 1H), [3.81–3.91, 3.73–3.80 and 3.63–3.68 (multiplets, total 4H)], 3.58 (dd, half of ABX pattern, $J = 10.2, 6.0$ Hz, 1H), 3.51 (dd, half of ABX pattern, $J = 10.2, 4.2$ Hz, 1H), 3.09–3.17 (m, 1H), 2.07 (ddd, $J = 14.1, 7.5, 2.2$ Hz, 1H), 1.57–1.69 (m, 1H).

(1*R*)-1-[(2*R*,4*R*,5*S*)-5-Amino-2-[(benzyloxy)methyl]-5-(2,4-difluorophenyl)tetrahydro-2*H*-pyran-4-yl]-2-fluoroethanol (**37**). To a mixture of **35** (18.0 g, 46.0 mmol) in acetic acid (153 mL) was added zinc dust (38.9 g, 595 mmol), and the reaction mixture was stirred at room temperature for 18 h. The zinc was removed via filtration through diatomaceous earth, and the filtrate was concentrated in vacuo and partitioned between ethyl acetate and aqueous 1 M sodium hydroxide solution. The aqueous layer was extracted twice with ethyl acetate, and the combined organic layers were washed with saturated aqueous sodium chloride solution, dried over sodium sulfate, filtered, and concentrated under reduced pressure; no chromatographic purification was carried out. Yield: 15.6 g, 39.4 mmol, 86%. LCMS m/z 396.2 [M + H]⁺. ¹H NMR (400 MHz, CD₃OD) δ 7.73 (ddd, $J = 9.1, 9.0, 6.5$ Hz, 1H), 7.26–7.40 (m, 5H), 6.96–7.02 (m, 1H), 6.92 (ddd, $J = 12.8, 8.9, 2.6$ Hz, 1H), 4.59 (s, 2H), [4.11–4.15 and 3.99–4.06 (multiplets, total 2H)], 3.90 (ddd, $J = 48.2, 9.5, 7.0$ Hz, 1H), 3.64–3.79 (m, 2H), 3.63 (dd, half of ABX pattern, $J = 10.4, 5.7$ Hz, 1H), 3.58 (dd, half of ABX pattern, $J = 10.4, 3.9$ Hz, 1H), 3.39 (d, $J = 11.3$ Hz, 1H), 2.73 (ddd, $J = 12.8, 4.4, 4.3$ Hz, 1H), 1.79–1.91 (m, 1H), 1.64 (ddd, $J = 13.7, 4.2, 2.6$ Hz, 1H).

N-[[(3*S*,4*R*,6*R*)-6-[(Benzyloxy)methyl]-3-(2,4-difluorophenyl)-4-[(1*R*)-2-fluoro-1-hydroxyethyl]tetrahydro-2*H*-pyran-3-yl]-carbamothioyl]benzamide (**41**). Benzoyl isothiocyanate (5.26 mL, 39.5 mmol) was added to a solution of **37** (15.6 g, 39.5 mmol) in dichloromethane (132 mL), and the reaction mixture was allowed to stir at room temperature for 18 h. Removal of solvent in vacuo afforded a solid that was purified by silica gel chromatography (gradient: 0–100% ethyl acetate in heptane) provided the product as a solid. Yield: 18.7 g, 33.5 mmol, 85%. This material was used directly in the next reactions.

N-[[(4*S*,4*aR*,6*R*,8*aS*)-6-[(Benzyloxy)methyl]-8*a*-(2,4-difluorophenyl)-4-(fluoromethyl)-4,4*a*,5,6,8,8*a*-hexahydropyrano[3,4-*d*][1,3]thiazin-2-yl]benzamide (**43**). To a solution of **41** (18.6 g, 33.3 mmol) in dichloromethane (444 mL) was added 1-chloro-*N,N*,2-trimethylprop-1-en-1-amine (6.88 mL, 49.9 mmol), and the reaction mixture was stirred at ambient temperature for 18 h. It was then partitioned between dichloromethane and water; the aqueous layer was extracted with dichloromethane, and the combined organic layers were washed with saturated aqueous sodium chloride solution, dried over magnesium sulfate, filtered, and concentrated in vacuo. Silica gel chromatography (gradient: 0–60% ethyl acetate in heptane) afforded the product as a solid. By ¹H NMR analysis, some reagent-derived material was still present. Corrected yield: 13.8 g, 25.5 mmol, 76%. LCMS m/z 541.3 [M + H]⁺. ¹H NMR (400 MHz, CDCl₃), product peaks only, characteristic peaks: δ 8.20 (br d, $J = 7$ Hz, 2H), 7.51–7.57 (m, 1H), 7.43–7.49 (m, 2H), 7.34–7.42 (m, 1H), 7.23–7.34 (m, 5H), 6.86–6.98 (m, 2H), 4.57 (AB quartet, $J_{AB} = 11.9$ Hz, $\Delta\nu_{AB} = 18.1$ Hz, 2H), [4.45–4.66 and 4.33–4.39 (multiplets, total 2H)], 4.19 (br d, $J = 12.0$ Hz, 1H), 3.82–3.94 (m, 2H), 3.63 (dd, half of ABX pattern, $J = 10.2, 6.2$ Hz, 1H), 3.5–3.57 (m, 1H), 3.49 (dd, half of ABX pattern, $J = 10.2, 4.4$ Hz, 1H), 3.21–3.29 (m, 1H).

N-[[(4*S*,4*aR*,6*R*,8*aS*)-8*a*-(2,4-Difluorophenyl)-4-(fluoromethyl)-6-(hydroxymethyl)-4,4*a*,5,6,8,8*a*-hexahydropyrano[3,4-*d*][1,3]thiazin-2-yl]benzamide (**39**). A solution of **43** (13.8 g, 25.5 mmol) in dichloromethane (130 mL) was cooled to 0 °C. Boron trichloride (1 M solution in toluene, 76.6 mL, 76.6 mmol) was added in a rapid dropwise manner at a rate such that the temperature of the reaction mixture remained at <5 °C throughout the addition. After 10 min at 0 °C, the reaction mixture was allowed to warm to room temperature and stirred for 30 min before being carefully quenched via dropwise addition of methanol (20 mL). The resulting solution was heated at reflux for 30 min, cooled to room temperature, and concentrated in vacuo. The residue was dissolved in methanol (460 mL) and

concentrated under reduced pressure; the resulting material was dissolved in dichloromethane and washed twice with 1 M aqueous sodium hydroxide solution and once with saturated aqueous sodium chloride solution, then dried over sodium sulfate and filtered. The organic layer was concentrated in vacuo to approximately 30% of its original volume and treated with heptane until a precipitate formed; this was collected via filtration to afford the product as a solid. Yield: 8.5 g, 19 mmol, 74%. LCMS m/z 451.3 [M + H]⁺. ¹H NMR (400 MHz, CD₃OD) δ 8.06–8.18 (m, 2H), 7.51–7.59 (m, 1H), 7.42–7.51 (m, 3H), 7.02–7.14 (m, 2H), 4.68 (ddd, $J = 46.6, 9.7, 6.5$ Hz, 1H), 4.51 (ddd, $J = 46.6, 9.7, 7.0$ Hz, 1H), 4.16 (br d, $J = 12$ Hz, 1H), 3.93 (d, $J = 11.9$ Hz, 1H), 3.69–3.78 (m, 1H), 3.59 (d, $J = 5.2$ Hz, 2H), 3.40–3.51 (br m, 1H), 3.23–3.3 (br m, 1H, assumed; partially obscured by solvent peak), 1.59–1.74 (m, 2H).

N-[[(4*S*,4*aR*,6*R*,8*aS*)-8*a*-(2,4-Difluorophenyl)-4-(fluoromethyl)-6-(hydroxymethyl)-4,4*a*,5,6,8,8*a*-hexahydropyrano[3,4-*d*][1,3]thiazin-2-yl]benzamide (**39**). To a stirring solution of thiourea **41** (32.83g, 58.77 mmol) in 1,2-dichloroethane (392 mL) was added anisole (19.1 g, 19.2 mL, 176 mmol) followed by triflic acid (26.5 g, 15.4 mL, 176 mmol) at room temperature. The reaction was then heated in an oil bath that was preheated to 60 °C for 2 h 15 min until starting material was consumed and debenylation and thioamidine product had formed by TLC and LCMS analysis. After cooling to room temperature, the reaction was diluted with dichloromethane and treated with 1*N* sodium hydroxide. The contents were extracted, separated, and the basic aqueous layer was backextracted 3 times with dichloromethane. The combined organic extracts were washed with brine, dried over sodium sulfate, filtered, and concentrated to give a crude solid which was triturated with dichloromethane. Filtration afforded a white solid. Yield: 17.18 g, @ @ mmol, 64.9%. Concentration of the filtrate followed by flash column chromatography (120 g SiO₂; gradient 0–60% ethyl acetate/heptanes), and subsequent trituration of that solid with dichloromethane afforded additional product as a white solid. Yield: 1.32 g, 5%. LCMS m/z 451.2 [M + H]⁺. ¹H NMR (400 MHz, CD₃OD) δ 8.12 (br s, 2H), 7.52–7.60 (m, 1H), 7.41–7.51 (m, 3H), 7.02–7.14 (m, 2H), 4.41–4.77 (m, 2H, both methylene fluoride protons grouped together as a multiplet), 4.17 (dd, $J = 0.68, 12.03$ Hz, 1H), 3.93 (d, $J = 11.9$ Hz, 1H), 3.74 (qd, $J = 4.8, 9.76$ Hz, 1H), 3.59 (d, $J = 5.3$ Hz, 2H), 3.40–3.51 (m, 1H), 3.21–3.29 (m, 1H), 1.59–1.75 (m, 2H).

N-[[(4*aR*,6*R*,8*aS*)-8*a*-(2,4-Difluorophenyl)-6-formyl-4,4*a*,5,6,8,8*a*-hexahydropyrano[3,4-*d*][1,3]thiazin-2-yl]benzamide (**51**). Triethylamine (16.7 mL, 120 mmol) was added in one rapid portion to a solution of *N*-[[(4*aR*,6*R*,8*aS*)-8*a*-(2,4-difluorophenyl)-6-(hydroxymethyl)-4,4*a*,5,6,8,8*a*-hexahydropyrano[3,4-*d*][1,3]thiazin-2-yl]benzamide (**44**) (4.18 g, 10.0 mmol) in dichloromethane (200 mL) that was immersed in a room temperature water bath. After 5 min, anhydrous dimethyl sulfoxide (9.94 mL, 140 mmol) was rapidly added, followed immediately by solid sulfur trioxide pyridine complex (98%, 13.0 g, 80.0 mmol) in a single portion. The resulting solution was stirred at ambient temperature for 6.5 h then diluted with a 1:1 mixture of water and saturated aqueous sodium chloride solution (200 mL) and stirred for 10 min. The aqueous layer was extracted with dichloromethane (2 × 200 mL), and the combined organic layers were washed with water (100 mL), washed with saturated aqueous sodium chloride solution (100 mL), dried over sodium sulfate, filtered, and concentrated in vacuo. Purification via silica gel chromatography (gradient: 0–100% ethyl acetate in heptane) gave the product as a white solid. Yield: 2.81 g, 6.75 mmol, 67%. LCMS m/z 414.9 [M – H]⁺. ¹H NMR (400 MHz, CDCl₃) δ 9.71 (s, 1H), 8.20 (br d, $J = 7$ Hz, 2H), 7.50–7.56 (m, 1H), 7.36–7.49 (m, 3H), 6.86–6.99 (m, 2H), 4.23 (br d, $J = 12.1$ Hz, 1H), 4.12 (dd, $J = 12.1, 2.9$ Hz, 1H), 3.94 (d, $J = 12.5$ Hz, 1H), 3.13–3.22 (m, 1H), 3.04 (dd, $J = 13.1, 4.1$ Hz, 1H), 2.69 (dd, $J = 13.1, 2.9$ Hz, 1H), 2.02–2.14 (m, 1H), 1.92–1.99 (m, 1H).

N-[[(4*aR*,6*R*,8*aS*)-8*a*-(2,4-Difluorophenyl)-6-(2-methoxyethenyl)-4,4*a*,5,6,8,8*a*-hexahydropyrano[3,4-*d*][1,3]thiazin-2-yl]benzamide (**54**). Commercial methoxymethyl(triphenyl)phosphonium chloride (9.49 g) was placed in a vacuum oven at 80 °C and low vacuum for 18 h. The resulting material (9.38 g, 27.4 mmol) was suspended in tetrahydrofuran (130 mL) and cooled to an internal temperature of 2

°C. A solution of potassium *tert*-butoxide (1.0 M in tetrahydrofuran, 23.5 mL, 23.5 mmol) was added over 2–3 min at a rate that kept the reaction temperature under 5 °C. The resulting solution was stirred for 5 min at 2 to 5 °C, then warmed to room temperature over 20 min. The reaction mixture was cooled to 3 °C internal temperature and treated with a solution of *N*-[(4*aR*,6*R*,8*aS*)-8*a*-(2,4-difluorophenyl)-6-formyl-4,4*a*,5,6,8,8*a*-hexahydropyrano[3,4-*d*][1,3]thiazin-2-yl]-benzamide **51** (3.20 g, 7.68 mmol) in tetrahydrofuran (20 mL) over 2–3 min while keeping the internal temperature below 6 °C. After 15 min at 3–6 °C, the reaction mixture was allowed to warm to room temperature over 25 min then cooled to 14 °C and quenched by addition of saturated aqueous sodium bicarbonate solution (125 mL). The resulting mixture was extracted with ethyl acetate (3 × 150 mL), and the combined organic layers were dried over sodium sulfate, filtered, and concentrated in vacuo. Purification via silica gel chromatography (gradient: 0–35% ethyl acetate in heptane) provided the product as a white solid, which was characterized by ¹H NMR as a roughly 1.4:1 mixture of geometrical isomers around the double bond. Yield: 2.66 g, 5.98 mmol, 78%. LCMS *m/z* 445.2 [M + H]⁺. ¹H NMR (400 MHz, CDCl₃) δ 8.24 (br d, *J* = 7.3 Hz, 2H), 7.48–7.54 (m, 1H), 7.37–7.48 (m, 3H), 6.85–6.96 (m, 2H), [6.68 (d, *J* = 12.7 Hz) and 5.99 (dd, *J* = 6.3, 0.9 Hz), total 1H], [4.86 (dd, *J* = 12.7, 8.0 Hz) and 4.55 (dd, half of ABX pattern, *J* = 8.1, 6.3 Hz), total 1H], 4.60–4.68 and 4.06–4.13 (2 m, total 1H), [4.20 (dd, *J* = 12.2, 1.9 Hz) and 4.19 (dd, *J* = 12.2, 2.0 Hz), total 1H], [3.81 (d, *J* = 12.2 Hz) and 3.79 (d, *J* = 12.2 Hz), total 1H], 3.66 and 3.55 (2 s, total 3H), 3.13–3.24 (m, 1H), 2.97–3.05 (m, 1H), 2.60–2.68 (m, 1H), 1.97–2.19 (m, 1H), 1.66–1.75 (m, 1H).

N-[(4*aR*,6*R*,8*aS*)-8*a*-(2,4-Difluorophenyl)-6-(1,1,3,3-tetramethoxypropan-2-yl)-4,4*a*,5,6,8,8*a*-hexahydropyrano[3,4-*d*][1,3]thiazin-2-yl]benzamide (**72**). To a stirring mixture of *N*-[(4*aR*,6*R*,8*aS*)-8*a*-(2,4-difluorophenyl)-6-(2-methoxyethenyl)-4,4*a*,5,6,8,8*a*-hexahydropyrano[3,4-*d*][1,3]thiazin-2-yl]benzamide (**54**) (70.0 mg, 0.157 mmol) in 1,2-dichloroethane (150 μL) was added trimethyl orthoformate (36.1 μL, 0.330 mmol), followed by boron trifluoride diethyl etherate (7.0 μL, 56 μmol), and the reaction mixture was stirred at room temperature for 30 min. At this point, additional trimethyl orthoformate (17 μL, 0.15 mmol) and boron trifluoride diethyl etherate (7.0 μL, 56 μmol) were introduced, and stirring was continued for 30 min. Boron trifluoride diethyl etherate (7.0 μL, 56 μmol) was added again, and the reaction mixture was stirred for 1 h then diluted with dichloromethane (1 mL) and transferred via pipet into a stirring mixture of saturated aqueous sodium bicarbonate solution (2 mL) and dichloromethane (5 mL). The aqueous layer was extracted with dichloromethane (5 mL), and the combined organic layers were dried over sodium sulfate, filtered, and concentrated in vacuo to afford the product as an off-white to pale-yellow foam. Yield: 75 mg, 0.14 mmol, 89%. LCMS *m/z* 549.1 [M + H]⁺. ¹H NMR (400 MHz, CDCl₃), characteristic peaks: δ 8.22–8.26 (m, 2H), 7.37–7.53 (m, 4H), 6.84–6.95 (m, 2H), 4.56 (d, *J* = 4.9 Hz, 1H), 4.52 (d, *J* = 3.8 Hz, 1H), 4.14 (dd, *J* = 12.2, 1.8 Hz, 1H), 4.03–4.09 (m, 1H), 3.78 (d, *J* = 12.2 Hz, 1H), 3.44 (s, 3H), 3.41 (s, 3H), 3.40 (s, 3H), 3.36 (s, 3H), 2.98 (dd, *J* = 12.8, 4.2 Hz, 1H), 2.65 (dd, *J* = 12.8, 2.7 Hz, 1H), 2.22–2.33 (m, 1H), 2.13–2.17 (m, 1H), 1.77 (ddd, *J* = 14.0, 4.0, 2.0 Hz, 1H).

Synthesis of (4*aR*,6*R*,8*aS*)-8*a*-(2,4-Difluorophenyl)-6-(1-methyl-1*H*-pyrazol-4-yl)-4,4*a*,5,6,8,8*a*-hexahydropyrano[3,4-*d*][1,3]thiazin-2-amine (5**).** Water (100 μL) was added to a mixture of *N*-[(4*aR*,6*R*,8*aS*)-8*a*-(2,4-difluorophenyl)-6-(1,1,3,3-tetramethoxypropan-2-yl)-4,4*a*,5,6,8,8*a*-hexahydropyrano[3,4-*d*][1,3]thiazin-2-yl]benzamide (**72**) (70 mg, 0.13 mmol) in methanol (150 μL). To the resulting gel was added methylhydrazine (10 μL, 0.19 mmol) followed by concentrated sulfuric acid (13 μL, 0.24 mmol). The mixture was vortexed for 2–3 min to break up the gel then heated to 45 °C for 2.5 h and to 60 °C for 20 h. After cooling to room temperature, the reaction mixture was partitioned between water (5 mL) and dichloromethane (2 mL). The aqueous layer was adjusted to pH 8–9 via dropwise addition of 1 M aqueous sodium hydroxide solution then extracted with ethyl acetate (2 × 10 mL). The combined organic layers were dried over sodium sulfate, filtered, and concentrated in

vacuo. Purification via silica gel chromatography (gradient: 0–18% methanol in dichloromethane) provided the product as an off-white solid. Yield: 19 mg, 52 μmol, 40%. LCMS *m/z* 365.1 [M + H]⁺. ¹H NMR (400 MHz, CDCl₃) δ 7.48 (s, 1H), 7.42 (s, 1H), 7.38 (ddd, *J* = 9.0, 9.0, 6.6 Hz, 1H), 6.85–6.91 (m, 1H), 6.82 (ddd, *J* = 12.5, 8.6, 2.5 Hz, 1H), 4.67 (dd, *J* = 11.5, 2.2 Hz, 1H), 4.22 (dd, *J* = 11.1, 2.4 Hz, 1H), 3.88 (s, 3H), 3.84–3.89 (m, 1H), 2.96–3.05 (m, 2H), 2.60–2.67 (m, 1H), 2.07–2.19 (m, 1H), 1.73–1.80 (m, 1H). ¹H NMR (400 MHz, CD₃OD) δ 7.58 (s, 1H), 7.45 (s, 1H), 7.31–7.41 (m, *J* = 6.7 Hz, 1H), 6.91–7.03 (m, 2H), 4.68 (dd, *J* = 2.4, 11.5 Hz, 1H), 4.23 (dd, *J* = 2.2, 11.2 Hz, 1H), 3.86 (s, 3H), 3.74 (d, *J* = 11.2 Hz, 1H), 2.96–3.08 (m, 1H), 2.90 (dd, *J* = 4.1, 12.5 Hz, 1H), 2.71 (dd, *J* = 2.9, 12.5 Hz, 1H), 2.00–2.16 (m, 1H), 1.75–1.86 (m, 1H); [α]_D²² = +17.24 (*c* = 0.58 g/100 mL; MeOH).

(4*aR*,6*R*,8*aS*)-8*a*-(2,4-Difluorophenyl)-6-(1*H*-pyrazol-4-yl)-4,4*a*,5,6,8,8*a*-hexahydropyrano[3,4-*d*][1,3]thiazin-2-amine (**6**). To compound **72** (620 mg, 1.13 mmol) dissolved in an ethanol/water mixture (3:1, 4 mL) was added hydrazine sulfate (150 mg, 1.15 mmol), and the mixture was heated at 60 °C for 16 h. Aqueous saturated sodium carbonate solution was added until a pH of 9 was obtained, followed by addition of methanol (1 mL) and extraction with ethyl acetate (3 × 25 mL). The combined organic layers were washed with saturated aqueous sodium chloride solution, dried over sodium sulfate, filtered, and concentrated in vacuo. Purification via silica gel chromatography (gradient: 0–17.5% methanol in dichloromethane) provided *N*-[(4*aR*,6*R*,8*aS*)-8*a*-(2,4-difluorophenyl)-6-(1*H*-pyrazol-4-yl)-4,4*a*,5,6,8,8*a*-hexahydropyrano[3,4-*d*][1,3]thiazin-2-yl]benzamide as a tan solid. Yield: 47 mg, 0.10 mmol, 9%. LCMS *m/z* 455.2 [M + H]⁺. ¹H NMR (400 MHz, CDCl₃) δ 8.20–8.22 (m, 2H), 7.39–7.53 (m, 6H), 6.86–6.96 (m, 2H), 4.77 (dd, *J* = 11.6, 2.1 Hz, 1H), 4.3 (dd, *J* = 12.1, 1.8 Hz, 1H), 3.89 (d, *J* = 12.1 Hz, 1H), 3.22–3.28 (m, 1H), 3.04 (dd, *J* = 12.8, 4.2 Hz, 1H), 2.67 (dd, *J* = 12.9, 2.7 Hz, 1H), 2.21–2.31 (m, 1H), 1.91–1.96 (m, 1H).

1,8-Diazabicyclo[5.4.0]undec-7-ene (DBU) (0.040 mmol, 6.1 mg, 6 μL) was added to a stirring solution of *N*-[(4*aR*,6*R*,8*aS*)-8*a*-(2,4-difluorophenyl)-6-(1*H*-pyrazol-4-yl)-4,4*a*,5,6,8,8*a*-hexahydropyrano[3,4-*d*][1,3]thiazin-2-yl]benzamide (26.3 mg, 0.058 mmol) in MeOH (0.4 mL) at room temperature then stirred at 60 °C for 18 h. The reaction was concentrated, partitioned with ethyl acetate (5 mL) and water (2 mL) then the phases were separated. The aqueous layer was washed with additional ethyl acetate (5 mL). The combined organic extracts were dried over magnesium sulfate, filtered, and concentrated in vacuo to give the crude residue, which was chromatographed on 4 g of SiO₂ (gradient: 0–17.5% methanol in DCM). The product fractions (eluted between 13% and 16% MeOH, visualized with I₂ on TLC that was run at 15% MeOH in DCM) were combined and concentrated to afford the desired product as a white solid. Yield: 15 mg, 0.42 mmol, 73.9%. LCMS *m/z* 351.5 [M + H]⁺. ¹H NMR (400 MHz, CD₃OD) δ 7.61 (s, 2H), 7.38 (dt, *J* = 6.6, 9.2 Hz, 1H), 6.95–7.04 (m, 2H), 4.75 (dd, *J* = 2.4, 11.7 Hz, 1H), 4.25 (dd, *J* = 1.9, 11.3 Hz, 1H), 3.77 (d, *J* = 11.3 Hz, 1H), 3.03–3.10 (m, 1H), 2.92 (dd, *J* = 4.3, 12.5 Hz, 1H), 2.74 (dd, *J* = 2.7, 12.5 Hz, 1H), 2.10 (dq, *J* = 2.3, 12.4 Hz, 1H), 1.82–1.88 (m, 1H).

N-[(4*S*,4*aR*,6*R*,8*aS*)-8*a*-(2,4-Difluorophenyl)-4-(fluoromethyl)-6-formyl-4,4*a*,5,6,8,8*a*-hexahydropyrano[3,4-*d*][1,3]thiazin-2-yl]benzamide (**53**). Triethylamine (0.817 mL, 5.86 mmol) was added rapidly to a solution of **39** (660 mg, 1.46 mmol) in dichloromethane (29 mL). After 5 min, anhydrous dimethyl sulfoxide (468 μL, 6.59 mmol) was rapidly added, followed immediately by solid sulfur trioxide pyridine complex (98%, 654 mg, 4.03 mmol) in a single portion. The resulting solution was stirred at ambient temperature for 3.5 h then diluted with a 1:1 mixture of water and saturated aqueous sodium chloride solution and stirred for 10 min. The aqueous layer was extracted twice with dichloromethane, and the combined organic layers were washed with water until the pH of the aqueous wash was pH 6–7. The organic layer was then washed twice with 0.2 M aqueous hydrochloric acid and once with saturated aqueous sodium chloride solution, dried over sodium sulfate, filtered, and concentrated in vacuo. Purification via silica gel chromatography (gradient: 0–75% ethyl acetate in heptane) provided the product as a solid. Yield: 0.54 g, 1.2

mmol, 82%. LCMS m/z 449.1 $[M + H]^+$. 1H NMR (400 MHz, $CDCl_3$) δ 9.69 (s, 1H), 8.14 (br d, $J = 7.0$ Hz, 2H), 7.50–7.57 (m, 1H), 7.46 (br dd, $J = 8, 7$ Hz, 2H), 7.36 (ddd, $J = 9.0, 8.8, 6.2$ Hz, 1H), 6.86–6.98 (m, 2H), 4.35–4.67 (m, 2H), 4.23 (br d, $J = 12.0$ Hz, 1H), 4.06–4.12 (m, 1H), 3.97 (d, $J = 12.1$ Hz, 1H), 3.46–3.56 (m, 1H), 3.25 (ddd, $J = 12.0, 4.0, 3.9$ Hz, 1H), 1.97 (ddd, $J = 13.5, 3.5, 3.5$ Hz, 1H), 1.74–1.86 (m, 1H).

N-[(4*S*,4*aR*,6*R*,8*aS*)-8*a*-(2,4-Difluorophenyl)-4-(fluoromethyl)-6-(2-methoxyethenyl)-4,4*a*,5,6,8,8*a*-hexahydropyrano[3,4-*d*][1,3]thiazin-2-yl]benzamide (**56**). To a stirring suspension of (methoxymethyl)triphenylphosphonium chloride (1.16 g, 3.38 mmol, previously oven-dried at 80 °C under vacuum overnight) in anhydrous tetrahydrofuran (15 mL) cooled to 2 °C internal under strong positive pressure of nitrogen was added potassium *tert*-butoxide (1 M in tetrahydrofuran, 2.9 mL, 2.90 mmol) over 3 min while keeping internal temperature under 5 °C. The resulting red solution was allowed to warm to room temperature over 30 min and was then cooled back down to 3 °C, at which point a solution of **53** (425 mg, 0.948 mmol) in anhydrous tetrahydrofuran (4 mL) was added over 2 min while ensuring that the internal temperature remained below 4 °C. The reaction mixture was allowed to stir at 3 to 6 °C for 30 min, was warmed to room temperature over 30 min, and was then cooled back down to 5 °C (internal), at which point saturated aqueous sodium bicarbonate solution (50 mL) was added. The mixture was extracted with ethyl acetate (3 × 60 mL), and the combined organic layers were dried over sodium sulfate, filtered, and concentrated under reduced pressure. Silica gel chromatography (gradient: 0–75% ethyl acetate in heptane) provided the product as ~60/40 mixture of *E/Z* isomers. Yield: 202 mg, 44.7%. LCMS m/z 477.3 $[M + H]^+$. 1H NMR (400 MHz, $CDCl_3$) δ 8.21 (d, $J = 7.4$ Hz, 2H), 7.50–7.58 (m, 1H), 7.43–7.50 (m, 2H), 7.34–7.43 (m, 1H), 6.86–6.99 (m, 2H), [6.69 (d, $J = 12.5$ Hz) and 5.99 (d, $J = 6.2$ Hz), total 1H], 4.45–4.89 (m, 3H), 4.05–4.41 (m, 2H), 3.76–3.88 (m, 1H), [3.66 (s) and 3.55 (s), total 3H], 3.47–3.54 (m, 1H), 3.23–3.35 (m, 1H), 1.64–1.93 (m, 2H).

N-[(4*S*,4*aR*,6*R*,8*aS*)-8*a*-(2,4-Difluorophenyl)-4-(fluoromethyl)-6-(1,1,3,3-tetramethoxypropan-2-yl)-4,4*a*,5,6,8,8*a*-hexahydropyrano[3,4-*d*][1,3]thiazin-2-yl]benzamide (**74**). To a solution of **56** (200 mg, 0.40 mmol) in dichloromethane (4.2 mL) cooled to 0 °C was added trimethyl orthoformate (0.0940 mL, 0.861 mmol) followed by dropwise addition of boron trifluoride diethyl etherate (58.4 μ L, 0.462 mmol). The reaction was stirred at 0 °C for 1.5 h then partitioned between dichloromethane and saturated aqueous sodium bicarbonate solution. The aqueous layer was extracted with dichloromethane, and the combined organic layers were washed with saturated aqueous sodium chloride solution, dried over sodium sulfate, filtered, and concentrated in vacuo. This material (300 mg) was carried into the subsequent step without further purification. LCMS m/z 583.3 $[M + H]^+$.

(4*S*,4*aR*,6*R*,8*aS*)-8*a*-(2,4-Difluorophenyl)-4-(fluoromethyl)-6-(1-methyl-1*H*-pyrazol-4-yl)-4,4*a*,5,6,8,8*a*-hexahydropyrano[3,4-*d*]-[1,3]thiazin-2-amine, Hydrochloride Salt (**14**). To a solution of **74** (material from the previous step, 300 mg, ≤ 0.40 mmol) in ethanol (3 mL) was added methylhydrazine (34.0 mg, 0.736 mmol) and water (1.3 mL). Concentrated sulfuric acid (51 μ L, 0.96 mmol) was added dropwise, and the reaction mixture was heated at 60 °C for 16 h. The reaction was partitioned between ethyl acetate and saturated aqueous sodium bicarbonate solution, and the aqueous layer was extracted three times with ethyl acetate. The combined organic layers were dried over sodium sulfate, filtered, and concentrated in vacuo. Purification via chromatography on silica gel (gradient: 0–4% methanol in dichloromethane) provided the free base of the product. This material was dissolved in dichloromethane and treated with excess hydrogen chloride (1 M in diethyl ether) to afford the product as a solid. Yield: 44.0 mg, 0.102 mmol, 26% over 2 steps. LCMS m/z 397.1 $[M + H]^+$. 1H NMR (400 MHz, CD_3OD) free base: δ 7.27–7.40 (m, 3H), 6.73–6.81 (m, 2H), 4.40–4.59 (m, 2H), 4.20–4.35 (m, 1H), 4.15 (dd, $J = 11.1, 2.1$ Hz, 1H), 3.78–3.81 (m, 4H), 3.39–3.40 (m, 1H), 3.03 (dt, $J = 11.8, 3.9$ Hz, 1H), 1.75–1.85 (m, 1H), 1.65 (dt, $J = 12.9, 3.1$ Hz, 1H); $[\alpha]^{25.7}_D = +12.00$ ($c = 0.10$ g/100 mL; MeOH).

N-[(4*R*,4*aR*,6*R*,8*aS*)-8*a*-(2,4-Difluorophenyl)-6-formyl-4-methyl-4,4*a*,5,6,8,8*a*-hexahydropyrano[3,4-*d*][1,3]thiazin-2-yl]benzamide (**52**). Triethylamine (5.88 mL, 42.2 mmol) was added in one rapid portion to a solution of **38** (1.52 g, 3.52 mmol) in anhydrous dichloromethane (70.3 mL) (mild exotherm from 20 to 23 °C noted internally). After 5 min, anhydrous dimethyl sulfoxide (3.5 mL, 49.2 mmol) was rapidly added, followed immediately by solid sulfur trioxide pyridine complex (98%, 4.57 g, 28.1 mmol) in a single portion (mild exotherm to 25 °C noted internally). The resulting pale-yellow solution was stirred at ambient temperature for 3.5 h (became pale amber) then diluted with a 1:1 mixture of water and saturated aqueous sodium chloride solution and stirred for 10 min. The aqueous layer (pH ~ 2) was extracted with dichloromethane (2 \times), and the combined organic layers were successively washed with water (until pH = 6–7), followed by 0.2 N HCl (2 \times) and saturated aqueous sodium chloride solution (1 \times). The separated organic extract was dried over sodium sulfate, filtered, and concentrated in vacuo. Purification via silica gel chromatography (gradient: 0–75% ethyl acetate in heptane) gave the product. Yield: 0.949 g, 62.7%. LCMS m/z 449.2 hydrate $[M - H^+ + H_2O]$. 1H NMR (400 MHz, $CDCl_3$) δ 9.72 (s, 1H), 8.19 (d, $J = 7.4$ Hz, 2H), 7.35–7.56 (m, 4H), 6.86–6.98 (m, 2H), 4.09 (dd, $J = 2.6, 12.2$ Hz, 1H), 3.95 (d, $J = 12.1$ Hz, 1H), 3.22–3.32 (m, 1H), 2.94 (td, $J = 3.8, 12.0$ Hz, 1H), 1.96–2.05 (m, 1H), 1.71–1.83 (m, 1H), 1.29 (d, $J = 7.0$ Hz, 3H).

N-[(4*R*,4*aR*,6*R*,8*aS*)-8*a*-(2,4-Difluorophenyl)-6-(2-methoxyvinyl)-4-methyl-4,4*a*,5,6,8,8*a*-hexahydropyrano[3,4-*d*][1,3]thiazin-2-yl]benzamide (**55**). To a stirring suspension of (methoxymethyl)triphenylphosphonium chloride (2.69 g, 7.85 mmol, previously oven-dried at 80 °C under vacuum overnight) in tetrahydrofuran (37 mL) cooled to 2 °C internal under strong positive pressure of nitrogen was added potassium *tert*-butoxide (1 M in tetrahydrofuran, 6.75 mL, 6.75 mmol) over 3 min while keeping internal temperature under 5 °C. The resulting red solution was allowed to warm to room temperature over 30 min and was then cooled back down to 3 °C, at which point a solution of **52** (949 mg, 2.20 mmol) in anhydrous tetrahydrofuran (6 mL) was added over 2 min while ensuring that the internal temperature remained below 6 °C. The reaction mixture was allowed to stir at 3–6 °C for 20 min, was warmed to room temperature over 30 min and was then cooled back down to 14 °C (internal), at which point saturated aqueous sodium bicarbonate solution was added. The mixture was extracted with ethyl acetate (3 \times), and the combined organic layers were dried over sodium sulfate, filtered, and concentrated under reduced pressure. Silica gel chromatography (gradient: 0–75% ethyl acetate in heptane) was isolated as an oil, which by 1H NMR analysis consisted of a roughly 1:1 mixture of the *E* and *Z* enol ethers. Yield: 795 mg, 1.73 mmol, 78.6%. LCMS m/z 459.2 $[M + H]^+$. 1H NMR (400 MHz, $CDCl_3$) δ 8.23 (d, $J = 7.2$ Hz, 2H), 7.48–7.55 (m, 1H), 7.33–7.48 (m, 3H), 6.82–6.97 (m, 2H), [6.69 (d, $J = 12.7$ Hz) and 5.99 (dd, $J = 6.2, 0.7$ Hz), total 1H], [4.86 (dd, $J = 12.7, 8.0$ Hz) and 4.55 (dd, half of ABX pattern, $J = 8.2, 6.3$ Hz), total 1H], [4.66–4.58 (m) and 4.11–4.04 (m), total 1H], [4.21 (dd, $J = 12.2, 1.7$ Hz) and 4.19 (dd, $J = 12.3, 1.8$ Hz), total 1H], [3.82 (d, $J = 12.3$ Hz) and 3.80 (d, $J = 12.3$ Hz), total 1H], [3.66 (s) and 3.55 (s), total 3H], 3.22–3.31 (m, 1H), 2.91–3.01 (m, 1H), 1.68–1.87 (m, 2H), [1.26 (d, $J = 7.0$ Hz) and 1.26 (d, $J = 7.0$ Hz), total 3H].

N-[(4*R*,4*aR*,6*R*,8*aS*)-8*a*-(2,4-Difluorophenyl)-4-methyl-6-(1,1,3,3-tetramethoxypropan-2-yl)-4,4*a*,5,6,8,8*a*-hexahydropyrano[3,4-*d*]-[1,3]thiazin-2-yl]benzamide (**73**). To a solution of **55** (795 mg, 1.73 mmol) in dichloromethane (3.5 mL) cooled to 1.6 °C internal was added trimethyl orthoformate (0.389 mL, 0.861 mmol) followed by dropwise addition of boron trifluoride diethyl etherate (0.221 mL, 1.76 mmol) at such a rate to never exceed 3 °C, resulting in a yellow solution. The reaction was stirred at 0 °C (external) for 1.5 h then partitioned between dichloromethane and saturated aqueous sodium bicarbonate solution. The aqueous layer was extracted with dichloromethane, and the combined organic layers were washed with saturated aqueous sodium chloride solution, dried over sodium sulfate, filtered, and concentrated in vacuo to give the crude product. Silica gel chromatography (30% ethyl acetate in heptanes isocratic) provided the product. Yield: 297 mg white solid, 0.52 mmol, 30.3%. LCMS m/z

565.4 [M + H]⁺. ¹H NMR (400 MHz, CDCl₃) δ 8.23 (d, J = 7.04 Hz, 2H), 7.35–7.51 (m, 4H), 6.84–6.95 (m, 2H), 4.56 (d, J = 5.5 Hz, 1H), 4.50 (d, J = 4.1 Hz, 1H), 4.15 (dd, J = 1.1, 12.23 Hz, 1H), 4.02–4.08 (m, 1H), 3.79 (d, J = 12.1 Hz, 1H), 3.42 (s, 3H), 3.40 (s, 3H), 3.38 (s, 3H), 3.37 (s, 3H), 3.26 (dd, J = 2.7, 7.4 Hz, 1H), 2.89–2.95 (m, 1H), 2.14 (td, J = 3.8, 5.09 Hz, 1H), 1.98–2.10 (m, 1H), 1.70–1.77 (m, 1H), 1.26 (d, J = 7.0 Hz, 3H).

(4*R*,4*aR*,6*R*,8*aS*)-8*a*-(2,4-Difluorophenyl)-4-methyl-6-(1-methyl-1*H*-pyrazol-4-yl)-4,4*a*,5,6,8,8*a*-hexahydropyrano[3,4-*d*][1,3]thiazin-2-amine (11). *N*-[(4*R*,4*aR*,6*R*,8*aS*)-8*a*-(2,4-Difluorophenyl)-4-methyl-6-(1,1,3,3-tetramethoxypropan-2-yl)-4,4*a*,5,6,8,8*a*-hexahydropyrano[3,4-*d*][1,3]thiazin-2-yl]benzamide (73) (297 mg, 0.526 mmol) was combined with ethanol (1.75 mL) and methyl hydrazine (36.4 mg, 0.789 mmol), followed by addition of water (0.6 mL). Concentrated sulfuric acid (55 μL, 1.0 mmol) was slowly added, and the reaction mixture was heated at 70 °C for 18 h. Saturated aqueous sodium bicarbonate solution was added, and the aqueous layer was extracted three times with ethyl acetate; the combined organic layers were extracted three times with 0.2 M aqueous hydrochloric acid, and the combined aqueous layers were washed with ethyl acetate. The pH was adjusted to 9–10 by addition of 1 M aqueous sodium hydroxide solution, and the mixture was extracted three times with ethyl acetate. The combined organic layers were dried over sodium sulfate, filtered, and concentrated under reduced pressure. Silica gel chromatography (gradient: 0–15% methanol in dichloromethane) provided the product as an off-white solid. Yield: 109 mg, 0.287 mmol, 55%. LCMS *m/z* 379.2 [M + H]⁺. ¹H NMR (400 MHz, CD₃OD) δ 7.48 (s, 1H), 7.36 (s, 1H), 7.22–7.28 (m, 1H), 6.85–6.92 (m, 2H), 4.57 (dd, J = 11.3, 2.3 Hz, 1H), 4.16 (dd, J = 11.1, 2.1 Hz, 1H), 3.76 (s, 3H), 3.69 (d, J = 11.3, 1H), 3.01–3.06 (m, 1H), 2.78 (dt, J = 11.9, 3.8 Hz, 1H), 1.75–1.80 (m, 1H), 1.59–1.68 (m, 1H), 1.10 (d, J = 7 Hz, 3H); [α]_D²⁴ = +24.52 (c = 0.31 g/100 mL; MeOH).

(4*R*,4*aR*,6*R*,8*aS*)-2-(Benzoylamino)-8*a*-(2,4-difluorophenyl)-4-methyl-4,4*a*,5,6,8,8*a*-hexahydropyrano[3,4-*d*][1,3]thiazine-6-carboxylic Acid (46). Tetrapropylammonium perruthenate (0.250 g, 0.711 mmol) was added in four equal portions to a mixture of 38 (3.24 g, 7.50 mmol) and 4-methylmorpholine *N*-oxide monohydrate (5.0 g, 37.0 mmol) in acetonitrile (20 mL). An exotherm was observed; the reaction flask was cooled in an ice–methanol slurry as needed and stirred for 2 h. 2-Propanol (15 mL) was added, and stirring was continued for 1 h at room temperature. After removal of solvent in vacuo, the residue was partitioned between dichloromethane (70 mL) and aqueous hydrochloric acid (1 M, 50 mL). The aqueous layer was extracted with dichloromethane (2 × 30 mL), and the combined organic layers were extracted with aqueous sodium hydroxide solution (0.25 M, 3 × 60 mL). The combined aqueous layers were adjusted to pH 1–2 with 5 M aqueous hydrochloric acid, and then extracted with dichloromethane (3 × 65 mL). The combined organic layers were dried over sodium sulfate, filtered, and concentrated under reduced pressure; purification via silica gel chromatography [gradient: 0–100% (89:10:1 dichloromethane/methanol/acetic acid) in dichloromethane] provided material that was then coconcentrated with toluene (3 × 5 mL). The resulting solid was partitioned between dichloromethane (20 mL) and aqueous sodium hydroxide solution (0.25 M, 60 mL). The organic layer was extracted with additional aqueous sodium hydroxide solution (0.25 M, 10 mL), and the combined aqueous layers were adjusted to pH 1–2 with 5 M aqueous hydrochloric acid. The aqueous layer was extracted with dichloromethane (3 × 50 mL), and the combined organic layers were dried over sodium sulfate, filtered, and concentrated in vacuo to afford the product as an off-white granular solid. Yield: 3.1 g, 6.85 mmol, 91%. LCMS *m/z* 447.1 [M + H]⁺. ¹H NMR (400 MHz, (CD₃)₂SO) δ 8.10–8.15 (m, 2H), 7.55–7.61 (m, 1H), 7.47–7.53 (m, 2H), 7.32–7.44 (m, 2H), 7.22 (ddd, J = 8.5, 8.5, 2.5 Hz, 1H), 4.28 (dd, J = 11.8, 2.4 Hz, 1H), 4.01 (br AB quartet, *J*_{AB} = 12 Hz, Δ*ν*_{AB} = 12 Hz, 2H), 3.06–3.16 (m, 1H), 2.95–3.04 (m, 1H), 1.99–2.07 (m, 1H), 1.53–1.66 (m, 1H), 1.21 (d, J = 6.9 Hz, 3H).

(4*R*,4*aR*,6*R*,8*aS*)-2-Benzamido-8*a*-(2,4-difluorophenyl)-*N*-(1-hydroxypropan-2-yl)-4-methyl-4,4*a*,5,6,8,8*a*-hexahydropyrano[3,4-*d*][1,3]thiazine-6-carboxamide (58). To a solution of (4*R*,4*aR*,6*R*,8*aS*)-

2-benzamido-8*a*-(2,4-difluorophenyl)-4-methyl-4,4*a*,5,6,8,8*a*-hexahydropyrano[3,4-*d*][1,3]thiazine-6-carboxylic acid 46 (2.68 g, 6.00 mmol) in dry dimethylformamide (15 mL) under nitrogen was added *N,N*-diisopropylethylamine (>99% Aldrich, 2.1 mL, 12 mmol). After 2 min, 2-(2-pyridon-1-yl)-1,1,3,3-tetramethyluronium tetrafluoroborate (TPTU, 2.0 g, 6.733 mmol) was added in one portion. The reaction was stirred at ambient temperature for 30 min. Additional TPTU (200 mg, 0.673 mmol) was added and further stirred at the same temperature for 35 min. At this point, 2-amino-1-propanol (98% from Aldrich, 1.0 mL, 12.6 mmol) was added and allowed to stir for 18 h at ambient temperature. At this time, the reaction was concentrated in vacuo to afford a thick amber gum, which was partitioned between ethyl acetate (120 mL) and 0.1 N HCl (120 mL). The phases were separated, and the aqueous layer extracted with additional ethyl acetate (1 × 40 mL). The combined organic extracts were washed with saturated aqueous Na₂CO₃ (100 mL), followed by water (100 mL) then brine (100 mL). The organic extract was dried over Na₂SO₄, filtered, and concentrated to afford (4*R*,4*aR*,6*R*,8*aS*)-2-benzamido-8*a*-(2,4-difluorophenyl)-*N*-(1-hydroxypropan-2-yl)-4-methyl-4,4*a*,5,6,8,8*a*-hexahydropyrano[3,4-*d*][1,3]thiazine-6-carboxamide as pale-tan solid. Yield: 2.730 g, 5.4 mmol, 90.3% yield. LCMS *m/z* 504.3 [M + H]⁺. ¹H NMR (400 MHz, CDCl₃) δ 8.21 (d, J = 7.8 Hz, 2H), 7.50–7.57 (m, 1H), 7.43–7.50 (m, 2H), 7.33–7.43 (m, 1H), 6.85–6.99 (m, 2H), 6.73 (d, J = 7.0 Hz, 0.5H), 6.66 (d, J = 7.4 Hz, 0.5H), 4.21 (d, J = 12.1 Hz, 1H), 3.99–4.10 (m, 1H), 3.90 (d, J = 12.5 Hz, 1H), 3.50–3.73 (m, 2H), 3.28 (m, 1H), 2.96 (m, 1H), 2.33 (m, 1H), 1.68–1.82 (m, 1H), 1.24–1.37 (m, 3H, pair of methyl doublets), 1.20 (m, 3H, pair of methyl doublets).

(4*R*,4*aR*,6*R*,8*aS*)-2-Benzamido-8*a*-(2,4-difluorophenyl)-4-methyl-*N*-(1-oxopropan-2-yl)-4,4*a*,5,6,8,8*a*-hexahydropyrano[3,4-*d*][1,3]thiazine-6-carboxamide (61). To a stirring solution of (4*R*,4*aR*,6*R*,8*aS*)-2-benzamido-8*a*-(2,4-difluorophenyl)-*N*-(1-hydroxypropan-2-yl)-4-methyl-4,4*a*,5,6,8,8*a*-hexahydropyrano[3,4-*d*][1,3]thiazine-6-carboxamide 58 (975.0 mg, 1.94 mmol) in anhydrous dichloromethane (9.0 mL, c = 0.22 M) at ambient temperature under N₂ was added Dess–Martin periodinane (1000.0 mg, 2.3 mmol) in one solid portion. The reaction was stirred at ambient temperature for 2.5 h. At this time, the reaction was diluted with DCM (80 mL) and quenched with saturated aqueous NaHCO₃ (60 mL) and saturated aqueous sodium thiosulfate (60 mL). The mixture was stirred for 20 min then the phases were separated. The aqueous phase was washed with dichloromethane (2 × 40 mL); the combined organic extracts were washed with brine (75 mL), dried (Na₂SO₄), filtered, and concentrated in vacuo to afford a pale-tan solid. This material was chromatographed on silica gel to afford (4*R*,4*aR*,6*R*,8*aS*)-2-benzamido-8*a*-(2,4-difluorophenyl)-4-methyl-*N*-(1-oxopropan-2-yl)-4,4*a*,5,6,8,8*a*-hexahydropyrano[3,4-*d*][1,3]thiazine-6-carboxamide as a 1:1 mixture of diastereomers. Yield: 588.0 mg, 1.18 mmol, 60.6%. LCMS *m/z* 502.4 [M + H]⁺. ¹H NMR (400 MHz, CDCl₃) δ 9.56 (s, 0.5H, first diastereomer), 9.53 (s, 0.5H, second diastereomer), 8.21 (d, J = 6.63 Hz, 2H), 7.50–7.57 (m, 1H), 7.43–7.50 (m, 2H), 7.34–7.43 (m, 1H), 7.02–7.09 (m, 1H), 6.85–6.99 (m, 2H), 4.50 (quin, J = 7.3 Hz, 1H), 4.41 (quin, J = 7.2 Hz, 1H), 4.15–4.27 (m, 2H), 3.94 (d, J = 12.1 Hz, 1H), 3.28 (dd, J = 3.5, 6.6 Hz, 1H), 2.96 (d, J = 12.5 Hz, 1H), 2.31 (dd, J = 3.5, 14.05 Hz, 1H), 1.72–1.87 (m, 1H), 1.39 (m, 3H pair of methyl doublets), 1.30 (m, 3H, pair of methyl singlets).

N-((4*R*,4*aR*,6*R*,8*aS*)-8*a*-(2,4-Difluorophenyl)-4-methyl-6-(4-methyloxazol-2-yl)-4,4*a*,5,6,8,8*a*-hexahydropyrano[3,4-*d*][1,3]thiazin-2-yl)benzamide (64). (4*R*,4*aR*,6*R*,8*aS*)-2-Benzamido-8*a*-(2,4-difluorophenyl)-4-methyl-*N*-(1-oxopropan-2-yl)-4,4*a*,5,6,8,8*a*-hexahydropyrano[3,4-*d*][1,3]thiazine-6-carboxamide 61 (292.0 mg, 1.10 mmol) and Burgess reagent (1-methoxy-*N*-triethylammoniosulfonylethanimidate, 350.0 mg, 1.47 mmol) were combined in anhydrous THF (11.0 mL, c = 0.0997 M) in a 20 mL microwave vial and vortexed until homogeneous. With stirring, the solution was microwaved at 120 °C for 2 min. The vial was cooled and uncapped, and the reaction concentrated in vacuo to a thick gum. This material was purified via silica chromatography (gradient: 0–100% ethyl acetate in heptanes) to afford *N*-((4*R*,4*aR*,6*R*,8*aS*)-8*a*-(2,4-difluorophenyl)-4-methyl-6-(4-methyloxazol-2-yl)-4,4*a*,5,6,8,8*a*-hexahydropyrano[3,4-*d*]-

[1,3]thiazin-2-yl)benzamide. Yield: 292 mg, 0.61 mmol, 55.1%. LCMS m/z 484.4 [M + H]⁺. ¹H NMR (400 MHz, CDCl₃) δ 8.18 (d, J = 7.8 Hz, 2H), 7.31–7.64 (m, 5H), 6.82–7.08 (m, 2H), 4.83 (d, J = 11.2 Hz, 1H), 4.33 (d, J = 12.1 Hz, 1H), 3.97 (d, J = 11.7 Hz, 1H), 3.21–3.35 (m, 1H), 3.02 (m, 1H), 2.27 (m, 1H), 2.10–2.20 (m, 4H), 1.31 (d, J = 7.0 Hz, 3H).

(4*R*,4*aR*,6*R*,8*aS*)-8*a*-(2,4-Difluorophenyl)-4-methyl-6-(4-methyl-oxazol-2-yl)-4,4*a*,5,6,8,8*a*-hexahydropyrano[3,4-*d*][1,3]thiazin-2-amine (**9**). *N*-((4*R*,4*aR*,6*R*,8*aS*)-8*a*-(2,4-Difluorophenyl)-4-methyl-6-(4-methyl-oxazol-2-yl)-4,4*a*,5,6,8,8*a*-hexahydropyrano[3,4-*d*][1,3]thiazin-2-yl)benzamide **64** (285 mg, 0.589 mmol) was dissolved in anhydrous methanol (3.50 mL, 0.168 M). DBU (60.0 μ L, 0.401 mmol) was then added. The mixture was stirred in a tightly capped vial at 60 °C for 16 h, at which time it was concentrated under N₂, transferred to scintillation vial with ethyl acetate (3 mL), and then diluted with ethyl acetate (10 mL) and water (4 mL). The phases were separated, and the aqueous layer extracted with additional ethyl acetate (10 mL). The combined organic extracts were dried over magnesium sulfate, filtered, and concentrated in vacuo. The crude residue obtained was chromatographed on silica (gradient: 0–15% methanol in dichloromethane) to afford (4*R*,4*aR*,6*R*,8*aS*)-8*a*-(2,4-difluorophenyl)-4-methyl-6-(4-methyl-oxazol-2-yl)-4,4*a*,5,6,8,8*a*-hexahydropyrano[3,4-*d*][1,3]thiazin-2-amine as white solid. Yield: 187 mg, 0.49 mmol, 83.6%. LCMS m/z 380.5 [M + H]⁺. ¹H NMR (400 MHz, CDCl₃) δ 7.42 (dt, J = 6.7, 9.0 Hz, 1H), 7.35 (d, J = 1.2 Hz, 1H), 6.76–6.90 (m, 2H), 5.32 (br s, 1H), 4.78 (dd, J = 2.6, 11.6 Hz, 1H), 4.26 (dd, J = 2.1, 11.1 Hz, 1H), 3.99 (d, J = 10.9 Hz, 1H), 3.17 (dq, J = 3.3, 6.9 Hz, 1H), 2.78 (td, J = 3.9, 12.0 Hz, 1H), 2.20 (d, J = 1.2 Hz, 3H), 1.99–2.10 (m, 1H), 1.89–1.96 (m, 1H), 1.21 (d, J = 7.0 Hz, 3H); [α]_D^{23.0} = +28.89 (c = 0.36 g/100 mL; MeOH).

(4*aR*,6*R*,8*aS*)-2-(Benzoylamino)-8*a*-(2,4-difluorophenyl)-4,4*a*,5,6,8,8*a*-hexahydropyrano[3,4-*d*][1,3]thiazine-6-carboxylic Acid (**45**). Tetrapropylammonium perruthenate (1.09 g, 3.10 mmol) was added to a mixture of **44** (13.0 g, 31.1 mmol) and 4-methylmorpholine *N*-oxide monohydrate (25.2 g, 186 mmol) in acetonitrile (207 mL), and the reaction mixture was stirred for 90 min at room temperature. After addition of 2-propanol (100 mL), it was stirred for an additional 2 h and then concentrated in vacuo. The residue was partitioned between ethyl acetate and 0.5 M aqueous sodium hydroxide solution. The organic layer was extracted twice with 0.5 M aqueous sodium hydroxide solution, and the combined aqueous layers were acidified to a pH of approximately 1 with 2 M aqueous hydrochloric acid then extracted three times with ethyl acetate. The combined ethyl acetate layers were dried over sodium sulfate, filtered, and concentrated under reduced pressure; the residue was dissolved in dichloromethane, washed with water and with saturated aqueous sodium chloride solution, dried over sodium sulfate, filtered, and concentrated in vacuo. Purification via chromatography on silica gel (gradient: 0–20% methanol in dichloromethane) provided the product as a reddish solid. Yield: 12.36 g, 28.58 mmol, 92%. LCMS m/z 433.2 [M + H]⁺. ¹H NMR (400 MHz, CD₃OD) δ 8.09–8.13 (m, 2H), 7.52–7.57 (m, 1H), 7.43–7.51 (m, 3H), 7.03–7.11 (m, 2H), 4.35 (dd, J = 11.2, 3.4 Hz, 1H), 4.19 (dd, J = 12.0, 1.4 Hz, 1H), 3.97 (d, J = 12.1 Hz, 1H), 3.20–3.27 (m, 1H), 2.96 (dd, half of ABX pattern, J = 13.1, 4.0 Hz, 1H), 2.78 (dd, half of ABX pattern, J = 13.2, 2.8 Hz, 1H), 2.03–2.15 (m, 2H).

(4*aR*,6*R*,8*aS*)-2-Benzamido-8*a*-(2,4-difluorophenyl)-*N*-(2,2-dimethoxyethyl)-4,4*a*,5,6,8,8*a*-hexahydropyrano[3,4-*d*][1,3]thiazine-6-carboxamide (**66**). A mixture of (4*aR*,6*R*,8*aS*)-2-(benzoylamino)-8*a*-(2,4-difluorophenyl)-4,4*a*,5,6,8,8*a*-hexahydropyrano[3,4-*d*][1,3]thiazine-6-carboxylic acid **45** [1.26 g, 2.91 mmol; this material had been azeotroped with toluene (2 \times 5 mL)], *N,N*-diisopropylethylamine (1.02 mL, 5.86 mmol), and 2-[2-oxo-1(2*H*)-pyridyl]-1,1,3,3-tetramethyluronium tetrafluoroborate (TPTU, 866 mg, 2.91 mmol) in *N,N*-dimethylformamide (10 mL) was stirred at room temperature for 25 min. 2,2-Dimethoxyethanamine (0.95 mL, 8.7 mmol) was added, and stirring was continued for 18 h, at which time the reaction mixture was diluted with saturated aqueous sodium bicarbonate solution (15 mL) and water (15 mL) and extracted with diethyl ether (3 \times 40 mL). The combined organic layers were dried over sodium sulfate, filtered,

and concentrated in vacuo. The resulting oil was combined with material derived from a similar reaction carried out on C19 (131 mg, 0.303 mmol) and purified via silica gel chromatography (gradient: 0–100% ethyl acetate in heptane) to afford (4*aR*,6*R*,8*aS*)-2-benzamido-8*a*-(2,4-difluorophenyl)-*N*-(2,2-dimethoxyethyl)-4,4*a*,5,6,8,8*a*-hexahydropyrano[3,4-*d*][1,3]thiazine-6-carboxamide as a white solid. Yield: 618 mg, 1.19 mmol, 37%. LCMS m/z 520.3 [M + H]⁺. ¹H NMR (400 MHz, CDCl₃) δ 8.17–8.28 (br m, 2H), 7.50–7.56 (m, 1H), 7.36–7.49 (m, 3H), 6.86–6.99 (m, 2H), 6.74 (br t, J = 6.0 Hz, 1H), 4.38 (t, J = 5.3 Hz, 1H), 4.15–4.24 (m, 2H), 3.90 (d, J = 12.3 Hz, 1H), 3.48–3.57 (m, 1H), 3.37 (s, 3H), 3.36 (s, 3H), 3.28–3.36 (m, 1H), 3.13–3.23 (br m, 1H), 3.03 (dd, J = 12.9, 3.9 Hz, 1H), 2.70 (br d, J = 13 Hz, 1H), 2.20–2.29 (m, 1H), 2.00–2.13 (m, 1H).

(4*aR*,6*R*,8*aS*)-2-Benzamido-8*a*-(2,4-difluorophenyl)-*N*-(2-oxoethyl)-4,4*a*,5,6,8,8*a*-hexahydropyrano[3,4-*d*][1,3]thiazine-6-carboxamide (**67**). (4*aR*,6*R*,8*aS*)-2-(Benzoylamino)-8*a*-(2,4-difluorophenyl)-*N*-(2,2-dimethoxyethyl)-4,4*a*,5,6,8,8*a*-hexahydropyrano[3,4-*d*][1,3]thiazine-6-carboxamide **66** (620 mg, 1.19 mmol) was dissolved in tetrahydrofuran (3.0 mL) and aqueous hydrochloric acid (2 M, 3 mL, 6 mmol) and stirred for 18 h at 38 °C. After cooling to room temperature, the reaction mixture was diluted with saturated aqueous sodium chloride solution (7 mL) and extracted with ethyl acetate (6 \times 10 mL). The combined organic layers were dried over sodium sulfate, filtered, and concentrated under reduced pressure. Purification via silica gel chromatography (gradient: 50–100% ethyl acetate in heptane) provided (4*aR*,6*R*,8*aS*)-2-benzamido-8*a*-(2,4-difluorophenyl)-*N*-(2-oxoethyl)-4,4*a*,5,6,8,8*a*-hexahydropyrano[3,4-*d*][1,3]thiazine-6-carboxamide as an off-white solid. Yield: 352 mg, 0.743 mmol, 62%. LCMS m/z 474.2 [M + H]⁺. ¹H NMR (400 MHz, CDCl₃) δ 9.63 (s, 1H), 8.34–8.44 (br m, 2H), 7.64–7.71 (br m, 1H), 7.54–7.62 (br m, 1H), 7.40–7.51 (br m, 1H), 7.28–7.37 (br m, 1H), 7.00–7.10 (br m, 1H), 6.91–7.00 (br m, 1H), 4.36–4.50 (br m, 1H), 4.23–4.35 (br m, 2H), 4.19 (br d, J = 11.0 Hz, 1H), 4.00–4.11 (br m, 1H), 3.29–3.46 (br m, 1H), 3.01–3.13 (br m, 1H), 2.76–2.89 (br m, 1H), 2.28–2.44 (br m, 1H), 1.85–2.02 (br m, 1H).

N-((4*aR*,6*R*,8*aS*)-8*a*-(2,4-difluorophenyl)-6-(oxazol-2-yl)-4,4*a*,5,6,8,8*a*-hexahydropyrano[3,4-*d*][1,3]thiazin-2-yl)benzamide (**68**). A mixture of (4*aR*,6*R*,8*aS*)-2-(benzoylamino)-8*a*-(2,4-difluorophenyl)-*N*-(2-oxoethyl)-4,4*a*,5,6,8,8*a*-hexahydropyrano[3,4-*d*][1,3]thiazine-6-carboxamide **67** [38 mg, 80 μ mol; this material had been azeotroped with toluene (2 \times 2 mL)], and Burgess reagent (1-methoxy-*N*-triethylammoniosulfonylmethanimidate, 38.1 mg, 0.160 mmol) in tetrahydrofuran (2.5 mL) was heated at reflux for 1.5 h, at which time it was cooled to room temperature and treated with additional Burgess reagent (19 mg, 80 μ mol). After an additional 3 h of heating at reflux, the reaction mixture was again allowed to cool to room temperature then concentrated in vacuo. Purification via silica gel chromatography (gradient: 0–100% ethyl acetate in heptane) afforded *N*-((4*aR*,6*R*,8*aS*)-8*a*-(2,4-difluorophenyl)-6-(oxazol-2-yl)-4,4*a*,5,6,8,8*a*-hexahydropyrano[3,4-*d*][1,3]thiazin-2-yl)benzamide as a white solid. Yield: 12 mg, 26 μ mol, 32%. LCMS m/z 456.2 [M + H]⁺. ¹H NMR (400 MHz, CD₃OD) δ 8.11 (br d, J = 7.4 Hz, 2H), 7.92–7.93 (m, 1H), 7.43–7.58 (m, 4H), 7.17–7.18 (m, 1H), 7.04–7.14 (m, 2H), 4.97 (dd, J = 12, 2 Hz, 1H), 4.32 (br d, J = 12 Hz, 1H), 4.01 (d, J = 11.9 Hz, 1H), 3.3–3.37 (m, 1H, assumed; obscured by solvent peak), 3.00 (dd, half of ABX pattern, J = 13.1, 4.1 Hz, 1H), 2.82 (dd, half of ABX pattern, J = 13, 2.6 Hz, 1H), 2.40–2.52 (m, 1H), 2.04–2.11 (m, 1H).

(4*aR*,6*R*,8*aS*)-8*a*-(2,4-Difluorophenyl)-6-(oxazol-2-yl)-4,4*a*,5,6,8,8*a*-hexahydropyrano[3,4-*d*][1,3]thiazin-2-amine (**2**). *N*-[(4*aR*,6*R*,8*aS*)-8*a*-(2,4-Difluorophenyl)-6-(1,3-oxazol-2-yl)-4,4*a*,5,6,8,8*a*-hexahydropyrano[3,4-*d*][1,3]thiazin-2-yl]benzamide **68** (25.0 mg, 54.9 μ mol) was combined with methanol (2.0 mL) and 1,8-diazabicyclo[5.4.0]undec-7-ene (2 drops) and heated to 75 °C for 18 h. The reaction mixture was cooled and concentrated in vacuo; purification using silica gel chromatography (gradient: 0–10% methanol in dichloromethane) provided (4*aR*,6*R*,8*aS*)-8*a*-(2,4-difluorophenyl)-6-(oxazol-2-yl)-4,4*a*,5,6,8,8*a*-hexahydropyrano[3,4-*d*][1,3]thiazin-2-amine as a white solid. Yield: 11.2 mg, 31.9 μ mol, 58%. LCMS m/z 352.1 [M + H]⁺. ¹H NMR (400 MHz, CD₃OD) δ 7.92 (d,

$J = 0.8$ Hz, 1H), 7.38 (ddd, $J = 9.6, 8.8, 6.6$ Hz, 1H), 7.17 (d, $J = 0.8$ Hz, 1H), 6.95–7.04 (m, 2H), 4.87 (dd, $J = 11.9, 2.3$ Hz, 1H), 4.27 (dd, $J = 11.2, 2.0$ Hz, 1H), 3.80 (d, $J = 11.3$ Hz, 1H), 3.03–3.10 (m, 1H), 2.93 (dd, half of ABX pattern, $J = 12.6, 4.2$ Hz, 1H), 2.76 (dd, half of ABX pattern, $J = 12.6, 2.8$ Hz, 1H), 2.35–2.46 (m, 1H), 1.90 (ddd, $J = 13.3, 4.1, 2.5$ Hz, 1H); $[\alpha]_{\text{D}}^{24} = +12.78$ ($c = 0.36$ g/100 mL; MeOH).

(4aR,6R,8aS)-2-Benzamido-8a-(2,4-difluorophenyl)-N-(1-hydroxypropan-2-yl)-4,4a,5,6,8,8a-hexahydropyrano[3,4-d][1,3]thiazine-6-carboxamide (57). To a round bottomed flask under nitrogen were added (4aR,6R,8aS)-2-benzamido-8a-(2,4-difluorophenyl)-4,4a,5,6,8,8a-hexahydropyrano[3,4-d][1,3]thiazine-6-carboxylic acid 45 (2.60 g, 6.0 mmol), dimethylformamide (87.1 mL, 0.069 M), diisopropylethylamine (2.09 mL, 12.0 mmol), and 2-(2-pyridon-1-yl)-1,1,3,3-tetramethyluronium tetrafluoroborate (1.96 g, 6.61 mmol). The mixture was stirred at ambient temperature for 30 min, at which point 2-amino-1-propanol (1.81 g, 24.0 mmol) was added. The mixture was stirred at ambient temperature for 18 h, after which it was diluted with saturated aqueous sodium bicarbonate solution and extracted with methyl *t*-butyl ether (3 \times). The combined organic extracts were washed with brine (1 \times), dried over Na₂SO₄, filtered, and concentrated to afford a material which was purified by silica gel chromatography (gradient: 0–100% ethyl acetate in heptane). (4aR,6R,8aS)-2-Benzamido-8a-(2,4-difluorophenyl)-N-(1-hydroxypropan-2-yl)-4,4a,5,6,8,8a-hexahydropyrano[3,4-d][1,3]thiazine-6-carboxamide was obtained as a yellow foam. Yield: 2.86 g, 5.82 mmol, 97%, as a 1:1 mixture of diastereomers. LCMS m/z 490.2 [M + H]⁺. ¹H NMR (400 MHz, CD₃OD) δ 8.11 (d, $J = 6.9$ Hz, 2H), 7.98 (s, 1H), 7.34–7.74 (m, 5H), 6.98–7.19 (m, 2H), 4.17–4.25 (m, 2H), 3.97–4.12 (m, 2H), 3.50 (dd, $J = 5.5, 6.5$ Hz, 2H), 3.2–3.2 (br s, 1H), 2.95–2.98 (m, 1H), 2.78–2.82 (m, 3H), 2.11–2.15 (m, 1H), 1.86–2.01 (m, 1H), 1.15 (m, 3H).

(4aR,6R,8aS)-2-Benzamido-8a-(2,4-difluorophenyl)-N-(1-oxopropan-2-yl)-4,4a,5,6,8,8a-hexahydropyrano[3,4-d][1,3]thiazine-6-carboxamide (60). (4aR,6R,8aS)-2-Benzamido-8a-(2,4-difluorophenyl)-N-(1-hydroxypropan-2-yl)-4,4a,5,6,8,8a-hexahydropyrano[3,4-d][1,3]thiazine-6-carboxamide 57 (2.86 g, 5.84 mmol) and Dess–Martin periodinane (4.96 g, 11.7 mmol) were combined in anhydrous methylene chloride (97 mL, 0.06 M) in a round-bottom flask at ambient temperature under nitrogen. The mixture was stirred at RT for 3 h, at which point the mixture was then diluted with saturated aqueous sodium bicarbonate solution (150 mL) and saturated aqueous sodium thiosulfate (150 mL) and stirred at ambient temperature for 20 min. The resulting solution was extracted with ethyl acetate (3 \times). The combined ethyl acetate extracts were dried over Na₂SO₄, filtered, and concentrated to afford a material which was purified by silica gel chromatography (gradient: 50–100% ethyl acetate/heptanes gradient). (4aR,6R,8aS)-2-Benzamido-8a-(2,4-difluorophenyl)-N-(1-oxopropan-2-yl)-4,4a,5,6,8,8a-hexahydropyrano[3,4-d][1,3]thiazine-6-carboxamide was isolated as a yellow foam as a 1:1 mixture of diastereomers. Yield: 2.11 g, 4.33 mmol, 74.1%. LCMS m/z 488.1 [M + H]⁺. ¹H NMR (400 MHz, CDCl₃) δ 9.56 (s, 0.5H, first diastereomer), 9.53 (s, 0.5H, second diastereomer), 8.16–8.28 (m, 2H), 7.35–7.57 (m, 4H), 6.85–7.12 (m, 3H), 4.45–4.55 (m, 1H), 4.37–4.45 (m, 1H), 4.19–4.28 (m, 2H), 3.90–3.96 (m, 1H), 3.14–3.24 (m, 1H), 3.00–3.07 (m, 1H), 2.67–2.75 (m, 1H), 2.20–2.30 (m, 1H), 2.06–2.17 (m, 1H), 1.39 (m, 3H).

N-((4aR,6R,8aS)-8a-(2,4-Difluorophenyl)-6-(4-methyloxazol-2-yl)-4,4a,5,6,8,8a-hexahydropyrano[3,4-d][1,3]thiazin-2-yl)benzamide (63). A mixture of (4aR,6R,8aS)-2-(benzoylamino)-8a-(2,4-difluorophenyl)-N-(1-oxopropan-2-yl)-4,4a,5,6,8,8a-hexahydropyrano[3,4-d][1,3]thiazine-6-carboxamide 60 (2.11 g, 4.33 mmol) and Burgess reagent (1-methoxy-*N*-triethylammoniosulfonylmethanimidate, 2.58 g, 10.8 mmol) in toluene (100 mL) was heated at 65 °C for 18 h then cooled to room temperature and concentrated in vacuo. The residue was partitioned between ethyl acetate and saturated aqueous sodium bicarbonate solution; the aqueous layer was extracted twice with ethyl acetate, and the combined organic layers were washed with saturated aqueous sodium chloride solution, dried over sodium sulfate, filtered, and concentrated under reduced pressure. Silica gel chromatography

(gradient: 0–100% ethyl acetate in heptane) provided *N*-((4aR,6R,8aS)-8a-(2,4-difluorophenyl)-6-(4-methyloxazol-2-yl)-4,4a,5,6,8,8a-hexahydropyrano[3,4-d][1,3]thiazin-2-yl)benzamide as a yellow solid. Yield: 1.0 g, 2.1 mmol, 48%. LCMS m/z 470.2 [M + H]⁺. ¹H NMR (400 MHz, CD₃OD), observed peaks: δ 8.12 (br d, $J = 7.0$ Hz, 2H), 7.61 (q, $J = 1.3$ Hz, 1H), 7.42–7.57 (m, 4H), 7.03–7.13 (m, 2H), 4.90 (dd, $J = 11.8, 2.4$ Hz, 1H), 4.30 (dd, $J = 11.9, 1.6$ Hz, 1H), 3.99 (d, $J = 11.9$ Hz, 1H), 2.99 (dd, half of ABX pattern, $J = 13.2, 4.2$ Hz, 1H), 2.81 (dd, half of ABX pattern, $J = 13.2, 2.8$ Hz, 1H), 2.37–2.50 (m, 1H), 2.14 (d, $J = 1.2$ Hz, 3H), 2.01–2.08 (m, 1H).

(4aR,6R,8aS)-8a-(2,4-Difluorophenyl)-6-(4-methyloxazol-2-yl)-4,4a,5,6,8,8a-hexahydropyrano[3,4-d][1,3]thiazin-2-amine (3). A mixture of *N*-[(4aR,6R,8aS)-8a-(2,4-difluorophenyl)-6-(4-methyl-1,3-oxazol-2-yl)-4,4a,5,6,8,8a-hexahydropyrano[3,4-d][1,3]thiazin-2-yl]benzamide 63 (1.0 g, 2.1 mmol) and 1,8-diazabicyclo[5.4.0]undec-7-ene (0.335 mL, 2.13 mmol) in methanol (34 mL) was heated to 70 °C for 18 h then cooled to room temperature and added to an aqueous solution of sodium bicarbonate. The mixture was extracted three times with ethyl acetate, and the combined organic layers were washed with saturated aqueous sodium chloride solution, dried over sodium sulfate, filtered, and concentrated in vacuo. Purification was carried out twice using silica gel chromatography (gradient: 0–10% methanol in dichloromethane, followed by a column eluted with ethyl acetate), affording (4aR,6R,8aS)-8a-(2,4-difluorophenyl)-6-(4-methyloxazol-2-yl)-4,4a,5,6,8,8a-hexahydropyrano[3,4-d][1,3]thiazin-2-amine as a white solid. Yield: 491 mg, 1.34 mmol, 64%. LCMS m/z 366.1 [M + H]⁺. ¹H NMR (400 MHz, CD₃OD) δ 7.60 (q, $J = 1.3$ Hz, 1H), 7.37 (ddd, $J = 9.6, 8.8, 6.6$ Hz, 1H), 6.94–7.03 (m, 2H), 4.80 (dd, $J = 11.9, 2.5$ Hz, 1H), 4.25 (dd, $J = 11.1, 2.0$ Hz, 1H), 3.78 (d, $J = 11.1$ Hz, 1H), 3.00–3.07 (m, 1H), 2.92 (dd, half of ABX pattern, $J = 12.5, 4.1$ Hz, 1H), 2.74 (dd, half of ABX pattern, $J = 12.6, 2.8$ Hz, 1H), 2.32–2.43 (m, 1H), 2.15 (d, $J = 1.2$ Hz, 3H), 1.87 (ddd, $J = 13.3, 4.0, 2.6$ Hz, 1H); $[\alpha]_{\text{D}}^{23.8} = +22.62$ ($c = 0.61$ g/100 mL; MeOH).

(4S,4aR,6R,8aS)-2-(Benzoylamino)-8a-(2,4-difluorophenyl)-4-(fluoromethyl)-4,4a,5,6,8,8a-hexahydropyrano[3,4-d][1,3]thiazine-6-carboxylic Acid (47). Tetrapropylammonium perfluorinated (1.02 g, 2.9 mmol) was added to a mixture of *N*-((4S,4aR,6R,8aS)-8a-(2,4-difluorophenyl)-4-(fluoromethyl)-6-(hydroxymethyl)-4,4a,5,6,8,8a-hexahydropyrano[3,4-d][1,3]thiazin-2-yl)benzamide 39 (13.0 g, 28.8 mmol) and 4-methylmorpholine *N*-oxide monohydrate (23.4 g, 173 mmol) in acetonitrile (210 mL), and the reaction mixture was stirred for 40 min at room temperature. After addition of 2-propanol (100 mL), it was stirred for an additional 2 h and then concentrated in vacuo. The residue was partitioned between ethyl acetate (250 mL) and aqueous sodium hydroxide solution (0.25 M, 250 mL). The organic layer was extracted with aqueous sodium hydroxide solution (0.25 M, 2 \times 150 mL), and the combined aqueous layers were acidified to a pH of approximately 1 with 2 M aqueous hydrochloric acid then extracted with ethyl acetate (3 \times 250 mL). The combined ethyl acetate layers were dried over sodium sulfate, filtered, and concentrated under reduced pressure. Purification via chromatography on silica gel (gradient: 0–100% (89:10:1 dichloromethane/methanol/acetic acid) in dichloromethane). (4S,4aR,6R,8aS)-2-Benzamido-8a-(2,4-difluorophenyl)-4-(fluoromethyl)-4,4a,5,6,8,8a-hexahydropyrano[3,4-d][1,3]thiazine-6-carboxylic acid was obtained as a solid. Yield: 9.9 g, 21 mmol, 74%. LCMS m/z 465.2 [M + H]⁺. ¹H NMR (400 MHz, CDCl₃) δ 9.09 (v br s, 2H), 8.07–8.12 (m, 2H), 7.52–7.58 (m, 1H), 7.46 (br dd, $J = 8.0, 7.0$ Hz, 2H), 7.32 (ddd, $J = 8.9, 8.9, 6.2$ Hz, 1H), 6.85–6.98 (m, 2H), 4.35–4.66 (m, 2H), 4.08–4.20 (m, 2H), 4.03 (d, half of AB quartet, $J = 12.2$ Hz, 1H), 3.43–3.52 (m, 1H), 3.22 (ddd, $J = 12.0, 3.9, 3.8$ Hz, 1H), 2.06–2.14 (m, 1H), 1.84–1.97 (m, 1H).

(4S,4aR,6R,8aS)-2-Benzamido-8a-(2,4-difluorophenyl)-4-(fluoromethyl)-N-(1-hydroxypropan-2-yl)-4,4a,5,6,8,8a-hexahydropyrano[3,4-d][1,3]thiazine-6-carboxamide (59). (4S,4aR,6R,8aS)-2-Benzamido-8a-(2,4-difluorophenyl)-4-(fluoromethyl)-4,4a,5,6,8,8a-hexahydropyrano[3,4-d][1,3]thiazine-6-carboxylic acid 47 (30.0 g, 64.6 mmol) was dissolved in DMF (215 mL). DIPEA (22.5 mL, 129 mmol) and TPTU (21.1 g, 71.0 mmol) were added sequentially, and the reaction stirred for 1 h. After this time, DL-2-amino-1-propanol

(10.1 mL, 129 mmol) was added and the reaction stirred. After 3 h, the reaction was concentrated and the residue taken up in aqueous 0.1 M HCl and ethyl acetate. The layers were separated, and the aqueous layer was extracted with ethyl acetate (2×). The combined organics were washed with aqueous NaHCO₃, brine, dried over sodium sulfate, and concentrated to yield crude product. Yield 33.6 g, 64.0 mmol, 99.7%. LCMS *m/z* 522.3 [M + H]⁺. ¹H NMR (400 MHz, CDCl₃) δ 8.11–8.29 (m, 2H), 7.48 (d, *J* = 7.0 Hz, 3H), 6.83–7.05 (m, 2H), 6.60–6.77 (m, 1H), 4.34–4.72 (m, 2H), 4.11–4.27 (m, 3H), 3.98–4.09 (m, 1H), 3.84–3.95 (m, 1H), 3.48–3.73 (m, *J* = 4.7, 6.5 Hz, 3H), 3.17–3.33 (m, 1H), 2.18–2.30 (m, 1H), 1.72–1.89 (m, 1H), 1.13–1.23 (m, 3H).

(4*S*,4*aR*,6*R*,8*aS*)-2-Benzamido-8*a*-(2,4-difluorophenyl)-4-(fluoromethyl)-*N*-(1-oxopropan-2-yl)-4,4*a*,5,6,8,8*a*-hexahydropyrano[3,4-*d*][1,3]thiazine-6-carboxamide (62). (4*S*,4*aR*,6*R*,8*aS*)-2-Benzamido-8*a*-(2,4-difluorophenyl)-4-(fluoromethyl)-*N*-(1-hydroxypropan-2-yl)-4,4*a*,5,6,8,8*a*-hexahydropyrano[3,4-*d*][1,3]thiazine-6-carboxamide 59 (5.0 g, 9.6 mmol) was dissolved in DCM (95.9 mL), to this was added Dess–Martin periodinane (4.88 g, 11.5 mmol). The reaction was stirred for 2 h before being diluted with aqueous NaHCO₃ and sodium thiosulfate. The layers were separated, and the aqueous layer was extracted with DCM (3×). The combined organic layers were washed with brine, dried over sodium sulfate, and concentrated to give crude product. No further purification was done. Yield: 5.09 g, 9.6 mmol, quantitative. LCMS *m/z* 520.2 [M + H]⁺. ¹H NMR (400 MHz, CDCl₃) δ 9.49–9.57 (m, 1H), 8.10–8.24 (m, 2H), 7.46 (m, 3H), 6.87–7.11 (m, 3H), 4.34–4.72 (m, 4H), 4.15–4.28 (m, 2H), 3.90–4.00 (m, 1H), 3.45–3.60 (m, 1H), 3.17–3.34 (m, 1H), 2.19–2.32 (m, 1H), 1.76–1.92 (m, 1H), 1.38 (dd, *J* = 4.4, 7.3 Hz, 3H).

N-((4*S*,4*aR*,6*R*,8*aS*)-8*a*-(2,4-Difluorophenyl)-4-(fluoromethyl)-6-(4-methyloxazol-2-yl)-4,4*a*,5,6,8,8*a*-hexahydropyrano[3,4-*d*][1,3]thiazin-2-yl)benzamide (65). To two 20 mL microwave vials were each added (4*S*,4*aR*,6*R*,8*aS*)-2-benzamido-8*a*-(2,4-difluorophenyl)-4-(fluoromethyl)-*N*-(1-oxopropan-2-yl)-4,4*a*,5,6,8,8*a*-hexahydropyrano[3,4-*d*][1,3]thiazine-6-carboxamide 62 (0.650 g, 1.25 mmol), dry tetrahydrofuran (13.1 mL, 0.095 M), and Burgess reagent (0.501 g, 2.13 mmol). The vials were capped, vortexed until homogeneous, then heated in a microwave for 2 min at 125 °C. After this time, the vials were cooled and the contents combined and diluted with methanol (1 mL). The volatiles were removed under vacuum, and the crude residue chromatographed on silica gel (gradient: 5–90% ethyl acetate/heptanes) to afford *N*-((4*S*,4*aR*,6*R*,8*aS*)-8*a*-(2,4-difluorophenyl)-4-(fluoromethyl)-6-(4-methyloxazol-2-yl)-4,4*a*,5,6,8,8*a*-hexahydropyrano[3,4-*d*][1,3]thiazin-2-yl)benzamide as a white solid. Yield: 711 mg, 57% yield. LCMS *m/z* 502.3 [M + H]⁺. ¹H NMR (400 MHz, CDCl₃) δ 8.04–8.23 (m, 2H), 7.32–7.60 (m, 4H), 6.85–7.00 (m, *J* = 7.6 Hz, 2H), 4.82 (dd, *J* = 2.5, 11.84 Hz, 1H), 4.37–4.73 (m, 2H), 4.33 (dd, *J* = 1.6, 11.9 Hz, 1H), 3.91–4.02 (m, 1H), 3.48–3.61 (m, 1H), 3.24–3.39 (m, 1H), 2.24–2.39 (m, 1H), 2.16 (d, *J* = 1.4 Hz, 3H), 2.06–2.14 (m, 1H).

(4*S*,4*aR*,6*R*,8*aS*)-8*a*-(2,4-Difluorophenyl)-4-(fluoromethyl)-6-(4-methyloxazol-2-yl)-4,4*a*,5,6,8,8*a*-hexahydropyrano[3,4-*d*][1,3]thiazin-2-amine (12). *N*-((4*S*,4*aR*,6*R*,8*aS*)-8*a*-(2,4-Difluorophenyl)-4-(fluoromethyl)-6-(4-methyloxazol-2-yl)-4,4*a*,5,6,8,8*a*-hexahydropyrano[3,4-*d*][1,3]thiazin-2-yl)benzamide 65 (0.12 g, 0.25 mmol) was dissolved in *n*-propylamine (2.5 mL) and stirred for 2 h then concentrated. Chromatography on silica gel (gradient: 0–60% ethyl acetate in heptane) afforded the product as a colorless solid. Yield: 0.09 g, 0.22 mmol, 87%. LCMS *m/z* 398.3 [M + H]⁺. ¹H NMR (400 MHz, CDCl₃) δ 7.49 (dt, *J* = 6.7, 9.0 Hz, 1H), 7.34 (q, *J* = 1.3 Hz, 1H), 6.77–6.92 (m, 2H), 4.80 (dd, *J* = 2.5, 11.7 Hz, 1H), 4.22–4.65 (m, 3H), 4.01 (d, *J* = 11.2 Hz, 1H), 3.51 (dtd, *J* = 4.1, 7.3, 11.6 Hz, 1H), 3.13 (td, *J* = 4.0, 12.1 Hz, 1H), 2.21 (d, *J* = 1.2 Hz, 3H), 2.02–2.16 (m, 1H), 1.81 (td, *J* = 3.3, 13.2 Hz, 1H). ¹H NMR (400 MHz, CD₃OD) δ 7.60 (q, *J* = 1.2 Hz, 1H), 7.31–7.41 (m, 1H), 6.94–7.07 (m, 2H), 4.78 (dd, *J* = 2.5, 11.9 Hz, 1H), 4.33–4.72 (m, 2H), 4.27 (dd, *J* = 1.9, 11.2 Hz, 1H), 3.81 (d, *J* = 11.4 Hz, 1H), 3.36–3.49 (m, 1H), 3.16 (td, *J* = 3.9, 12.1 Hz, 1H), 2.07–2.21 (m, 4H), 1.81–1.90 (m, 1H); [α]_D^{25.7} = +24.72 (*c* = 0.36 g/100 mL; MeOH).

(4*R*,4*aR*,6*R*,8*aS*)-2-(Benzoylamino)-8*a*-(2,4-difluorophenyl)-*N*-methoxy-*N*,4-dimethyl-4,4*a*,5,6,8,8*a*-hexahydropyrano[3,4-*d*][1,3]thiazine-6-carboxamide (49). To a solution of 46 (893 mg, 2.00 mmol) in 1,2-dichloroethane (5 mL) was added 1,1'-carbonyldiimidazole (389 mg, 2.40 mmol), and the reaction mixture was stirred at room temperature for 2 h. *N*,*O*-Dimethylhydroxylamine hydrochloride (273 mg, 2.80 mmol) was added, and stirring was continued for 2 h, whereupon the reaction mixture was partitioned between water (60 mL) and dichloromethane (50 mL). The organic layer was washed sequentially with aqueous hydrochloric acid (0.5 M, 20 mL), saturated aqueous sodium bicarbonate solution (20 mL), and saturated aqueous sodium chloride solution (20 mL), dried over sodium sulfate, filtered, and concentrated in vacuo. The residue was azeotroped with dichloromethane (3 × 10 mL) to afford the product as an off-white solid. Yield: 953 mg, 1.95 mmol, 98%. LCMS *m/z* 490.3 [M + H]⁺. ¹H NMR (400 MHz, CDCl₃) δ 8.18 (v br d, *J* = 7.0 Hz, 2H), 7.49–7.55 (m, 1H), 7.36–7.48 (m, 3H), 6.90–6.97 (m, 1H), 6.89 (ddd, *J* = 12.3, 8.3, 2.5 Hz, 1H), 4.53 (br d, *J* = 11.5 Hz, 1H), 4.22 (br d, *J* = 12 Hz, 1H), 3.92 (br d, *J* = 12 Hz, 1H), 3.76 (s, 3H), 3.18–3.31 (m, 4H), 2.90–2.99 (m, 1H), 2.06–2.20 (m, 1H), 1.88 (br d, *J* = 13 Hz, 1H), 1.27 (d, *J* = 6.9 Hz, 3H).

N-((4*R*,4*aR*,6*R*,8*aS*)-8*a*-(2,4-Difluorophenyl)-4-methyl-6-(3-methyl-1,2-oxazol-5-yl)-4,4*a*,5,6,8,8*a*-hexahydropyrano[3,4-*d*][1,3]thiazin-2-yl)benzamide (70). A solution of *N*-hydroxypropan-2-imine (272 mg, 3.72 mmol) in tetrahydrofuran (10 mL) was cooled in an ice bath. *n*-Butyllithium (2.5 M solution in hexanes, 3.00 mL, 7.50 mmol) was added to the cold solution over 8 min. The cooling bath was removed, and the reaction mixture was allowed to warm to room temperature, whereupon it was cooled in an ice bath and treated with a solution of 49 (617 mg, 1.26 mmol) in tetrahydrofuran (5 mL) over 15 min. Stirring was continued under ice cooling for 2 min, at which time concentrated sulfuric acid (1.01 mL, 18.9 mmol) was slowly added. The reaction mixture was stirred at room temperature for 1.5 h then cooled in an ice bath and quenched via addition of 15% aqueous sodium hydroxide solution until the pH of the aqueous phase reached 9–10. The mixture was partitioned between water (60 mL) and ethyl acetate (50 mL), and the aqueous layer was extracted with ethyl acetate (2 × 50 mL). The combined organic layers were dried over sodium sulfate, filtered, and concentrated in vacuo. Chromatography on silica gel (gradient: 0–80% ethyl acetate in heptane) provided the product as a white solid. Yield: 491 mg, 1.02 mmol, 81%. LCMS *m/z* 484.2 [M + H]⁺. ¹H NMR (400 MHz, CDCl₃) δ 8.19 (br d, *J* = 7 Hz, 2H), 7.50–7.56 (m, 1H), 7.36–7.49 (m, 3H), 6.87–6.98 (m, 2H), 6.14 (s, 1H), 4.86 (br dd, *J* = 11.8, 2.4 Hz, 1H), 4.31 (dd, *J* = 12.2, 1.5 Hz, 1H), 3.94 (d, *J* = 12.2 Hz, 1H), 3.26–3.34 (m, 1H), 3.00–3.08 (m, 1H), 2.28 (s, 3H), 2.12–2.20 (m, 1H), 1.94–2.05 (m, 1H), 1.30 (d, *J* = 7.0 Hz, 3H).

(4*R*,4*aR*,6*R*,8*aS*)-8*a*-(2,4-Difluorophenyl)-4-methyl-6-(3-methyl-1,2-oxazol-5-yl)-4,4*a*,5,6,8,8*a*-hexahydropyrano[3,4-*d*][1,3]thiazin-2-amine (10). 1,8-Diazabicyclo[5.4.0]undec-7-ene (47.5 μL, 0.318 mmol) was added to a solution of 70 (154 mg, 0.318 mmol) in methanol (3 mL), and the reaction mixture was heated at 60 °C for 18 h. Solvent was removed in vacuo, and the residue was partitioned between ethyl acetate and aqueous sodium bicarbonate solution. The aqueous layer was extracted twice with ethyl acetate, and the combined organic layers were washed with saturated aqueous sodium chloride solution, dried over sodium sulfate, filtered, and concentrated under reduced pressure. Silica gel chromatography (gradient: 0–15% methanol in dichloromethane) afforded the product as a white solid. Yield: 103 mg, 0.271 mmol, 85%. LCMS *m/z* 380.2 [M + H]⁺. ¹H NMR (400 MHz, (CD₃)₂SO) δ 7.33 (ddd, *J* = 9.0, 9.0, 7.0 Hz, 1H), 7.23 (ddd, *J* = 12.6, 9.1, 2.6 Hz, 1H), 7.08–7.14 (m, 1H), 6.30 (s, 1H), 6.22 (br s, 2H), 4.80 (dd, *J* = 11.7, 2.1 Hz, 1H), 4.09 (dd, *J* = 10.6, 2.1 Hz, 1H), 3.69 (d, *J* = 10.8 Hz, 1H), 2.96 (qd, *J* = 6.9, 3.3 Hz, 1H), 2.71 (ddd, *J* = 11.9, 4, 3 Hz, 1H), 2.22 (s, 3H), 1.81–1.88 (m, 1H), 1.62–1.73 (m, 1H), 1.10 (d, *J* = 6.9 Hz, 3H). ¹H NMR (400 MHz, methanol-*d*₄) δ 7.31–7.39 (m, 1H), 6.93–7.03 (m, 2H), 6.24 (s, 1H), 4.82–4.88 (m, 1H), 4.27 (dd, *J* = 1.95, 11.32 Hz, 1H), 3.82 (d, *J* = 10.93 Hz, 1H), 3.12 (dq, *J* = 3.32, 6.96 Hz, 1H), 2.89 (td, *J* = 3.76, 12.00 Hz, 1H), 1.95 (td, *J* = 3.41, 13.07 Hz, 1H), 1.75–1.86 (m, 1H),

1.20 (d, $J = 6.63$ Hz, 3H); $[\alpha]_D^{24.6} = +40.86$ ($c = 0.35$ g/100 mL; MeOH).

(4*S*,4*aR*,6*R*,8*aS*)-2-(Benzoylamino)-8*a*-(2,4-difluorophenyl)-4-(fluoromethyl)-*N*-methoxy-*N*-methyl-4,4*a*,5,6,8,8*a*-hexahydropyrano[3,4-*d*][1,3]thiazine-6-carboxamide (50). 1,1'-Carbonyldiimidazole (4.40 g, 27.1 mmol) was added to a solution of 47 (9.7 g, 21 mmol) in 1,2-dichloroethane (70 mL), and the reaction mixture was stirred at room temperature for 1.5 h. *N,O*-Dimethylhydroxylamine hydrochloride (3.06 g, 31.4 mmol) was then added, and stirring was continued for 18 h. The reaction mixture was partitioned between water and dichloromethane, and the organic layer was washed sequentially with 0.5 M aqueous hydrochloric acid, saturated aqueous sodium bicarbonate solution, and saturated aqueous sodium chloride solution then dried over sodium sulfate, filtered, and concentrated in vacuo. The residue was azeotroped with dichloromethane (3 × 100 mL) to afford the product as a solid. Yield: 7.6 g, 15 mmol, 71%. LCMS m/z 508.2 $[M + H]^+$.

N-[(4*S*,4*aR*,6*R*,8*aS*)-8*a*-(2,4-Difluorophenyl)-4-(fluoromethyl)-6-(3-methyl-1,2-oxazol-5-yl)-4,4*a*,5,6,8,8*a*-hexahydropyrano[3,4-*d*][1,3]thiazin-2-yl]benzamide (71). A solution of *N*-hydroxypropan-2-imine (3.28 g, 44.9 mmol) in tetrahydrofuran (150 mL) was cooled to an internal temperature of -9 °C. *n*-Butyllithium (2.5 M solution in hexanes, 35.9 mL, 89.8 mmol) was slowly added to the cold solution. The cooling bath was removed, and the reaction mixture was allowed to warm to room temperature, whereupon it was cooled to -8 °C and treated dropwise over less than 20 min with a solution of 50 (7.6 g, 15 mmol) in a minimum volume of tetrahydrofuran at a rate such that the internal reaction temperature never exceeded -5 °C. Stirring was continued at -5 °C for 2 min, then at 0 °C for 10 min, at which time concentrated sulfuric acid (12.0 mL, 225 mmol) was slowly added. The reaction mixture was stirred at room temperature for 1 h then cooled to -5 °C and slowly quenched via addition of 15% aqueous sodium hydroxide solution until the pH of the aqueous phase reached 9–10. The mixture was partitioned between water and ethyl acetate, and the aqueous layer was extracted with ethyl acetate. The combined organic layers were dried over sodium sulfate, filtered, and concentrated in vacuo. Chromatography on silica gel (gradient: 0–20% ethyl acetate in heptane) provided the product as a solid. Yield: 5.65 g, 11.3 mmol, 75%. $^1\text{H NMR}$ (400 MHz, CDCl_3) δ 8.17 (br s, 2H), 7.43–7.59 (m, 3H), 7.33–7.43 (m, 1H), 6.89–7.00 (m, 2H), 6.14 (s, 1H), 4.87 (dd, $J = 10.7$, 3.5 Hz, 1H), 4.61 (ddd, $J = 46.9$, 9.6, 7.9 Hz, 1H), 4.46 (ddd, $J = 46.1$, 9.7, 6.2 Hz, 1H), 4.33 (dd, $J = 12.1$, 1.3 Hz, 1H), 3.96 (d, $J = 12.1$ Hz, 1H), 3.50–3.62 (br m, 1H), 3.32–3.43 (br m, 1H), 2.28 (s, 3H), 2.0–2.16 (m, 2H).

(4*S*,4*aR*,6*R*,8*aS*)-8*a*-(2,4-Difluorophenyl)-4-(fluoromethyl)-6-(3-methyl-1,2-oxazol-5-yl)-4,4*a*,5,6,8,8*a*-hexahydropyrano[3,4-*d*][1,3]thiazin-2-amine (13). Methylamine (33% solution in absolute ethanol, 23.8 mL, 200 mmol) was added to a solution of 71 (1.00 g, 1.99 mmol) in ethanol (40 mL), and the reaction mixture was allowed to stir for 2 h. After concentration under reduced pressure, the residue was purified via silica gel chromatography (gradient: 0–60% ethyl acetate in heptane) to afford the product. Yield: 0.71 g, 1.8 mmol, 90%. LCMS m/z 398.0 $[M + H]^+$. $^1\text{H NMR}$ (400 MHz, CDCl_3) δ 7.36 (ddd, $J = 9.0$, 8.8, 6.6 Hz, 1H), 6.81–6.92 (m, 2H), 6.14 (s, 1H), 4.78–4.84 (m, 1H), 4.56 (ddd, $J = 46.8$, 9.5, 7.3 Hz, 1H), 4.37 (ddd, $J = 46.3$, 9.5, 6.7 Hz, 1H), 4.24 (dd, $J = 11.2$, 2.0 Hz, 1H), 3.93 (d, $J = 11.3$ Hz, 1H), 3.47–3.57 (m, 1H), 3.10–3.17 (m, 1H), 2.30 (s, 3H), 1.88–2.00 (m, 2H); $[\alpha]_D^{25.0} = +34.57$ ($c = 0.35$ g/100 mL; MeOH).

Methyl (4*aR*,6*R*,8*aS*)-2-(Benzoylamino)-8*a*-(2,4-difluorophenyl)-4,4*a*,5,6,8,8*a*hexahydropyrano[3,4-*d*][1,3]thiazine-6-carboxylate (48). To a stirring suspension of (4*aR*,6*R*,8*aS*)-2-(benzoylamino)-8*a*-(2,4-difluorophenyl)-4,4*a*,5,6,8,8*a*-hexahydropyrano[3,4-*d*][1,3]thiazine-6-carboxylic acid (45) (245 mg, 0.567 mmol) in dichloromethane (2.85 mL) was added oxalyl chloride (100 μL , 1.16 mmol) in a dropwise fashion, followed by *N,N*-dimethylformamide (7.0 μL , 90 μmol). The reaction mixture was stirred for 15 min, at which time additional oxalyl chloride (50 μL , 0.58 mmol) was added. After 20 min, methanol (1 mL) was added, and the reaction mixture was stirred for 10 min. Removal of solvents in vacuo was followed by silica gel chromatography (gradient: 0–60% ethyl acetate in heptane), affording

the product as a white solid. Yield: 208 mg, 0.466 mmol, 82%. LCMS m/z 447.2 $[M + H]^+$. $^1\text{H NMR}$ (400 MHz, CDCl_3) δ 68.18 (br d, $J = 7.0$ Hz, 2H), 7.50–7.56 (m, 1H), 7.36–7.49 (m, 3H), 6.85–6.97 (m, 2H), 4.33 (dd, $J = 12.0$, 2.6 Hz, 1H), 4.19 (dd, $J = 12.2$, 1.6 Hz, 1H), 3.94 (d, $J = 12.3$ Hz, 1H), 3.80 (s, 3H), 3.13–3.22 (m, 1H), 3.03 (dd, half of ABX pattern, $J = 13.1$, 4.0 Hz, 1H), 2.67 (dd, half of ABX pattern, $J = 13.0$, 2.8 Hz, 1H), 2.21–2.34 (m, 1H), 2.05–2.12 (m, 1H).

N-[(4*aR*,6*R*,8*aS*)-8*a*-(2,4-Difluorophenyl)-6-(3-methyl-1,2-oxazol-5-yl)-4,4*a*,5,6,8,8*a*-hexahydropyrano[3,4-*d*][1,3]thiazin-2-yl]benzamide (69). To a solution of propan-2-one oxime (23.0 mg, 0.315 mmol) in tetrahydrofuran (L25 mL) at 0 °C was added a solution of *n*-butyllithium in hexanes (2.5 M, 0.25 mL, 0.62 mmol). The ice bath was removed, and the mixture was stirred at room temperature for 30 min. After the reaction mixture had been recooled to 0 °C, a solution of methyl (4*aR*,6*R*,8*aS*)-2-(benzoyl amino)-8*a*-(2,4-difluorophenyl)-4,4*a*,5,6,8,8*a*-hexahydropyrano[3,4-*d*][1,3]thiazine-6-carboxylate 48 (70.0 mg, 0.157 mmol) in tetrahydrofuran (0.75 mL) was added dropwise. The reaction mixture was allowed to warm to room temperature and stirred for 1 h then cooled once again in an ice bath. Concentrated sulfuric acid (35 μL , 0.66 mmol) was added, and the flask was allowed to warm to room temperature for 1 h. After recooling the reaction mixture to 0 °C, it was neutralized with 5 M aqueous sodium hydroxide solution. Water (2 mL) was added, and the mixture was extracted with ethyl acetate (3 × 5 mL). The combined organic layers were dried over sodium sulfate, filtered, and concentrated in vacuo. Silica gel chromatography (gradient: 0–50% ethyl acetate in heptane) provided the product as a white solid; the relative stereochemistry of the isoxazole side chain was confirmed via nuclear Overhauser enhancement study. Yield: 18 mg, 38 μmol , 24%. LCMS m/z 470.2 $[M + H]^+$. $^1\text{H NMR}$ (400 MHz, CDCl_3) δ 8.18–8.22 (m, 2H), 7.50–7.55 (m, 1H), 7.38–7.48 (m, 3H), 6.88–6.99 (m, 2H), 6.14 (s, 1H), 4.88 (dd, $J = 11.7$, 2.4 Hz, 1H), 4.31 (dd, $J = 12.1$, 1.6 Hz, 1H), 3.93 (d, $J = 12.3$ Hz, 1H), 3.24–3.31 (m, 1H), 3.06 (dd, $J = 12.9$, 4.1 Hz, 1H), 2.70 (dd, $J = 13.0$, 2.8 Hz, 1H), 2.28 (s, 3H), 2.26–2.38 (m, 1H), 2.11 (ddd, $J = 13.6$, 4.2, 2.7 Hz, 1H).

(4*aR*, 6*R*, 8*aS*)-8*a*-(2,4-Difluorophenyl)-6-(3-methyl-1, 2-oxazol-5-yl)-4,4*a*,5,6,8,8*a*-hexahydropyrano [3,4-*d*][1,3]thiazin-2-amine (4). *N*-[(4*aR*,6*R*,8*aS*)-8*a*-(2,4-Difluorophenyl)-6-(3-methyl-1,2-oxazol-5-yl)-4,4*a*,5,6,8,8*a*-hexahydropyrano[3,4-*d*][1,3]thiazin-2-yl]benzamide (69) (14 mg 0.030 mmol) was dissolved in methanol (0.75 mL) and was treated with DBU (4.1 mg, 4.0 μL , 0.027 mmol). The reaction mixture was heated to 80 °C in a sealed vial for 16 h. Analysis by LCMS indicated that starting material had been consumed. The solvent was evaporated under a stream of nitrogen, and then the residue was partitioned between water (3 mL) and ethyl acetate (5 mL) to afford the product as a white solid. The layers were extracted and separated. The aqueous layer was washed with further ethyl acetate (5 mL). The combined organic extracts were dried over Na_2SO_4 , filtered, and concentrated to give the crude product. The residue was dry loaded on 5 g of silica and then chromatographed on a CombiFlash Rf (4 g of RediSep Gold; gradient: 0–15% methanol in dichloromethane over 15 min; 18 mL/min flow rate). The combined fractions were concentrated to afford product as a white solid. Yield: 8.9 mg, 24 μmol , 80%. LCMS m/z 366.1 $[M + H]^+$. $^1\text{H NMR}$ (400 MHz, CDCl_3) δ 6.734 (ddd, $J = 9.0$, 9.0, 6.6 Hz, 1H), 6.86–6.92 (m, 2H), 6.83 (ddd, $J = 12.5$, 8.6, 2.5 Hz, 1H), 4.82 (dd, $J = 11.9$, 2.4 Hz, 1H), 4.23 (dd, $J = 11.2$, 2.2 Hz, 1H), 3.91 (d, $J = 11.2$ Hz, 1H), 2.98–3.08 (m, 2H), 2.65–2.71 (m, 1H), 2.30 (s, 3H), 2.11–2.22 (m, 1H), 1.91–1.98 (m, 1H); $[\alpha]_D^{23.1} = +22.37$ ($c = 0.76$ g/100 mL; MeOH).

■ ASSOCIATED CONTENT

Supporting Information

Drug exposure data and absolute $A\beta$ concentrations in brain, plasma, and CSF compartments following acute administration of compounds 5, 10, 12, and 13 for in vivo mouse experiments; data collection/refinement statistics for 5 with BACE1 and the CYP2D6 structures for compounds 5 and 6; 2D ROESY spectrum for compound 32 and 2D COSY spectrum for compound 33; single X-ray structure of compound 38, 39, and

the benzoyl precursor to compound **5**; ^1H NMR for key analogues **5**, **10**, **12**, and **13** and HSQC for compound **8**. This material is available free of charge via the Internet at <http://pubs.acs.org>.

Accession Codes

Atomic coordinates and structure factors for the BACE cocrystal structure have been deposited with the RCSB: compound **5** (PDB ID code 4XXS). Atomic coordinates and structure factors for the CYP2D6 cocrystal structures have been deposited with the RCSB: compound **5** (4XRY code S15) and **6** (4XRZ code S16). Atomic coordinates and structure factors for compounds **38**, **39**, and benzoyl protected precursor to compound **5** have been deposited with the Cambridge Crystallographic Data Centre (CCDC): compound **38** (Z510), compound **39** (Z231), and protected compound **5** (Z171).

AUTHOR INFORMATION

Corresponding Author

*Phone: 617 395 0706. E-mail: michael.a.brodney@pfizer.com.

Notes

The authors declare no competing financial interest.

ACKNOWLEDGMENTS

We thank Hui Kim and Lacey Samp for synthetic expertise along with Yasong Lu for PK–PD modeling support. We thank Dr. Brian Samas for obtaining single crystal X-ray structures. We thank Dennis Anderson for 2D NMR structural analysis. This work was supported in part by National Institutes of Health grant R01GM031001 (to E.F.J.). Portions of this research were carried out at the Stanford Synchrotron Radiation Lightsource (SSRL), a national user facility operated by Stanford University on behalf of the United States Department of Energy, Office of Basic Energy Sciences. The SSRL Structural Molecular Biology Program is supported by the United States Department of Energy, Office of Biological and Environmental Research, and by the National Center for Research Resources, Biomedical Technology Program, and NIGMS of the National Institutes of Health. Use of the IMCA-CAT beamline 17-ID at the Advanced Photon Source was supported by the companies of the Industrial Macromolecular Crystallography Association through a contract with Hauptman–Woodward Medical Research Institute. Use of the Advanced Photon Source (APS) was supported by the U.S. Department of Energy, Office of Science, Office of Basic Energy Sciences, under contract no. DE-AC02-06CH11357. Compounds **12** (PF-06691283 (catalogue no. PZ0260)), **10** (PF-06649283 (catalogue no. PZ0261)), and **13** (PF-06663195 (catalogue no. PZ0262)) are now commercially available from Sigma-Aldrich.

ABBREVIATIONS USED

BACE1, β -secretase; DDI, drug–drug interaction; AD, Alzheimer's disease; $A\beta$, amyloid- β ; sAPP β , N-terminal ectodomain of APP; C99, C-terminal fragment; CatD, cathepsin D; WCA, whole cell assay; RPE, retinal pigment epithelium; LipE, lipophilic efficiency; CFA, cell-free assay; P-gp, P-glycoprotein; HLM, human liver microsomes; HHEP, human hepatocytes; rCYP, recombinant human P450s; THP, tetrahydropyran; TEA-3HF, triethylamine hydrofluoride; TPP-DEAD, triphenylphosphine and diethyl azodicarboxylate; FP, fluorescence polarization; EDTA, ethylenediaminetetraacetic

acid; DELFIA, dissociation-enhanced lanthanide fluorescent immunoassay; ELISA, platform enzyme-linked immunosorbent assay

REFERENCES

- (1) (a) Hardy, J.; Allsop, D. Amyloid deposition as the central event in the aetiology of Alzheimer's disease. *Trends Pharmacol. Sci.* **1991**, *12* (10), 383. (b) Walsh, D. M.; Minogue, A. M.; Sala Frigerio, C.; Fadeeva, J. V.; Wasco, W.; Selkoe, D. J. The APP family of proteins: similarities and differences. *Biochem. Soc. Trans.* **2007**, *35* (2), 416–420.
- (2) Tanzi, R. E.; Bertram, L. Twenty years of the Alzheimer's disease amyloid hypothesis: a genetic perspective. *Cell* **2005**, *120* (4), 545–555.
- (3) De Strooper, B. Proteases and proteolysis in Alzheimer disease: a multifactorial view on the disease process. *Physiol. Rev.* **2010**, *90* (2), 465–494.
- (4) Vassar, R.; Kovacs, D. M.; Yan, R.; Wong, P. C. The beta-secretase enzyme BACE in health and Alzheimer's disease: regulation, cell biology, function, and therapeutic potential. *J. Neurosci.* **2009**, *29* (41), 12787–12794.
- (5) Marks, N.; Berg, M. J. BACE and gamma-secretase characterization and their sorting as therapeutic targets to reduce amyloidogenesis. *Neurochem. Res.* **2010**, *35* (2), 181.
- (6) (a) Citron, M.; Eckman, C. B.; Diehl, T. S.; Corcoran, C.; Ostaszewski, B. L.; Xia, W.; Levesque, G.; St. George Hyslop, P.; Younkin, S. G.; Selkoe, D. J. Additive effects of PS1 and APP mutations on secretion of the 42-residue amyloid β -protein. *Neurobiol. Dis.* **1998**, *5* (2), 107–116. (b) Jonsson, T.; Atwal, J. K.; Steinberg, S.; Snaedal, J.; Jonsson, P. V.; Bjornsson, S.; Stefansson, H.; Sulem, P.; Gudbjartsson, D.; Maloney, J.; Hoyte, K.; Gustafson, A.; Liu, Y.; Lu, Y.; Bhangale, T.; Graham, R. R.; Huttenlocher, J.; Bjornsdottir, G.; Andreassen, O. A.; Joansson, E. G.; Palotie, A.; Behrens, T. W.; Magnusson, O. T.; Kong, A.; Thorsteinsdottir, U.; Watts, R. J.; Stefansson, K. A mutation in APP protects against Alzheimer's disease and age-related cognitive decline. *Nature* **2012**, *488* (7409), 96–99.
- (7) Yuan, J.; Venkatraman, S.; Zheng, Y.; McKeever, B. M.; Dillard, L. W.; Singh, S. B. Structure-based design of beta-site APP cleaving enzyme 1 (BACE1) inhibitors for the treatment of Alzheimer's disease. *J. Med. Chem.* **2013**, *56* (11), 4156–4180.
- (8) (a) Fielden, M. R.; Werner, J.; Coppi, A.; Dunn, R. T., II; Trueblood, E.; Afshari, C. A.; Lightfoot-Dunn, R.; Jamison, J. A.; Hickman, D.; Zhou, L., Retinal Toxicity Induced by a Novel β -Secretase Inhibitor in the Sprague–Dawley Rat. *Toxicol. Pathol.* **2014**, *0192623314553804*. (b) May, P. C.; Dean, R. A.; Lowe, S. L.; Martenyi, F.; Sheehan, S. M.; Boggs, L. N.; Monk, S. A.; Mathes, B. M.; Mergott, D. J.; Watson, B. M.; Stout, S. L.; Timm, D. E.; Smith Labell, E.; Gonzales, C. R.; Nakano, M.; Jhee, S. S.; Yen, M.; Ereshefsky, L.; Lindstrom, T. D.; Calligaro, D. O.; Cocke, P. J.; Greg Hall, D.; Friedrich, S.; Citron, M.; Audia, J. E. Robust central reduction of amyloid-beta in humans with an orally available, non-peptidic beta-secretase inhibitor. *J. Neurosci.* **2011**, *31* (46), 16507–16516.
- (9) Lilly Voluntarily Terminates Phase II Study for LY2886721, a Beta Secretase Inhibitor, Being Investigated as a Treatment for Alzheimer's Disease; Eli Lilly Pharmaceuticals: Indianapolis, IN, June 13, 2013; <https://investor.lilly.com/releaseDetail.cfm?ReleaseID=771353>.
- (10) Butler, C. R.; Brodney, M. A.; Beck, E. M.; Barreiro, G.; Nolan, C. E.; Pan, F.; Vajdos, F.; Parris, K.; Varghese, A. H.; Helal, C. J.; Lira, R.; Doran, S.; Riddell, D. R.; Buzon, L. M.; Dutra, J. K.; Martinez-Alsina, L. A.; Ogilvie, K.; Murray, J. C.; Young, J. M.; Atchison, K.; Robshaw, A.; Gonzales, C.; Wang, J.; Zhang, Y.; O'Neill, B. T., Discovery of a Series of Efficient, Centrally Efficacious BACE1 Inhibitors through Structure-Based Drug Design. *J. Med. Chem.* **2015**, *58*, 2678–2702, DOI: 10.1021/jm501833t.
- (11) Stepan, A. F.; Walker, D. P.; Bauman, J.; Price, D. A.; Baillie, T. A.; Kalgutkar, A. S.; Aleo, M. D. Structural alert/reactive metabolite concept as applied in medicinal chemistry to mitigate the risk of idiosyncratic drug toxicity: a perspective based on the critical

examination of trends in the top 200 drugs marketed in the United States. *Chem. Res. Toxicol.* **2011**, *24* (9), 1345–410.

(12) Freeman-Cook, K. D.; Hoffman, R. L.; Johnson, T. W. Lipophilic efficiency: the most important efficiency metric in medicinal chemistry. *Future Med. Chem.* **2013**, *5* (2), 113–115.

(13) Hitchcock, S. A. Structural modifications that alter the P-glycoprotein efflux properties of compounds. *J. Med. Chem.* **2012**, *55* (11), 4877–4895.

(14) Lu, Y.; Riddell, D.; Hajos-Korcsok, E.; Bales, K.; Wood, K. M.; Nolan, C. E.; Robshaw, A. E.; Zhang, L.; Leung, L.; Becker, S. L.; Tseng, E.; Barricklow, J.; Miller, E. H.; Osgood, S.; O'Neill, B. T.; Brodney, M. A.; Johnson, D. S.; Pettersson, M. Cerebrospinal fluid amyloid- β ($A\beta$) as an effect biomarker for brain $A\beta$ lowering verified by quantitative preclinical analyses. *J. Pharmacol. Exp. Ther.* **2012**, *342* (2), 366–375.

(15) (a) Rendic, S.; Di Carlo, F. J. Human cytochrome P450 enzymes: a status report summarizing their reactions, substrates, inducers, and inhibitors. *Drug Metab. Rev.* **1997**, *29* (1,2), 413–580. (b) Teh, L. K.; Bertilsson, L. Pharmacogenomics of CYP2D6: molecular genetics, interethnic differences and clinical importance. *Drug Metab. Pharmacokinet.* **2012**, *27* (1), 55–67. (c) Bertilsson, L.; Dahl, M.-L.; Dalen, P.; Al-Shurbaji, A. Molecular genetics of CYP2D6: clinical relevance with focus on psychotropic drugs. *Br. J. Clin. Pharmacol.* **2002**, *53* (2), 111–122.

(16) Wang, A.; Savas, U.; Hsu, M.-H.; Stout, C. D.; Johnson, E. F. Crystal structure of human cytochrome P 450 2D6 with prinomastat bound. *J. Biol. Chem.* **2012**, *287* (14), 10834–10843.

(17) (a) Sanguinetti, M. C.; Tristani-Firouzi, M. hERG potassium channels and cardiac arrhythmia. *Nature* **2006**, *440* (7083), 463–469. (b) Sanguinetti, M. C.; Jiang, C.; Curran, M. E.; Keating, M. T. A mechanistic link between an inherited and an acquired cardiac arrhythmia: hERG encodes the IKr potassium channel. *Cell* **1995**, *81* (2), 299–307. (c) Roden, D. M. Drug-induced prolongation of the QT interval. *N. Engl. J. Med.* **2004**, *350* (10), 1013–1022.

(18) Waring, M. J.; Johnstone, C. A quantitative assessment of hERG liability as a function of lipophilicity. *Bioorg. Med. Chem. Lett.* **2007**, *17* (6), 1759–1764.

(19) Ginman, T.; Viklund, J.; Malmstroem, J.; Blid, J.; Emond, R.; Forsblom, R.; Johansson, A.; Kers, A.; Lake, F.; Sehgelmeble, F.; Sterky, K. J.; Bergh, M.; Lindgren, A.; Johansson, P.; Jeppsson, F.; Faeltling, J.; Gravenfors, Y.; Rahm, F. Core Refinement toward Permeable β -Secretase (BACE-1) Inhibitors with Low hERG Activity. *J. Med. Chem.* **2013**, *56* (11), 4181–4205.

(20) (a) Jamieson, C.; Moir, E. M.; Rankovic, Z.; Wishart, G. Medicinal chemistry of hERG optimizations: highlights and hang-ups. *J. Med. Chem.* **2006**, *49* (17), 5029–5046. (b) Price, D. A.; Armour, D.; de Groot, M.; Leishman, D.; Napier, C.; Perros, M.; Stammen, B. L.; Wood, A. Overcoming hERG affinity in the discovery of maraviroc; a CCR5 antagonist for the treatment of HIV. *Curr. Top. Med. Chem.* **2008**, *8* (13), 1140–1151.

(21) Morgenthaler, M.; Schweizer, E.; Hoffmann-Roder, A.; Benini, F.; Martin, R. E.; Jaeschke, G.; Wagner, B.; Fischer, H.; Bendels, S.; Zimmerli, D.; Schneider, J.; Diederich, F.; Kansy, M.; Muller, K. Predicting and tuning physicochemical properties in lead optimization: amine basicities. *ChemMedChem* **2007**, *2* (8), 1100–1115.

(22) Motoki, T.; Takeda, K.; Kita, Y.; Takaishi, M.; Suzuki, Y.; Ishida, T. Preparation of novel fused aminodihydrothiazine derivatives as β -secretase 1 (BACE 1) inhibitors. WO2010038686A1, 2010.

(23) (a) Morwick, T.; Hrapchak, M.; DeTuri, M.; Campbell, S. A Practical Approach to the Synthesis of 2,4-Disubstituted Oxazoles from Amino Acids. *Org. Lett.* **2002**, *4* (16), 2665–2668. (b) Kim, K. S.; Kimball, S. D.; Misra, R. N.; Rawlins, D. B.; Hunt, J. T.; Xiao, H.-Y.; Lu, S.; Qian, L.; Han, W.-C.; Shan, W.; Mitt, T.; Cai, Z.-W.; Poss, M. A.; Zhu, H.; Sack, J. S.; Tokarski, J. S.; Chang, C. Y.; Pavletich, N.; Kamath, A.; Humphreys, W. G.; Marathe, P.; Bursuker, I.; Kellar, O. K. A.; Roongta, U.; Batorsky, R.; Mulheron, J. G.; Bol, D.; Fairchild, C. R.; Lee, F. Y.; Webster, K. R. Discovery of Aminothiazole Inhibitors of Cyclin-Dependent Kinase 2: Synthesis, X-ray Crystallographic Analysis, and Biological Activities. *J. Med. Chem.* **2002**, *45* (18),

3905–3927. (c) Cooper, J. P.; Cobb, J. E.; Shearer, B. G.; Minick, D. J.; Rutkowske, R. D. Synthesis and identification of a novel 6,5,6-tricyclic lactam. *Heterocycles* **2003**, *60* (3), 607–613.

(24) Nitz, T. J.; Volkots, D. L.; Aldous, D. J.; Oglesby, R. C. Regiospecific Synthesis of 3-Substituted 5-Alkylisoxazoles from Oxime Dianions and *N*-Methoxy-*N*-Methylalkylamides. *J. Org. Chem.* **1994**, *59* (19), 5828–5832.

(25) (a) O'Sullivan, P. T.; Buhr, W.; Fuhry, M. A. M.; Harrison, J. R.; Davies, J. E.; Feeder, N.; Marshall, D. R.; Burton, J. W.; Holmes, A. B. A concise synthesis of the octalactins. *J. Am. Chem. Soc.* **2004**, *126* (7), 2194–2207. (b) Werner, A.; Sanchez-Migallon, A.; Fruchier, A.; Elguero, J.; Fernandez-Castano, C.; Foces-Foces, C. Porphyrins with four azole substituents in meso positions: X-ray crystal structure of meso-tetrakis-(1-benzylpyrazol-4-yl)porphyrin at 200 K. *Tetrahedron* **1995**, *51* (16), 4779–4800. (c) Alberti, C.; Zerbi, G. Synthesis of alkylpyrazoles. *Farmaco Sci.* **1961**, *16*, 527–539.

(26) Tius, M. A.; Reddy, N. K. Cembrane synthesis. An advanced intermediate for crassin acetate. *Tetrahedron Lett.* **1991**, *32* (30), 3605–3608.

(27) Williams, D. R.; Harigaya, Y.; Moore, J. L.; D'Sa, A. Stereocontrolled transformations of orthoester intermediates into substituted tetrahydrofurans. *J. Am. Chem. Soc.* **1984**, *106* (9), 2641–2644.

(28) (a) Middleton, W. J. New fluorinating reagents. Dialkylamino-sulfur fluorides. *J. Org. Chem.* **1975**, *40* (5), 574–578. (b) Singh, R. P.; Shreeve, J. M. Recent advances in nucleophilic fluorination reactions of organic compounds using deoxofluor and DAST. *Synthesis* **2002**, *17*, 2561–2578. (c) Kirk, K. L. Fluorination in Medicinal Chemistry: Methods, Strategies, and Recent Developments. *Org. Process Res. Dev.* **2008**, *12* (2), 305–321. (d) Al-Maharik, N.; O'Hagan, D. Organo-fluorine chemistry. Deoxyfluorination reagents for C–F bond synthesis. *Aldrichimica Acta* **2011**, *44* (3), 65–75.

(29) (a) Messina, P. A.; Mange, K. C.; Middleton, W. J. Aminosulfur trifluorides: relative thermal stability. *J. Fluorine Chem.* **1989**, *42* (1), 137–143. (b) Middleton, W. J. Explosive hazards with DAST [diethylaminosulfur trifluoride]. *Chem. Eng. News* **1979**, *57* (21), 43.

(30) L'Heureux, A.; Beaulieu, F.; Bennett, C.; Bill, D. R.; Clayton, S.; La Flamme, F.; Mirmehrabi, M.; Tadayon, S.; Tovell, D.; Couturier, M. Aminodifluorosulfonium Salts: Selective Fluorination Reagents with Enhanced Thermal Stability and Ease of Handling. *J. Org. Chem.* **2010**, *75* (10), 3401–3411.

(31) (a) Devos, A.; Remion, J.; Frisque-Hesbain, A. M.; Colens, A.; Ghosez, L. Synthesis of acyl halides under very mild conditions. *J. Chem. Soc., Chem. Commun.* **1979**, *24*, 1180–1181. (b) Ghosez, L. α -Chloroenamines. New reagents for organic synthesis. *Angew. Chem., Int. Ed. Engl.* **1972**, *11* (9), 852–853.

(32) Burgess, E. M.; Penton, H. R., Jr.; Taylor, E. A. Thermal reactions of alkyl *N*-carbomethoxysulfamate esters. *J. Org. Chem.* **1973**, *38* (1), 26–31.

(33) Kalvass, J. C.; Maurer, T. S. Use of plasma and brain unbound fractions to assess the extend of brain distribution of 34 drugs: comparison of unbound concentration ratios to in vivo P-glycoprotein efflux ratios. *Biopharm. Drug Dispos.* **2002**, *23* (8), 327.

(34) Kutchinsky, J.; Friis, S.; Asmild, M.; Taborski, R.; Pedersen, S.; Vestergaard, R. K.; Jacobsen, R. B.; Krzywkowski, K.; Schroder, R. L.; Ljungstrom, T.; Helix, N.; Sorensen, C. B.; Bech, M.; Willumsen, N. J. Characterization of Potassium Channel Modulators with QPatch Automated Patch-Clamp Technology: System Characteristics and Performance. *Assay Drug Dev. Technol.* **2003**, *1* (5), 685–693.

(35) Bridges, K. G.; Chopra, R.; Lin, L.; Svenson, K.; Tam, A.; Jin, G.; Cowling, R.; Lovering, F.; Akopian, T. N.; DiBlasio-Smith, E.; Annis-Freeman, B.; Marvell, T. H.; LaVallie, E. R.; Zollner, R. S.; Bard, J.; Somers, W. S.; Stahl, M. L.; Kriz, R. W. A novel approach to identifying β -secretase inhibitors: Bis-statinine peptide mimetics discovered using structure and spot synthesis. *Peptides (N. Y., N. Y., U. S. A.)* **2006**, *27* (7), 1877–1885.

(36) Otwinowski, Z.; Minor, W. Processing of x-ray diffraction data collected in oscillation mode. *Methods Enzymol.* **1997**, *276*, 307–326 Macromolecular Crystallography, Part A.

(37) Murshudov, G. N.; Vagin, A. A.; Dodson, E. J. Refinement of Macromolecular Structures by the Maximum-Likelihood Method. *Acta Crystallogr., Sect. D: Biol. Crystallogr.* **1997**, *D53*, 240–255.

(38) Emsley, P.; Cowtan, K. Coot: model-building tools for molecular graphics. *Acta Crystallogr., Sect. D: Biol. Crystallogr.* **2004**, *D60* (12, Pt. 1), 2126–2132.

(39) Bricogne, G.; Blanc, E.; Brandl, M.; Flensburg, C.; Keller, P.; Paciorek, W.; Roversi, P.; Smart, O. S.; Vonrhein, C.; Womack, T. O. *BUSTER*, 2.8.0; Global Phasing Ltd.: Cambridge, UK, 2009.

(40) Wang, A.; Stout, C. D.; Zhang, Q.; Johnson, E. F. Contributions of Ionic Interactions and Protein Dynamics to Cytochrome P450 2D6 (CYP2D6) Substrate and Inhibitor Binding. *J. Biol. Chem.* **2015**, *290*, 5092–5104.

(41) Kabsch, W. XDS. *Acta Crystallogr. D Biol. Crystallogr.* **2010**, *66* (Pt 2), 125–132.

(42) Adams, P. D.; Afonine, P. V.; Bunkoczi, G.; Chen, V. B.; Davis, I. W.; Echols, N.; Headd, J. J.; Hung, L.-W.; Kapral, G. J.; Grosse-Kunstleve, R. W.; McCoy, A. J.; Moriarty, N. W.; Oeffner, R.; Read, R. J.; Richardson, D. C.; Richardson, J. S.; Terwilliger, T. C.; Zwart, P. H. PHENIX: a comprehensive Python-based system for macromolecular structure solution. *Acta Crystallogr., Sect. D: Biol. Crystallogr.* **2010**, *66* (Pt 2), 213–221.